

BMP signaling in the dorsal-ventral patterning system of the
milkweed bug *Oncopeltus fasciatus*

I n a u g u r a l - D i s s e r t a t i o n

zur

Erlangung des Doktorgrades

der Mathematisch-Naturwissenschaftlichen Fakultät

der Universität zu Köln

vorgelegt von

Lena Mareike Sachs

aus Dachau

Köln

2014

Berichterstatter:

Prof. Dr. Siegfried Roth

Prof. Dr. Günter Plickert

Vorsitzende der Prüfungskommission:

Prof. Dr. Ute Höcker

Tag der mündlichen Prüfung:

1.7.2014

Table of Contents

Zusammenfassung	6
Abstract.....	8
1. Introduction	9
1.1 The milkweed bug, <i>Oncopeltus fasciatus</i>.....	9
1.1.1 Formation of the blastoderm.....	10
1.1.2 Gastrulation and embryonic movements	11
1.1.3 Segmentation	13
1.1.4 Preliminary fate map of <i>Oncopeltus fasciatus</i>	13
1.2 BMP and Toll signaling.....	15
1.2.1 Toll signaling pathway.....	15
1.2.2 BMP signaling pathway.....	16
1.3 DV patterning in <i>Drosophila melanogaster</i>	17
1.4 Evolution of DV patterning.....	18
1.5 Aim of this study	19
2. Material and Methods.....	20
2.1 Material	20
2.1.1 Chemicals & Enzymes	20
2.1.2 Reagent Kits.....	20
2.1.3 Buffers and Solutions	20
2.1.4 Antibodies	25
2.1.5 Oligonucleotides and PCR programs.....	25
2.2 Methods	28
2.2.1 <i>Oncopeltus</i> husbandry	28
2.2.2 RNA interference (RNAi).....	29
2.2.2.1 Synthesis of dsRNA.....	29
2.2.2.2 Phenol chloroform extraction and 2-propanol precipitation of dsRNA.....	30
2.2.2.3 Injection of dsRNA into adult females	30
2.2.3 <i>In situ</i> hybridization (ISH)	30
2.2.3.1 Embryo fixation.....	30
2.2.3.2 Synthesis of RNA probes.....	31
2.2.3.3 Preparing of embryos for the hybridization	31
2.2.3.4 Hybridization.....	31
2.2.3.5 Removal of excessive probe.....	32
2.2.3.6 Detection.....	32

2.2.4 Fuchsin staining	32
2.2.5 Antibody staining	33
2.2.5.1 Standard Antibody staining	33
2.2.5.2 Antibody staining using the PerkinElmer TSA PLUS DNP HRP enhancer Kit	33
2.2.7 RNA isolation and cDNA synthesis	34
2.2.7.1 RNA isolation	34
2.2.7.2 cDNA synthesis	34
2.2.8 Identification of transcripts	35
2.2.9 Cloning of PCR products	35
2.2.9.1 Electroschock Transformation	35
2.2.9.2 Mini Prep	35
2.2.9.3 Restriction of the extracted plasmids	36
3. Results	37
3.1 Disrupting BMP signaling severely impairs morphogenesis of <i>O. fasciatus</i>	37
3.1.1 Disrupting BMP signaling leads to a failure in katarrepsis	37
3.1.2 Knockdown of <i>decapentaplegic</i> impairs germ band formation	40
3.1.3 Defective germ band elongation upon impaired BMP signaling	41
3.2 BMP signaling appears not to be involved in body segmentation	42
3.3 BMP signaling plays a major role in DV patterning of <i>Oncopeltus fasciatus</i>	45
3.3.1 BMP signaling and DV marker expression in wild type embryos	45
3.3.1.1 BMP signaling activity is dynamic in <i>Oncopeltus fasciatus</i> blastoderm stage embryos ...	45
3.3.1.2 Expression patterns of BMP signaling components in <i>Oncopeltus fasciatus</i>	47
3.3.1.3 Expression patterns of DV marker genes in <i>Oncopeltus fasciatus</i>	49
3.3.2 BMP ligands have distinct roles in DV patterning of <i>Oncopeltus fasciatus</i>	52
3.3.2.1 Depletion of the BMP ligand Decapentaplegic leads to strongly ventralized embryos	52
3.3.2.2 The anterior is more sensitive to <i>dpp</i> knockdown than the posterior	58
3.3.2.3 Knockdown of <i>glass bottom boat</i> leads to lateralization	59
3.3.2.4 The consequences of <i>gbb</i> knockdown differ along the AP axis	65
3.3.3 BMP receptors are required for a proper BMP signal transduction	68
3.3.3.1 Knockdown of <i>punt</i> causes a <i>dpp</i> knockdown-resembling DV phenotype	68
3.3.3.2 Knockdown of <i>thickveins</i> causes ventralization	69
3.3.3.3 Knockdown of <i>saxophone</i> causes ventralization	70
3.3.3.4 Partial recovery of DV marker expression in <i>sax</i> -RNAi germ band stage embryos	71
3.3.4 Extracellular modulators strongly influence BMP signaling activity during DV patterning	73

3.3.4.1 Ventral fates require protection from BMP signaling.....	73
by Twisted gastrulation and Short gastrulation.....	73
3.3.4.2 DV patterning of <i>sog</i> knockdown embryos is less impaired in the abdomen compared to the head and thorax	81
3.3.4.3 <i>dpp</i> is epistatic to <i>sog</i>	81
3.3.4.4 Sterility effects caused by loss of <i>dpp</i> and <i>tsg</i> are cumulative	82
3.3.4.5 Tolloid is essential for BMP signaling activity	84
3.3.5 Toll signaling is essential for DV polarity formation.....	85
3.3.5.1 The DV phenotype of <i>dpp</i> is epistatic to <i>Toll</i>	85
3.3.5.2 Toll is not required for the early activation of <i>sog</i>	88
4. Discussion	91
4.1 BMP signaling seems to be required for extraembryonic membrane function	91
4.2 Excursus: Crosstalk between DV and AP patterning during head specification	95
4.3 BMP gradient formation requires Tsg and Sog	97
4.4 The main DV patterning function of Tsg is dependent on Sog	98
4.5 Growth zone patterning might dependent on posterior signaling centers established at the onset of gastrulation.....	100
4.6 BMP heterodimers might be required for shaping of the BMP signaling activity gradient	104
4.7 BMP heterodimers might contribute to robust patterning	105
4.8 BMP signaling restricts mesoderm formation.....	106
4.9 BMP signaling represses <i>sog</i>	107
4.10 The evolution of Toll signaling in DV patterning: From a trigger to a ruler	108
4.11 Evolution of DV patterning.....	111
5. Outlook.....	115
5.1 The future of the system <i>Oncopeltus fasciatus</i>	115
5.2 Towards a broader perspective.....	117
6. References	118
7. Supplementary Information	132
7.1 Cell distributions differ between <i>dpp</i> -RNAi and <i>Toll-dpp</i> -RNAi embryos at the onset of gastrulation	132
7.2 <i>tsg</i> expression is not lost in <i>Toll</i> -RNAi embryos	133
7.3 Transcript sequences.....	134
Acknowledgments/Danksagungen.....	136
Erklärung.....	138
Lebenslauf.....	139

Zusammenfassung

Der BMP Signalweg spielt in der gesamten Tierwelt eine konservierte und wichtige Rolle während der Musterbildung entlang der dorsoventralen (DV) Achse. In Insekten übt allerdings auch der Toll Signalweg einen bemerkenswerten Einfluss auf die DV Musterbildung aus und scheint in abgeleiteteren Insekten einige Aufgaben, die ursprünglich dem BMP Signalweg unterlagen, übernommen zu haben. Um diese Annahme zu überprüfen wurde der relative Beitrag beider Signalwege zur DV Musterbildung in verschiedenen Insekten verglichen. Dabei hat sich herausgestellt, dass das DV Musterbildungssystem der sehr abgeleiteten Taufliege *Drosophila melanogaster* extrem abhängig vom Toll Signalweg ist, welcher sogar die räumliche Verteilung des BMP Signals weitgehend festlegt. Die Bedeutung des Toll Signalwegs für die DV Musterbildung scheint in basaler abzweigenden Insekten abzunehmen, während das Gegenteil auf den BMP Signalweg zutrifft. In der Wespe *Nasonia vitripennis*, welche zu den basalsten holometabolen Insekten, den Hymenopteren, zählt, wird der Toll Signalweg zur Mesoderm Induktion verwendet. In dieser Studie wurde zum ersten mal das DV Musterbildungssystem eines hemimetabolen Insektes, der Baumwollwanze *Oncopeltus fasciatus*, analysiert. *O. fasciatus* ist ein Kurzkeim Insekt, d.h. seine posterioren Segmente werden, nach Beginn der Gastrulation, sukzessive von einer posterior gelegenen Wachstumzone gebildet. Seine anterioren Segmente werden dagegen während des Blastoderm Stadiums etabliert. Unterschiede in der Entstehung anteriorer und posteriorer Segmente könnten sich möglicherweise auch in der DV Musterbildung widerspiegeln. Um das DV Musterbildungssystem von *O. fasciatus* zu verstehen wurde die Aktivität von Kandidatengenen mit Hilfe von parentaler RNA Interferenz (pRNAi) herunterreguliert. Die daraus resultierenden Phänotypen wurden auf molekulare und morphologische Abweichungen vom Wildtyp hin untersucht. Zu diesem Zweck wurden Kernfärbungen, *in situ* Hybridisierungen (ISH) sowie Antikörperfärbungen unternommen. Es stellte sich heraus, dass der BMP Signalweg das ventralste Schicksal, das Mesoderm, limitiert und sogar vollständig unterdrücken kann. Desweiteren reprimiert der BMP Signalweg auch *short gastrulation (sog)*, einen Inhibitor von BMP Liganden. Der Verlust der DV Polarität als Folge des Fehlens der BMP Inhibitoren Twisted gastrulation (Tsg) und Sog war ein weiterer Hinweis auf den enormen Einfluss des BMP Signalwegs auf die DV Musterbildung von *O. fasciatus*. Das Fehlen DV Asymmetrie in der Abwesenheit von *Toll* schien durch den Verlust späterer, nicht jedoch initialer *sog* Expression begründet zu sein.

Diese Ergebnisse führen zur Annahme, dass die DV Musterbildung in *O. fasciatus* ein selbst regulierendes System darstellt, das von BMP und seinen extrazellulären Modulatoren dominiert und durch den Toll Signalweg lediglich polarisiert wird. Außerdem deuten Unterschiede in den RNAi Phänotypen von Blastoderm- und Keimstreifembryonen daraufhin, dass das DV Musterbildungssystem für den Übergang vom Blastoderm zur Wachstumszone die Etablierung zweier gegensätzlich wirkender Signalzentren am posterioren Pol benötigt.

Abstract

BMP signaling plays an essential role in dorsal-ventral (DV) axis patterning throughout the animal kingdom. However, in insects Toll signaling also has a remarkable influence on DV patterning and, in higher branching lineages, fulfills some functions, which depend on BMP signaling in more basally branching lineages. Thus, the DV patterning system of the highly derived fruit fly *Drosophila melanogaster* is extremely dependent on Toll, which determines also the pattern of dorsal cell fates by specifying the polarity of BMP signaling. However, the wasp *Nasonia vitripennis*, which belongs to the most basally branching holometabolous lineage, the hymenopterans, uses Toll signaling only as mesoderm inductor. In this study for the first time the DV patterning system of a hemimetabolous insect, the milkweed bug *Oncopeltus fasciatus* was analyzed. *O. fasciatus* is a short germ insect, *i.e.* its posterior segments successively arise from a posterior growth zone, after the onset of gastrulation. In contrast, the anterior segments are synchronously established during the blastoderm stage. A different emergence of anterior and posterior segments might also be reflected in the DV patterning system. To understand the DV patterning system of *O. fasciatus* candidate genes were knocked down via parental RNA interference (pRNAi) and the resulting phenotypes were investigated for morphological as well as molecular deviations from wild type embryos. Nuclear staining techniques, *in situ* hybridization (ISH) and antibody staining were performed for this purpose. BMP signaling was found to be able to completely repress mesodermal fates and to be required to restrict it to the ventral side. Furthermore the repression of the BMP inhibitor *short gastrulation (sog)* seemed also to be mediated by BMP signaling. The lack of DV polarity upon depletion of the extracellular BMP inhibitors Sog and Twisted gastrulation provided further evidence for the high impact of BMP signaling on the *O. fasciatus* DV patterning system. The absence of DV asymmetry upon depletion of *Toll* was indicated to be due to a loss of later but not initial expression of *sog*. These results led to the proposal of a highly self-regulating BMP-dependent DV patterning system for *O. fasciatus*, which is only polarized by Toll signaling. In addition, differences between the early blastoderm and the later germ band DV pattern in knockdown embryos suggested that the transition of the two dimensional blastoderm DV patterning system into the three dimensional growth zone DV patterning system requires the establishment of two opposing signaling center located close to the posterior pole at the onset of gastrulation.

1. Introduction

The diversity of body plans, sizes and shapes among animals is incredibly amazing. However, despite their morphological variety the vast majority of animals possess two major body axes, the anterior posterior (AP) and the dorsal-ventral (DV) axis, which need to be established during embryogenesis. Remarkable similarities in setting up these axes are found on the molecular level. It appears that the gene regulatory networks (GRN) used for axis formation are partially conserved (Petersen & Reddien 2009; Little & Mullins 2006). For example most bilaterians, analyzed so far, use Wnt signaling to set up the AP axis (Petersen & Reddien 2009). Despite of such commonalities, GRNs underlying axial patterning also underwent major changes in the course of evolution. Our research group attempts to reconstruct the evolution of the GRN guiding DV patterning in arthropods, especially in insects.

Insects are appropriate to study evolution as they have a small body size, often exhibit a short life cycle, and many species produce a large number of offspring relative to other animals, e.g. mammals. For these reasons a lot of insects are easy and inexpensive to culture and especially suitable for studying embryonic development. In addition, insects are the most diverse class of animals, so it is possible to examine many different sampling points (Nentwig et al. 2007).

1.1 The milkweed bug, *Oncopeltus fasciatus*

This study focuses on the analysis of the DV patterning network with special regard to Bone morphogenetic protein (BMP) signaling using the milkweed bug *Oncopeltus fasciatus* as sampling point for investigation.

O. fasciatus is a true bug (order: Hemiptera, suborder: Heteroptera), with widespread distribution in the new world (Butt 1949). Its phylogenetic position within the group of winged insects (Pterygota) is shown in Figure 1-1. The duration of its embryogenesis is dependent on temperature and humidity. With conditions in our laboratory (25°C, approximately constant humidity), hatching from the approximately 1.2 mm long egg occurs after seven days.

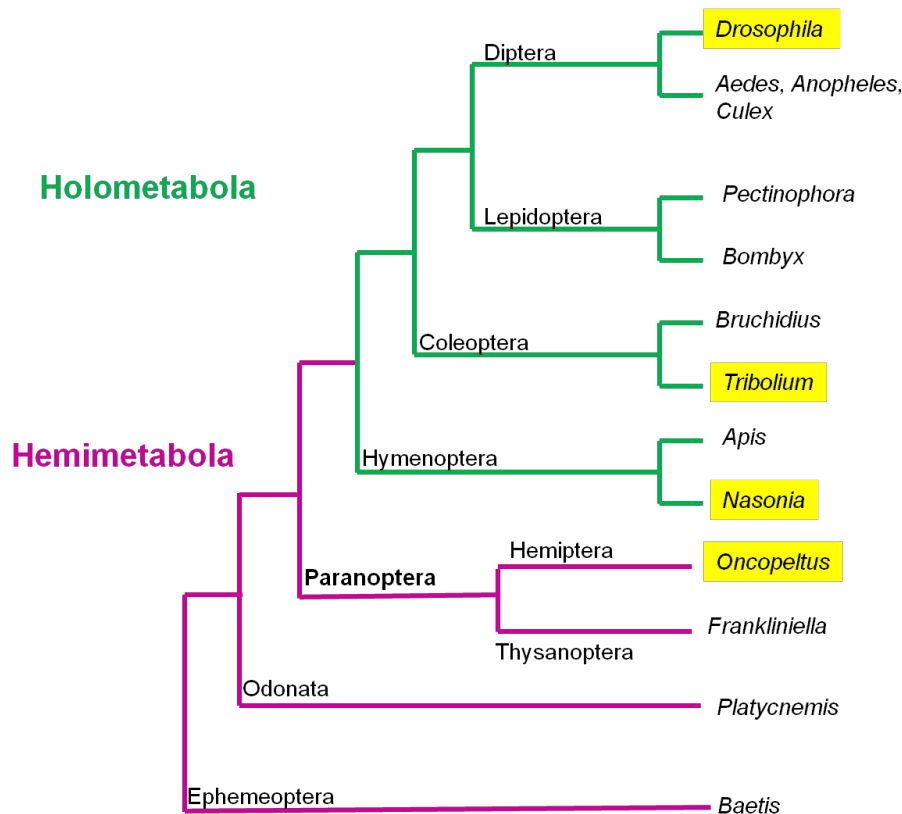


Figure 1-1: Phylogenetic tree of Pterygota

The tree was drawn after information from the publications Lynch & Roth 2011; Roth 2004. The clade indicated with green branches is the Holometabola; the assemblage indicated with lilac branches are hemimetabolous (paraphyletic with respect to the Holometabola). Orders and superorders are written on top or below the respective branches, orders in non-bold fonts, superorders in bold font. Genera are written in italic font; dorsal-ventral patterning mechanisms of species with genera highlighted in yellow are discussed later.

1.1.1 Formation of the blastoderm

Insects typically form a superficial, mono-layered "blastoderm" embryo during early embryogenesis (Roth 2004; Counce & Waddington 1973). The blastoderm is established during the first 15 hours of embryogenesis in *O. fasciatus*. After fertilization and egg activation (concomitant with oviposition), the zygotic nucleus starts to divide. Most of the emerging nuclei migrate as energids (the nucleus itself and an associated island of cytoplasm) towards the periphery of the egg. Some nuclei remain in the yolk and are referred to as vitellophages. The nuclei located close to the egg cortex undergo several rounds of synchronous division. Finally, cellularization is initiated, *i.e.* the syncytial uniform blastoderm is transformed into a cellularized, uniform blastoderm (Figure 1-2 A; Butt 1949).

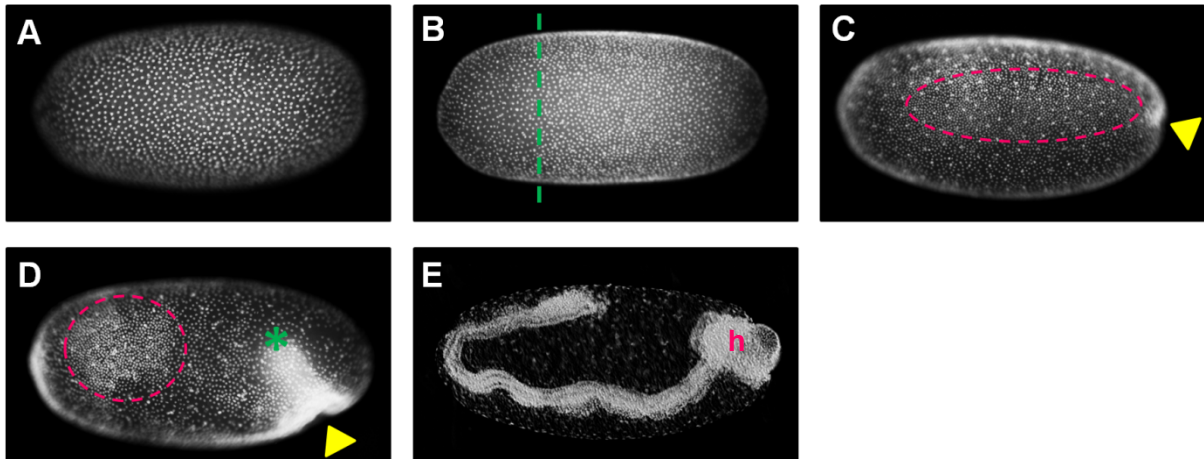


Figure 1-2: Early embryogenesis of *Oncopeltus*

The nuclei were stained with SYTOX-green (A-D) or with fuchsin (E). In all images the anterior of the egg is oriented to the left. All embryos are shown in a lateral view with egg-dorsal to the top (hence the embryo in (E) has embryo-ventral oriented to the top). Image (A) shows a uniform, cellularized blastoderm stage embryo (~20 hours post fertilization (hpf)). (B) pictures an embryo at the late uniform¹ blastoderm stage (~28 hpf). The dashed green line approximately separates an anterior region of low nuclear density from the remaining blastoderm. The embryo in C (~30 hpf) is at the differentiated blastoderm stage with a yellow arrowhead pointing towards the (future) invagination site. Laterally condensed cells are highlighted by a pink oval. The embryo in (D) is at the anatrepsis stage (~40 hpf). The green asterisk marks the posterior end of the germ rudiment (which already invaginated into the yolk). The embryo in (E) has finished anatrepsis (1.1.2), and it therefore has an inverse orientation with respect to the egg axes, *i.e.* its head (marked by an h) is at the egg posterior. Abbreviations: hpf: hours post fertilization, h: head.

1.1.2 Gastrulation and embryonic movements

During the second day of embryogenesis the cells become unevenly distributed within the blastoderm. First they become more widely spaced in the anterior 25% of the embryo (Figure 1-2 B)¹. The serosa is proposed to be located within this region (1.1.4; Figure 1-3 A; Figure 1-4). The serosa as well as the amnion are extraembryonic tissues covering the complete embryo and the yolk, or the ventral side of the embryo, respectively, during a certain stage of development (Roth 2004).

Around 30 hours post fertilization (hpf) cells become more widely spaced in the ventral region, while they start to condense in the lateral region and form a slight indentation at the posterior pole (Figure 1-2 C). The formation of the posterior indentation marks the

¹ Blastoderm embryos before gastrulation (*i.e.* before they formed a posterior indentation) are considered as uniform blastoderm embryos, although the cells are not completely equal distributed throughout this stage.

onset of gastrulation, which is defined as the sum of (morphological) processes that lead to the formation of the three germ layers (Solnica-Krezel & Sepich 2012).

At the end of the second day several patches of highly condensed cells emerge in the lateral region of the germ rudiment (Figure 1-2 D). This process occurs during the complete invagination of the germ rudiment into the yolk, whereby the embryonic orientation becomes inversed relative to the axes of the egg, a movement which is termed anatrepsis (Figure 1-2 D, E; Figure 1-3 B, C; Panfilio et al. 2006; Panfilio 2008). During anatrepsis the mono-layered surface (*i.e.* blastoderm embryo) becomes transformed into a multi-layered embryo, which is referred to as germ band in insects. This transformation includes internalization of the mesoderm and is directly followed by elongation of the newly formed germ band (Butt 1949; Panfilio et al. 2006; Roth 2004).

Around mid-embryogenesis (early on the fourth day) the orientation of the embryo becomes reversed again with respect to the egg axes, during an embryonic movement termed katatrepsis (Panfilio et al. 2006; Panfilio 2008). This event is preceded by the fusion of the amnion and serosa at the posterior pole of the egg (*i.e.* at the anterior end of the germ band) (Figure 1-3 D). The fused membranes rupture, which permits the contracting serosa to pull the germ rudiment out of the yolk (Figure 1-3 E; Panfilio et al. 2006; Panfilio 2008).

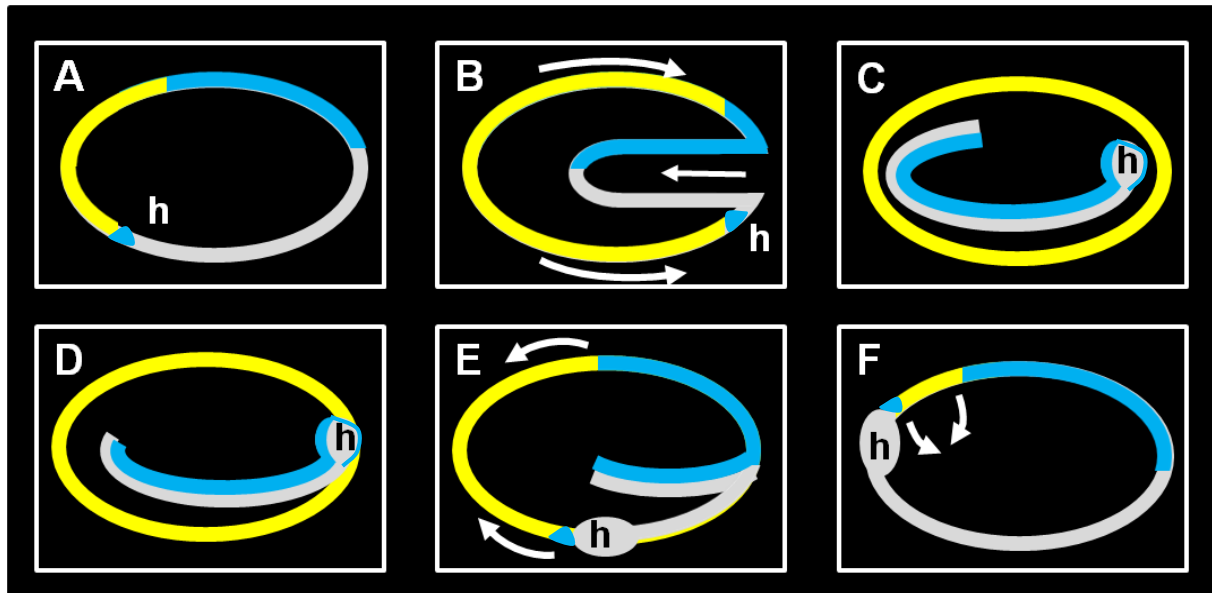


Figure 1-3: Schematic drawing of embryonic movements of *Oncopeltus fasciatus*

The serosa is depicted in yellow, the amnion in blue, the embryo in gray and the gray thickening indicates the head. Anterior is to the top, ventral to the left, regarding egg axes. The directions of movements are indicated with arrows. The egg and embryonic axes correspond to each other during the blastoderm stage (A). During anatrepsis the whole germ rudiment invaginates into the yolk (B). This leads to the formation of a germ band with inversed axes relative to the egg axes, which is surrounded by yolk and serosa (C). The amnion covers the embryo on the ventral side (C, D). Around mid embryogenesis the amnion and serosa fuse (D). Afterwards the

serosa contracts and pulls the germ rudiment out of the yolk (E). In this manner the egg and the embryonic axes become again correlated to each other (F). Abbreviations: h: head. This schematic drawing was based on the publication Panfilio 2008.

1.1.3 Segmentation

Segmentation starts already before germ band elongation, during the blastoderm stage. The head segments and the three thoracic segments are determined at this stage (Birkan et al. 2011; Liu & Kaufman 2004). However, the 11 abdominal segments arise successively from a posterior growth zone, after the onset of gastrulation (Liu & Kaufman 2004). If posterior segments are established after the onset of germ band elongation the mode of development is referred to as extreme short, short or intermediate germ, depending on the number of segmental primordia present before germ band elongation (Roth 2004). For simplification this study refers to all of these modes as short germ development.

In contrast to embryos with short germ development, embryos with long germ development establish all segments during the blastoderm stage. Long germ development is exclusively found in a subset of holometabolous insects (Roth 2004).

1.1.4 Preliminary fate map of *Oncopeltus fasciatus*

Like segmentation, the specification of DV fates starts also already during the blastoderm stage. From 25 hpf onwards several known marker genes are expressed in distinct regions along the DV axis in *O. fasciatus* (Francois et al. 1994; Jiménez et al. 1995; Kasai et al. 1992; Leptin 1991; Miller-Bertoglio et al. 1997; van der Zee et al. 2006; Handel et al., 2005; Sommer & Tautz 1994).

The anterior 25% of the blastoderm is largely excluded from the expression of those markers. This would be consistent with this region having a serosal identity, as the serosa does not contribute to the germ layers (Roth 2004). However, some head patterning genes are expressed in this region, indicating that it contains anterior head anlagen as well (Birkan et al. 2011; Weisbrod et al. 2013). In addition, it was proposed that at least a part of the serosa anlage is dorsally located within the *O. fasciatus* blastoderm (Ben-David & Chipman 2010).

However, the anterior region of the blastoderm is usually specified as serosa in short germ insects (Roth 2004). The anterior half as well as the dorsal 30% of the anterior quarter of the *O. fasciatus* blastoderm are not reported to express head patterning genes during specification of head tissue (Birkan et al. 2011; Weisbrod et al. 2013). Therefore, it is proposed in this study that the serosa anlage covers this region (Figure 1-4).

The expression of the highly conserved mesodermal marker *twist* (*twi*) was observed in the ventral 20 to 30% of the posterior 75% of the blastoderm (Drechsler 2007; Leptin 2004; Roth 2004; Sachs 2009; Figure 3-7 A, E, I). This indicates that the ventral-most tissue corresponds to the mesoderm anlage, since *twi* expression is indicative for mesoderm in all insects analyzed so far (Handel et al. 2005; Lynch & Roth 2011; Roth 2004).

The arrangement of the remaining DV fates seems also to be widely conserved among insects (Lynch & Roth 2011). The position of the future neuroectoderm in the ventral-lateral region was verified by the expression pattern of marker genes like *ventral nervous system defective* (*vnd*), *short gastrulation* (*sog*) and *single minded* (*sim*) (Sachs 2011; Figure 3-7 B, C, F, G, J, K; unpublished data of Yen-Ta Chen). Usually the non-neurogenic, also referred to as dorsal, embryonic ectoderm is located dorsally adjacent to the neuroectoderm, while the amnion (dorsal, extraembryonic ectoderm) is often positioned in the dorsal-most region of insect blastoderm fate maps (Goltsev et al. 2007; Lynch & Roth 2011; Nunes da Fonseca et al. 2008). This arrangement could not be assured by the expression of marker genes, as those dorsal marker genes which are known from holometabolous insects are not expressed in the same manner in *O. fasciatus* (data not shown).

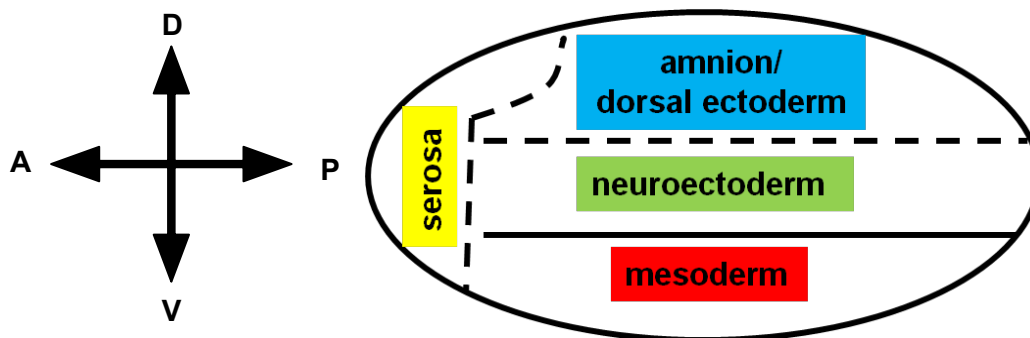


Figure 1-4: Presumptive blastoderm fate map of *Oncopeltus fasciatus*

The schematic embryo is orientated in a lateral view with dorsal to the top and anterior to the left. The mesoderm anlage is positioned in the ventral 20-30% of the egg circumference, followed by the neuroectoderm, dorsally to which the dorsal, embryonic ectoderm and amnion are located. The serosa is assumed to be located in the anterior 15% of the egg with a dorsal, posterior pointing protrusion. The position of the borders between the neuroectoderm and the dorsal ectoderm as well as of the serosa is uncertain (dashed lines). Abbreviations: A: anterior, D: dorsal, P: posterior, V: ventral.

1.2 BMP and Toll signaling

To establish DV fates insects use the BMP and the Toll signaling pathway both of which are conserved among metazoans (Hibino et al. 2006; Hughes & Piontkivska 2008; Satake & Sasaki 2010; Valanne et al. 2011; Guo & Wang 2009).

1.2.1 Toll signaling pathway

The Toll signaling pathway is involved in various processes, e.g. pathogen recognition, cell adhesion and development (Anderson et al. 1985; Eldon et al. 1994; Hughes & Piontkivska 2008; Tauszig et al. 2000). Toll signaling is especially famous for its conserved role in immunity (Hughes & Piontkivska 2008; Satake & Sasaki 2010; Zhong et al. 2012; Zheng et al. 2012; Pradeep et al. 2013; Yeh et al. 2013; Han-Ching Wang et al. 2010; Satake & Sekiguchi 2012).

Despite the broad conservation of the pathway's immune function, some deviations are found with regard to signaling components. Among these are remarkable differences between insect and vertebrate Toll ligands. Insects express an endogenous² Toll1-ligand, referred to as Spätzle, which is cleaved and thereby activated (Moussian & Roth 2005). This is in contrast to vertebrates, where Toll-like receptors (TLRs) are activated by direct, or co-receptor-mediated, binding of pathogen associated molecular patterns (PAMPs) or danger associated molecular patterns (DAMPs) (Santegoets et al. 2011).

The activated Toll receptors recruit DEATH domain proteins as adaptors, e.g. MyD88, which enable the docking of other DEATH domain proteins, at least one of them containing an additional kinase domain. Examples for the latter are IL-1R associated kinases (IRAKs) or their insect homologs Pelle and Tube or Tube-like kinases (TTLK) (Hughes & Piontkivska 2008; Santegoets et al. 2011; Towb et al. 2009; Valanne et al. 2011). This intracellular signaling cascade leads finally to the phosphorylation of I κ B, in insects referred to as Cactus, thereby initiating its degradation. Cactus prevents the transcription factor Dorsal, in vertebrates termed Nuclear factor κ B (NF- κ B), from nuclear translocation by masking its nuclear localization signal. After degradation of Cactus, Dorsal translocates into the nucleus and regulates the transcription of target genes (Moussian & Roth 2005; Valanne et al. 2011).

² Endogenous ligand is here used as expression for a genome encoded ligand, which does not include DAMPs, e.g. fragments of gene products which are only formed upon an injury.

1.2.2 BMP signaling pathway

The BMP signal transduction cascade is known to be involved in several developmental processes; one of them is DV patterning (Guo & Wang 2009; Dutko & Mullins 2011). In this regard, Decapentaplegic (Dpp) is the most important BMP ligand, which is homologous to BMP 2/4 in vertebrates (Johnston & Gelbart 1987; Miyazono et al. 2005). Other ligands of this signaling pathway are, for example, Glass bottom boat (Gbb) and Screw (Scw), which are homologous to the vertebrate BMP5/6/7/8 ligands (Miyazono et al. 2005). All BMP ligands are secreted proteins, which are synthesized as pro-proteins and require processing by proteases before they can act as ligands. They dimerize through the formation of disulfide bonds and subsequently bind to two type II BMP receptors and two type I BMP receptors (Figure 1-5; Miyazono et al. 2005; Sun & Davies 1995; Constam & Robertson 1999; Cui et al. 1998). Type I receptors, like Saxophone (Sax) or Thickveins (Tkv), are responsible for the ligand specificity (Nguyen et al. 1998; Haerry et al. 1998; ten Dijke et al. 1994). The receptors tetramerize upon ligand binding and BMP type II receptors, e.g. Punt (Put) and Wishful thinking (Wit), which are constitutively active kinases, activate BMP type I receptors via phosphorylation (Figure 1-5; Miyazono et al. 2005; Little & Mullins 2006). The activated type I receptors specifically interact with and phosphorylate receptor-associated Smad proteins (r-Smads), e.g. Mothers against Dpp (Mad) in the case of BMP signaling in insects (Figure 1-5; Feng & Derynck 1997; Little & Mullins 2006; Miyazono et al. 2005). These form complexes with Medea, in vertebrates referred to as common Smad (co-Smad), which then translocate into the nucleus and regulate transcription (Figure 1-5; Little & Mullins 2006; Miyazono et al. 2005).

The BMP signaling cascade, or rather its spatial activity, can be influenced by extracellular BMP modulators. These can facilitate or impede BMP ligand activity (Ben-zvi et al. 2008; De Robertis & Kuroda 2004; Little & Mullins 2006; van der Zee et al. 2006). The best known extracellular modulator is Short gastrulation (Sog), whose vertebrate ortholog is Chordin (Chd). It sequesters BMP dimers and thus prevents binding to their respective receptors (Little & Mullins 2006; Marqués et al. 1997; Piccolo et al. 1996; Ross et al. 2001; Shimmi & O'Connor 2003; Xie & Fisher 2005). The metalloprotease Tolloid (Tld) is responsible for the cleavage of Sog and hence for the release of BMP dimers from Sog-BMP ligand complexes (Ben-zvi et al. 2008; Connors et al. 1999; Little & Mullins 2006; Marqués et al. 1997; Shimmi & O'Connor 2003).

Another extracellular modulator is Twisted gastrulation (Tsg), or its homolog

Crossveinless 1 (Cv 1). The molecular mechanism as well as the general function of Tsg is not completely understood. Nevertheless, Tsg appears to be conserved in invertebrates and vertebrates and its functional depletion or over-activation clearly impairs BMP signaling (Ben-zvi et al. 2008; Little & Mullins 2006; Nunes da Fonseca et al. 2010).

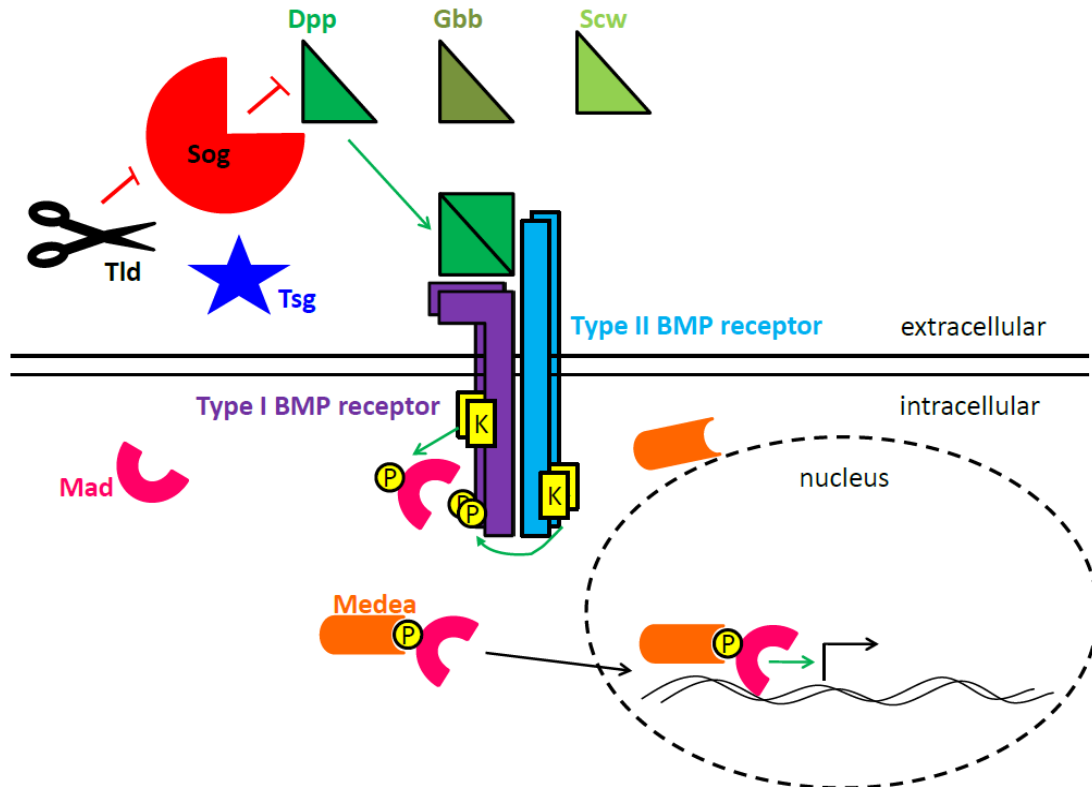


Figure 1-5: Scheme of the BMP signal transduction

Red lines with a blunt end indicate inhibition, green arrows activation and black arrows translocation. A detailed description of the signal transduction is provided in the text. Abbreviations: Dpp: Decapentaplegic, Gbb: Glass bottom boat, K: kinase; Mad: Mothers against Dpp, P: phosphate, Scw: Screw, Tld: Toll, Tsg: Twisted gastrulation.

1.3 DV patterning in *Drosophila melanogaster*

The best understood DV patterning system within insects is that of the fruit fly *Drosophila melanogaster*. In the following the function of Toll and BMP signaling in this system will be elucidated.

The BMP signaling pathway is required to pattern the dorsal 40% of *D. melanogaster* embryos. To this end a gradient of nuclear phosphorylated Mad (pMad) is established via the extracellular modulators Sog, Tsg and Tld. Sog and Tsg form complexes with BMP ligands, which quickly diffuse away from the source of Sog, *i.e.* the ventral-lateral region, towards the dorsal side. At this side of the embryo, BMP dimers bind to their receptors as they are freed

from Sog by Tld (Ben-zvi et al. 2008; Connors et al. 1999; Little & Mullins 2006; Marqués et al. 1997; Shimmi & O'Connor 2003).

The ventral side is patterned by the Toll signaling pathway: upon activation of the Toll receptor, a nuclear Dorsal gradient is formed in the ventral 60% of the egg circumference. Nuclear Dorsal shows peak levels at the ventral side and gradually decreases towards the dorsal side (Moussian & Roth 2005; Roth et al. 1989). This morphogen gradient is sufficient for establishing most cell fates along the DV axis and even regulates BMP signaling in several regards (Roth et al. 1989; Rusch & Levine 1996; Jazwińska et al. 1999; Reeves & Stathopoulos 2009).

1.4 Evolution of DV patterning

Although Toll signaling plays such an important role in *D. melanogaster* DV patterning it was never found to participate in DV axis formation outside of arthropods (Hughes & Piontkivska 2008; Satake & Sasaki 2010).³

In contrast, BMP signaling appears to be involved in DV patterning in almost all bilaterally symmetric animals (Akiyama-Oda & Oda 2006; Ben-zvi et al. 2008; De Robertis & Kuroda 2004; Kishimoto et al. 1997; Lapraz et al. 2009; Lowe et al. 2006; van der Zee et al. 2006; Kuo et al. 2012; Raftery & Sutherland 2003). This pathway is especially important for the specification of fates on the non-neuronal side (dorsal in insects, ventral in vertebrates). However, while the BMP pathway is in *D. melanogaster* largely under the control of Toll signaling and only responsible for patterning the dorsal, embryonic ectoderm as well as the extraembryonic amnioserosa, it has a more fundamental role in establishing fates along the DV axis in many other bilaterians (Akiyama-Oda & Oda 2006; Ben-zvi et al. 2008a; De Robertis & Kuroda 2004; Kishimoto et al. 1997; Lapraz et al. 2009; Lowe et al. 2006). For instance, vertebrate DV patterning is almost completely dependent on BMP signaling (Ben-zvi et al. 2008; De Robertis & Kuroda 2004; Kishimoto et al. 1997).

Comparing the situation in several insects, BMP signaling appears to gain relevance in DV patterning whereas the NF- κ B/Toll pathway loses it, towards more basally branching species of the insect phylogeny (Ferguson & Anderson 1992a; Nunes da Fonseca et al. 2008; van der Zee et al. 2006; Özüak 2014; Buchta 2014). For example, upon a functional

³ There might be one exception: there is vague evidence that TLR signaling might have a role in *Xenopus* DV patterning (Armstrong et al. 2012; Prothmann et al. 2000; Armstrong et al. 1998).

knockdown of *sog* the neuroectoderm is completely lost in *T. castaneum*, while it is only reduced in *D. melanogaster* (Francois et al. 1994; Raftery & Sutherland 2003; van der Zee et al. 2006). Furthermore, the depletion of Dpp causes a stronger ventralization in the wasp *Nasonia vitripennis* than in *D. melanogaster* (Ferguson & Anderson 1992a; Özüak 2014; phylogenetic position is indicated in Figure 1-1).

The conserved contribution of BMP signaling in DV patterning, together with functional data demonstrating its profound impact on this process in most animals, suggests an ancestral involvement of BMP signaling in DV axis establishment.

1.5 Aim of this study

This evolutionary assumption implies that Toll signaling might have been recruited for DV patterning during arthropod evolution. In the course of arthropod evolution the relevance of Toll signaling in establishing cell fates along the DV axis may have successively increased at the expense of the importance of BMP signaling in this regard.

It is not only of interest to confirm this hypothesis, but to find out how, and maybe also why, such a change could have occurred in the course of evolution. Studies in this context will also improve the general understanding of the evolution of complex gene regulatory networks (GRN) and possibly about stimuli for such evolutionary changes.

Therefore, it is valuable to gain knowledge about the evolution of DV axis establishment by analyzing this process in further insects, thereby generating additional sampling points for a comparative analysis. As we already have insights into the DV patterning systems of several holometabolous insects, it is reasonable to analyze for the first time the DV patterning systems of a hemimetabolous insect.

O. fasciatus is appropriate for such a study for several reasons: its husbandry is inexpensive with a high, year-round yield of embryonic material (2.2.1). Transcriptome data are available; blastoderm stages are amenable for *in situ* hybridization (ISH) and antibody as well as nuclear staining techniques. It is possible to synchronously knock down maternally and zygotically transcribed genes via parental RNA interference (pRNAi) (Liu & Kaufman 2004). The above mentioned techniques were used to analyze the function of some BMP signaling components of *O. fasciatus* in order to elucidate the mechanism of DV axis formation in this species.

2. Material and Methods

2.1 Material

2.1.1 Chemicals & Enzymes

Chemicals were purchased from BAUER, Merck, PFALTZ, Roche, Roth, Sigma and VWR. Chemicals ordered from other companies were marked as such. Enzymes were purchased from Ambion, Fermentas, Invitrogen and Roche.

2.1.2 Reagent Kits

Table 2-1: List of used Reagent Kits

Reagent Kit	Company
QUIAGEN Plasmid Miniprep Kit	Quiagen
TOPO ® TA Cloning (pCR®IIvector)	Invitrogen
Zymoclean™ Gel DNA Recovery Kit	ZYMO RESEARCH
MEGAscript ® RNAi	Ambion
MAXIscript ® In vitro Transcription Kit	Ambion
High-Fidelity PCR Kit	Invitrogen
TSA PLUS DNP HRP enhancer Kit	PerkinElmer
SuperScript® VILO™ cDNA Synthesis Kit	Invitrogen
SMARTer™ RACE cDNA Amplification Kit	Clontech

2.1.3 Buffers and Solutions

The pH was adjusted with HCl or NaOH. The solutions were sterilized either by filtration or by autoclaving. Applied water was either autoclaved or filter-sterilized.

For general use:

Phosphate buffered saline (PBS), 1x

NaCl	137 mM
KCl	2.7 M
Na ₂ HPO ₄	8 mM
KH ₂ PO ₄	1.7 mM

PBS with Tween (PBT), 1x

PBS, 1x	99.9%
Tween-20	0.1%

Sodium Dodecyl Sulfate (SDS), 10%

C ₁₂ H ₂₅ SO ₄ Na	10%
--	-----

Saline sodium citrate (SSC), 20x, pH 5

NaCl	3 M
Na ₃ C ₆ H ₅ O ₇	300 mM

Injection buffer (IB)

KCl	5 mM
Na ₂ HPO ₄	0.1 mM

Tris acetate EDTA (TAE) buffer

Tris	40 mM
acetic acid	20 mM
EDTA	1 mM

Lysogeny broth (LB) medium, pH 7

yeast extract	0.5%
NaCl	1%
tryptone	1%

Super-optimal broth with catabolite repression (SOC) medium

bacto-tryptone	2%
bacto-yeast extract	0.5%
NaCl	10 mM
KCl	2.5 mM
MgCl ₂	10 mM
glucose	20 mM

Fuchsin staining solutions:**Alcoholic fuchsin staining solution**

(stored at room temperature (RT))

Pararosaniline	5 mg/ml
Ethanol	80%

Solution C

Ethanol	50%
Solution D/BBBA	50%

Solution D/BBBA

Benzyl benzoate	80%
Benzyl alcohol	20%

In situ Hybridization and Antibody Staining Solutions:

Hybridization buffer (HYBE)

Formamide	50%
SSC, pH 5	5x
Heparin	100 µg/ml
salmon sperm DNA (ssDNA)	100 µg/ml
transfer-RNA (t-RNA)	100 µg/ml
SDS	1%
Tween-20	0.1%

Blocking solution

PBS	1x
Bovine serum albumin (BSA)	2 mg/ml
Goat serum	5%
Tween-20	0.1%

Alkaline phosphatase (AP) buffer, pH 9.5

Tris, pH 9.5	0.1 M
MgCl ₂	50 mM
NaCl	100 mM
Tween-20	0.05%

Probe resuspension buffer

Formamide	50%
SSC, pH 5	2x

Antibody staining solutions required for the PerkinElmer TSA PLUS DNP HRP enhancer Kit:

TNT

Tris-HCl, pH 7.5	0.1 M
NaCl	0.15 M
Tween20	0.05%

TNB

Tris-HCl, pH 7.5	0.1 M
NaCl	0.15 M
Blocking reagent (PerkinElmer)	0.5%

The blocking reagent was added slowly in small amounts to the buffer while stirring. Afterwards the buffer was gradually heated to 60°C while stirring to completely dissolve the blocking reagent.

DNP Amplification reagent working solution

The DNP Amplification stock (PerkinElmer) was 1:50 diluted with 1x Plus amplification diluent (PerkinElmer). This solution was always freshly prepared.

DAB staining solution

3,3-Diaminobenzidine (DAB)	0.3-0.5 mg
Ammonium nickel sulfate	0.05%
PBS	1x
Tween20	0.05%

2.1.4 Antibodies

Table 2-2: Applied antibodies

Antibodies were stored at 4°C or -20°C. Abbreviation: AP: alkaline phosphatase, DNP: dinitrophenol, HRP: horse radish peroxidase, IgG: heavy chain of Immunoglobulin G.

Order	Target, Designation	Animal in which it is generated	Coupled substance	Applied dilution
1°	Engrailed, 4D9	mouse	-	1:250
1°	Phospho-Smad1/5 (Ser463/465), 41D10	rabbit	-	1:30
2°	Rabbit IgG, α-rabbit::HRP	goat	HRP	1:100
2°	Mouse IgG, α-Mouse::AP	?	AP	1:400
2°	Digoxigenin, α-DIG::AP	sheep	AP	1:2000
3°	DNP, α-DNP::HRP	rat	HRP	1:100

2.1.5 Oligonucleotides and PCR programs

Table 2-3: Oligonucleotides

All oligonucleotides were purchased from Sigma. The online version of the program Primer3 (<http://frodo.wi.mit.edu/>) was used in order to design oligonucleotides. Also oligonucleotides designed by Yen-Ta Chen (indicated in parentheses) and general available oligonucleotides (M13, T7-SP6, T7) were used. T7 adaptor sequences are written in lowercase.

Designation	Sequence 5' -> 3'
LS_Of collagenIV m Fwd	ggccgcggGCAATTATGCTAGCCGGAAT
LS_Of collagenIV m Rev	cccggggcATTACAATATAACAAGAAAGACATTT
LS_Of croc m2 Fwd	ggccgcggAGAAGAGGTGTACGCTCAAC
LS_Of croc m Fwd	ggccgcggGGAGTCACCAGTGTGGATG
LS_Of croc m Rev	cccggggc GCATCTCCTGCTGCCTCTT
LS_Of gbb Fwd	ggccgcggTCAGTGAAACTATTGTTGGAGCA
LS_Of gbb Rev	cccggggcTTGGAGCACAACAAGGCTTA
LS_Of gbb small Fwd	ggccgcggTTGAAGTCCGTAACAATGAAGTT
LS_Of gbb intern Rev	cccggggcTGCTCCAACAATAGTTTCACTGA
LS_Of gbb intern Rev	cccggggcTGCTCCAACAATAGTTTCACTGA
LS_Of dpp intern Fwd	ggccgcggTCCTGGTGAAGTGGCGAG
LS_Of dpp intern Rev	cccggggcTTGCGGACCTCACATGGCGT
LS_Of dpp mp Fwd	ggccgcggACGCGGGGAGTAGCTAGCC
LS_Of dpp mp Rev	cccggggcCTTCTACATCCACAGCCAACC

LS_Of dlp m Fwd	ggccgcggCTACGAACAGAATGCCTATCTC
LS_Of dlp m Rev	cccggggcTTTAAACAATATCAGCTGACACACG
Msh pF (Yen-Ta Chen)	ggccgcggACCTGCGAAGCAGAAGC
Msh pR (Yen-Ta Chen)	cccggggcTCTGATTTGCTATAATAATGAACTGC
M 13 Fwd	GTAAAACGACGGCCAG
M13 Rev	CAGGAAACAGCTATGAC
LS_Of perlecan m Fwd	ggccgcggCAAGGACGACACCAAGGACT
LS_Of perlecan m Rev	cccggggcATTTGGGACCATCTGGAACA
LS_Of pent- Contig7096 Fwd	ggccgcggAGGTGATTGCTTGACTGACC
LS_Of pent- Contig7096 Rev	cccggggcCTAGTTGAAACATCTTGAAAGCA
LS_Of punt marg Fwd2	ggccgcggTGTGGACCCTAGTCCCCTC
LS_Of punt intern Rev	cccggggcTTGTTGGCACCTCATTGAAA
LS_Of punt marg Rev2	cccggggcTCCAGGCGATCAGTAGAGGT
LS_Of punt intern Fwd	ggccgcggTTCCTGAGAATTGACATGTATGC
LS_Of_qPCR_HMBS Fwd 1	TGGAAGTGTGGACTTGGTTG
LS_Of_qPCR_HMBS Rev 2	TTTCTTGTCCGCTGTTATTGG
LS_Of_qPCR_atubulin Fwd 3	CCCTCGTCTGATCTCCTTGA
LS_Of_qPCR_atubulin Rev 2	AACAGGGAGGTGAATCCAGA
LS_Of-sax-17917 Fwd	ggccgcggTGGTACACAGGGAAAACCAAG
LS_Of-sax-17917 Rev	cccggggcTTGGGCAAACAGGTCTTCT
LS_Of-sax17917 int Rev	cccggggcCTTTTGGTTCCCACACGAGTG
LS_Of-sax17917 int Fwd	ggccgcggATACATGGGTCCAGAGCTCC
sim 28 Fwd (Yen-Ta Chen)	CCTCCATCATCAGACTGACC
sim 771R (Yen-Ta Chen)	GCGAGAAGTGTATGATGAGAATA
LS_Of slalom m Fwd	ggccgcggAAAGACTGGAAATACTAGCCATTCA
LS_Of slalom m Rev	cccggggcGATGTTGGAGAAAGAACAGTATGC
sog0_1F (Yen-Ta Chen)	ggccgcggGTTTGGCAAGTCGTTTCGTA
sog1_2328R (Yen-Ta Chen)	cccggggcCCGTGCGATTACACTGAGCAA
sogF2P_1339F (Yen-Ta Chen)	ggccgcggATTGCAGTTGACCCACAATG
sogR2P_1182R (Yen-Ta Chen)	cccggggcTTCTACCAGCCTTGGTGAGG
LS_Of sox21 m2 Fwd	ggccgcggCATCAAGAGGGAACACACA
LS_Of sox21 m2 Rev	cccggggcAGCAAGGACGAGTGGCTTT
SoxN 400 F	GGCCGCGGCAGCACCTCATCAT

(Yen-Ta Chen)	
SoxN 1338 R (Yen-Ta Chen)	CCCGGGCAGGTTGGCACTGGGA
LS_Of syndecan m Fwd	ggccgcggTAGGAGGAGCTGTTGTTGGA
LS_Of syndecan m Rev	cccggggcGGAGAGGAGCGGTCTGATAA
LS_Of-tkv-15135 m Fwd	ggccgcggGGAAGTGGGAGGTATGGTGA
LS_Of-tkv-15135 m Rev	cccggggcGGAGGTGAGCTAGACCAGAAGA
LS_Of tld nd Fwd	ggccgcggCTTGGTTCCTATGTCTGCTGGTGTC
LS_Of tld nd Rev	cccggggcAGTCTTATTCGGTGGCCTGGAGTAG
Of-tsg marginal forward	ggccgcggAAGTGATTCTCTGAAGGAAGTG
Of-tsg marginal reverse	cccggggcTACTGGATGAACATATGTCT
LS_Of tsg intern FWD	ggccgcggACAAGAAGTTGATCCAGCCAA
Of-tsg-probe -reverse	cccggggcGTTCTCCAATACTCACAGC
twi_89F (Yen-Ta Chen)	ggccgcggCGACTCACTATAGGGCAAGCAG
twi-711R (Yen-Ta Chen)	cccggggcGGAATAGTAACATTTCTGGCTTGG
T3359 F (Yen-Ta Chen)	ggccgcggGGCAGTTCACACTCACATTGAATTACT
T3359 R (Yen-Ta Chen)	cccggggcGGATATGTGACTGTCAAGCAA
T7-Sp6 (SP6 is changed to T7)	TAATACGACTCACTATAGGATTTAGGTGACACTATAGA
T7 5' universal (fwd)	GAGAATTCTAATACGACTCACTATAGGGCCGCGG
T7 3' universal (Rev)	AGGGATCCTAATACGACTCACTATAGGGCCCGGGC

PCR programs:

The reaction volume was always 25 µl. As template served complementary DNA (cDNA) mixtures or plasmids. The reagent mix REDTaq[®] ReadyMix[™] PCR Reaction Mix (Sigma) and my-Budget 5 x PCR-Mastermix (Bio-Budget) were applied.

standard PCR program

95°C,	5 min	
95°C,	30 sec	} 34 x
50 - 60°C,	30 sec	
72°C,	0.5 - 2 min	
72°C,	6 min	
12°C		

For semi-quantitative PCR the standard program was used with a reduced cycle number (25). *alpha-tubulin* and *HMBS* transcripts were amplified as control.

colony PCR program

97°C,	10 min	
95°C,	30 sec	} 34 x
50 - 60°C,	30 sec	
72°C,	0.5 - 2 min	
72°C,	6 min	
12°C		

touch down PCR program

95°C,	5 min	
95°C,	30 sec	} 20 x
50 - 60°C, -0.5°C/cycle	30-90 sec	
72°C,	0.5 - 2 min	
95°C,	30 sec	} 34 x
50 - 60°C,	30 sec	
72°C,	0.5 - 2 min	
72°C,	6 min	
12°C		

The touch-down PCR program was applied if it was difficult to amplify the respective sequence with the standard PCR program.

2.2 Methods

2.2.1 *Oncopeltus* husbandry

The milkweed bugs were fed with sunflower seeds, and wet paper towels served as water source. They were also equipped with pieces of cotton. The eggs were usually deposited into the cotton, from which they could be easily removed with a brush.

Injected females were housed each individually in large petri dishes (Greiner Bio-one GmbH, size 145/20 mm) together with two un-injected males.

2.2.2 RNA interference (RNAi)

This paragraph is based on the review article “A three-dimensional view of the molecular machinery of RNA interference” (Jinek & Doudna 2009).

This gene knockdown method exploits a defense mechanism against viruses that is present in (almost) all multicellular organisms.

Long double stranded RNA molecules (dsRNAs) that often result from viral transcription are recognized and cleaved by Dicer, a RNase III enzyme. Therefore arise small dsRNAs (21-25 nucleotides), which are labeled via mono-phosphate groups on the five prime ends and dinucleotide overhangs on the three prime ends. These small dsRNAs are bound by argonoute proteins. This association forms the core complex of the RNA induced silencing complex (RISC). The argonoute proteins are responsible for the cleavage and binding of the target single-stranded RNA (ssRNA).

This mechanism can be experimentally exploited by injection of long dsRNA molecules (about 200 bp to 1.5 kb) corresponding to an exonic region of the respective target gene. This leads to a knockdown of the target gene.

This method is very successful and easy to apply in *Oncopeltus*. It is possible to perform a parental RNA interference (pRNAi) knockdown via injection of dsRNA into adult females. Embryos with a loss of function phenotype can be obtained for several weeks (Liu & Kaufman 2004).

2.2.2.1 Synthesis of dsRNA

In the first PCR target gene-specific primers were used, which were endowed with an overhang complementary to the end of the T7 Universal Fwd and Rev primers (Table 2-3). In the second PCR the first PCR reaction served as template and T7 Universal primers were applied with a T7 polymerase binding site overhang (Table 2-3). The templates exhibited a size between 200 bp and 1.5 kb.

In vitro transcription was complied with instruction of the MEGAscript protocol, but the reaction was allowed to proceed over night.

2.2.2.2 Phenol chloroform extraction and 2-propanol precipitation of dsRNA

Table 2-4: Pipetting scheme of the RNA extraction reaction

dsRNA synthesis reaction	20 μ l
Nuclease free water (Ambion)	115 μ l
Ammonium acetate	15 μ l
Final volume	150 μ l

After mixing of the reagents, listed in Table 2-4, 150 μ l of phenol/chloroform (1:1) were added. Afterwards the mixture was vortexed for 60 sec and then centrifuged with 5000 rpm for 5 min at RT. The upper aqueous phase was transferred into a new tube. Thereupon 150 μ l 2-propanol were added and the tube was inverted. Then the reaction was incubated over night at -20°C. Subsequently centrifugation for 5 min with 13000 rpm at 4 °C followed. The supernatant was removed, 300 μ l of ethanol (100%) were added and the tube was inverted. Then the reaction was centrifuged for 5 min with 1300 rpm at 4°C. The RNA pellet was freed from the ethanol and dried 5 min at RT. Resuspension of the pellet was done in 50 μ l IB. Afterwards the RNA concentration and length was estimated via gelelectrophoresis.

2.2.2.3 Injection of dsRNA into adult females

Injection was performed using a 10 μ l syringe (Hamilton). Each 5 μ l of dsRNA were injected into the belly of adult, virgin females. The dsRNA concentration were between 8 μ g/ μ l and 0.5 μ g/ μ l. IB without dsRNA was injected as negative control. The real amount of absorbed dsRNA was not completely clear, because it is insecure how much of the injected liquid is taken up in the animal's body.

2.2.3 In situ hybridization (ISH)

The Hybridization method was previously described by Liu & Kaufman 2005.

2.2.3.1 Embryo fixation

The applied embryo fixation method is based on a description of Liu & Kaufman 2004.

Between the chorion of *O. fasciatus* eggs and the embryo is much pressure. In order to crack the eggshell without damaging the embryo, the egg was initially heat-fixed. Therefore the eggs were transferred into a screw top tube and covered with distilled H₂O. The tube was

submerged into boiling water for 70 sec to 90 sec. Afterwards it was immediately cooled down in ice water. Then the eggs were vortexed in heptane and 1x PBS with 4% formaldehyde (1:1) for 5 min. The lower aqueous phase was removed. The addition of methanol initiated the cracking of the chorion. The embryos were fixed in 1x PBS with 4% formaldehyde for 45 min to 2 h. The fixation works via a nucleophile attack of primary amino functional groups, which are mainly found in lysine side chains, to carbonyl functional groups of formaldehyde. This leads to hemiaminals that condensate with further amino functional groups. Thus the proteins become connected to each other. The fixed embryos were stored in methanol at -20°C.

2.2.3.2 Synthesis of RNA probes

Probes were synthesized applying the MAXIscript Kit (Ambion) or T7 polymerase of Roche or Ambion with RNase protector (Roche) and a digoxigenin (DIG) RNA labeling mix (Roche). The probes were resuspended in 100 µl probe resuspension buffer and stored at -20 °C. Sense probes were synthesized and applied for the negative control samples.

2.2.3.3 Preparing of embryos for the hybridization

The embryos were stepwise conveyed from methanol to 1x PBT and then washed with 1x PBT (2x rinsing, 1x ≥ 30 min). Afterwards they were gradually transferred into HYBE and rinsed twice with HYBE. Then the endogenous alkaline phosphatase was inactivated by incubation of the embryos at 70°C for 30 min. Subsequently the embryos were prehybridized by incubation at 60°C for at least 30 min.

2.2.3.4 Hybridization

1 to 10 µl probe were added in 500 µl HYBE. Hybridization was performed at 60°C for 12 to 18 h.

The success and specificity of a hybridization of nucleic acids mainly depends on an appropriate concentration of salt, formamide and on a suitable temperature. Salt (SDS, SSC) facilitates hybridization because the positively charged cations neutralize the negative charge of the phosphate backbone of nucleic acids. In contrast, formamide is a hydrogen bond-breaking substance, so it prevents unspecific hybridization. A high temperature also prevents unspecific hybridization. Additionally, ssDNA also should inhibit unspecific hybridization (because it binds unspecifically to nucleic acids). t-RNA is added to protect the probe against

RNAses (because the concentration of t-RNA is much higher than the probe concentration it is more likely as a substrate for RNAses).

2.2.3.5 Removal of excessive probe

Excessive probe was removed by six washes in HYBE at 60°C (2 x rinsing, 4 x ≥ 20 min) and two subsequent washings at RT (2 x 5 min) first in 5x SSC/ 50% formamide/ 0.1% Tween-20 and second in 2x SSC/ 50% formamide/ 0.1% Tween-20. Afterwards the embryos were gradually transferred into 1x PBT and then washed in 1x PBT (2 x rinsing, 2x ≥ 15 min). Subsequently the embryos were once rinsed and afterwards blocked for at least 1.5 h at RT in blocking solution.

2.2.3.6 Detection

The α -DIG::AP Antibody (Table 2-2) and the nucleic acid stain SYTOX-green (Nuclear probes) was added in fresh blocking solution. The embryos were incubated overnight at 4°C. The excessive antibody was removed by several washes in 1x PBT at RT (4 x rinsing, 2 x ≥ 20 min). The embryos were stepwise transferred into AP buffer. This buffer contains ions and has an alkaline pH, so the enzyme can work efficiently. After several washings in AP buffer (2 x rinsing, 1 x ≥ 20 min) nitro blue tetrazolium chloride (NBT)/5bromo-4chlor-3indolyl-phosphate (BCIP) solution was added in fresh buffer to initiate the color reaction. Alkaline phosphatase dephosphorylates BCIP which becomes then oxidized by NBT and adds to a blue indigo colorant while NBT is reduced to a blue diformazan. The reaction was stopped by several washes in 1x PBT.

2.2.4 Fuchsin staining

Fixed embryos (as described in section 2.2.3.1) were transferred into glass vials and washed in 70% ethanol (4 x 20 min). The ethanol was removed, 2 N HCl were added and the embryos were incubated at 60°C for 10 min. Afterwards one washing with distilled H₂O (5 min) and two with 70% ethanol (2 x 5 min) were performed. Subsequently the embryos were incubated in alcoholic fuchsin staining solution for 30 min. Then excessive color was removed by washing in 95% ethanol (3 x 10-20 min). Afterwards the embryos were dehydrated by washing in 100% ethanol (2 x 3 min). The ethanol was removed and solution C was added. As soon as the embryos sank to the bottom of the tubes, solution C was substituted by solution D.

The BBBA alcohol mixture is responsible for optical clearing of the yolk and was also applied for the analysis of germ band stage embryos stained for a transcript or a protein, and of end stage phenotypes. The stained embryos were stored at 4°C or RT, protected from light.

2.2.5 Antibody staining

2.2.5.1 Standard Antibody staining

The fixed embryos (as described in section 2.2.3.1) were stepwise conveyed from methanol into 1x PBT. Then they were washed with 1x PBT (1 x rinsing, 3 x 5 min, 1 x \geq 30 min). Subsequently they were rinsed with blocking solution. Blocking was performed for at least 1.5 h at RT, or alternatively overnight at 4°C. The primary antibodies (Table 2-2) were added in fresh blocking solution and incubated 16 to 22 h at 4°C, or alternatively 2.5 to 3 h at RT. No primary antibody was added to the negative control samples. The excessive antibodies were removed via several washes in 1x PBT at RT (1 x rinsing, 2 x \geq 20 min, 1 x \geq 30 min). The embryos were blocked a second time in blocking solution for at least 1 h at RT. The secondary antibodies were added in fresh blocking solutions together with SYTOX-green (Nuclear probes). The embryos were incubated for 16 to 22 h at 4°C, or alternatively for 2.5 to 3 h at RT, protected from light. Subsequently the embryos were washed in 1x PBT (1 x rinsing, 2 x \geq 20 min, 1 x \geq 30 min, 1x \geq 1 h). Then the embryos were stepwise transferred into AP buffer. After several washings in AP buffer (2 x rinsing, 1 x \geq 20 min), NBT (nitro blue tetrazolium chloride) /BCIP (5bromo-4chlor-3indolyl-phosphate) solution was added in fresh buffer to initiate the color reaction. The reaction was stopped by several washes in 1x PBT. The standard antibody staining protocol was used to monitor Engrailed.

2.2.5.2 Antibody staining using the PerkinElmer TSA PLUS DNP HRP enhancer Kit

The instructions of the PerkinElmer TSA PLUS DNP HRP enhancer Kit manual are adapted to sections and the protocol had to be modified to successfully stain *O. fasciatus* whole mounts.

Antibody staining was first performed as described above using a secondary antibody that was coupled to HRP. The excess secondary antibody was removed by washing with TNT (2x rinsing, 2x \geq 20 min, 1x \geq 30 min, 1x \geq 1 h). Afterwards the embryos were incubated for 40 min to 60 min in DNP Amplification reagent working solution and then washed with TNT (2x rinsing, 1x \geq 10 min, 1x \geq 20 min, 1x \geq 1 h). It followed blocking by incubating the

embryos for 1 to 2 h in TNB. Then the embryos were incubated with the third antibody (α -DNP-HRP) diluted in TNB for 3 to 4 h at RT or 16 to 22 h at 4°C. The excess antibody was removed by washing with TNT (2-3x rinsing, 1x \geq 10 min, 1x \geq 20 min, 1x \geq 1 h).

Subsequently the embryos were incubated in DAB staining solution for at least 30 min. The staining reaction was initiated by adding drop wise H₂O₂ (0.3%), which was diluted in 1x PBS. The reaction was stopped by several washes in 1x PBT or TNT.

2.2.7 RNA isolation and cDNA synthesis

2.2.7.1 RNA isolation

The protocol was adapted from the Ambion TRIzol® Reagent manual.

10 to 100 embryos were transferred into a 1.5 ml tube and grinded in 50-100 μ l TRIzol (Ambion). The grinded embryos could be optionally stored at -80°C. TRIzol was added to a final volume of 1 ml and the tube was vortexed for 3 sec and afterwards incubated at RT for approximately 5 min. It followed centrifugation with 12000 rpm for 15 min at 4°C. The liquid was transferred into a new tube, while solid components were discarded. 200 μ l trichlormethane were added, the tube was vortexed for 20 sec and incubated at RT for 2 to 3 min before it was centrifuged with 12000 rpm for 10 min at 4°C. The upper aqueous phase was transferred into a new tube and the phenol-chloroform extraction was repeated. Afterwards the aqueous phase was mixed with an equal volume of 2-propanol (600 μ l) by inverting the tube. The tube was incubated at -20° C for at least 30 min. In this manner the RNA was precipitated. The supernatant was removed and the RNA-pellet was washed with ethanol (80%) for 5 min at RT. The ethanol was removed and the pellet was allowed to dry on air. Afterwards it was resuspended in nuclease-free water and incubated at 55°C for 5 min. Concentration and quality was estimated by measuring the absorption at 230, 260 and 280 nm with a NanoDrop (Thermo Scientific). In addition, (ribosomal) RNA was monitored on an agarose gel to confirm that the isolated RNA is not degraded. The isolated RNA was stored at -80°C.

2.2.7.2 cDNA synthesis

The SuperScript® VILO™ cDNA Synthesis Kit or the SMARTer™ RACE cDNA amplification Kit were used for cDNA synthesis. Instruction of the manuals were followed. The cDNA was stored at -20°C or -80°C.

2.2.8 Identification of transcripts

Transcripts of orthologous genes were searched in the transcriptome published by Ewen-Campen et al. 2011. BioEdit was used for local BLAST (basic local alignment search tool) searches (tblastx) with query sequences from different species. Promising hits were verified by BLASTing (using tblastx provided by www.ncbi.gov) them against sequences of the query species and the complete nucleotide collection available on www.ncbi.gov. The identity of transcripts, which were used for functional analysis, was additionally confirmed by phylogenetic analysis with tools accessible on www.phylogeny.fr (Dereeper et al. 2008). In addition, sequence information was sometimes obtained by degenerate and RACE-PCR (Table 2-1). Contribution of other people to this work and identifiers of the genes are indicated in Table 7-1.

2.2.9 Cloning of PCR products

2.2.9.1 Electroshock Transformation

The invitrogen TOPO TA cloning Kit and DH 5 α *E. coli* cells were used and the instructions from the manual were followed. Competent *E. coli* cells were stored at -80°C and thawed on ice. After adding the ligation reaction, the bacteria were exposed to an electroshock of 1700 V. Immediately after the electroshock, the cells were transferred into SOC medium and incubated at 37°C for at least 1 h, while shaking. Then the bacteria were spread on LB-agar plates (LB medium plus 1.5% agar) with ampicillin, isopropyl β -D-1-thiogalactopyranoside (IPTG) and 5-Brom-4-chlor-3-indoxyl- β -D-galactopyranosid (X-Gal) and grown at 37°C over night. The pCRII vector contains an *Ampicillin resistance* gene and the cloning site is located in the *LacZ* gene. So bacteria with the pCRII vector were selected positively and it was possible to distinguish between colonies with an insertion in the pCRII vector (white) and with an empty vector (blue).

2.2.9.2 Mini Prep

White colonies were picked and each was allowed to grow in 3 ml LB medium with ampicillin at 37°C over night, while it was shaken. The picked colonies were additionally used as templates for colony PCRs with M13 primers. For plasmid extraction the QUIAGEN Plasmid Miniprep Kit was used and all instructions from the manual were followed.

2.2.9.3 Restriction of the extracted plasmids

The extracted plasmids were digested with EcoRI and subsequently loaded on an agarose gel (1% agarose in TAE buffer plus 0.05 µg/ml ethidium bromide (Sigma)). Gelectrophoresis was done in order to examine the length of the cloned PCR products. Sequencing was performed to finally confirm the cloning of the desired PCR product.

3. Results

This section will start with a description of germ band and end stage morphological defects in knockdown embryos (3.1). Afterwards analyses of blastoderm, anatrepsis and germ band stages of wild type and knockdown embryos by monitoring protein and mRNA distributions will be presented. This will comprise a short glance at segmentation in embryos with impaired BMP signaling (3.2) and a more detailed analysis of dorsal-ventral (DV) patterning in wild type (3.3.1) and distinct knockdown embryos (3.3.2-5). In this scope consequences of depletion of BMP ligands (3.3.2), BMP receptors (3.3.3) and BMP extracellular modulators (3.3.4) on DV marker gene expression and BMP signaling activity will be described. Finally, the DV fate map of *Toll-dpp*-RNAi and *Toll*-RNAi embryos will be delineated (3.3.5).

3.1 Disrupting BMP signaling severely impairs morphogenesis of *O. fasciatus*

3.1.1 Disrupting BMP signaling leads to a failure in katarrepsis

The BMP signaling pathway is known to participate in several developmental processes. For example, it is involved in skeletal development and organogenesis in vertebrates, as well as in limb development in vertebrates and insects (Hogan 1996; Wan & Cao 2005; Blank et al. 2008; Ahn et al. 2001; Jockusch et al. 2000; Weber 2006). It was therefore not surprising that knocking down genes encoding single components of this pathway caused embryonic lethality. After at least seven days of embryogenesis, when wild type embryos hatched (shortly after stages shown in Figure 3-1 A-B), unhatched knockdown embryos were categorized for end stage phenotype and analyzed further (Figure 3-1 C-L). For better visualization, the yolk was optically cleared with a mixture of benzyl benzoate and benzyl alcohol in some cases (2.2.4). In some end stage eggs only small fragments of pigmented embryonic epidermis were left after this time (depending on the target and dsRNA concentration ~5 to 30% of the end stage phenotypes) (Figure 3-1 L). This indicated an early disruption of embryogenesis followed by death and degradation of tissues. Other end stage phenotypes also suggested a severe defect occurring already during early embryogenesis. For example, the typical *dpp* knockdown end stage phenotype was an egg separated into two parts by a constriction: one part consisted presumably mainly of yolk, whereas the other one contained a big orange blob, which might have been the head, as it often exhibited a red pigmented dot, presumably an eye (Figure 3-1 K). The constriction divided the eggs into two,

either equal-sized parts, or the part containing the head was smaller (Figure 3-1 K). This part was typically located at the posterior pole of the egg, less often at the anterior pole and, in rare cases, the two parts were sitting on top of each other, *i.e.* one was more ventral than the other (Figure 3-1 K; data not shown). The inversion of the embryonic AP axis relative to the egg AP axis was also observed for *dpp*-RNAi embryos in which it was possible to identify residual body fragments in addition to the head (Figure 3-1 F). Furthermore, this phenomenon appeared to be common among all investigated intracellular and extracellular BMP signaling component encoding gene (*BMPsc*) knockdown embryos (Figure 3-1 C-G, J, K). The orientation of the embryo could be determined by the position of the head and sometimes through body pigmentation. This is possible as wild type embryos exhibit (from about 5 days post fertilization (dpf) onwards) an orange-colored head and thorax while the orange gradually darkens into red towards the posterior of the abdomen (Figure 3-1 A, B).

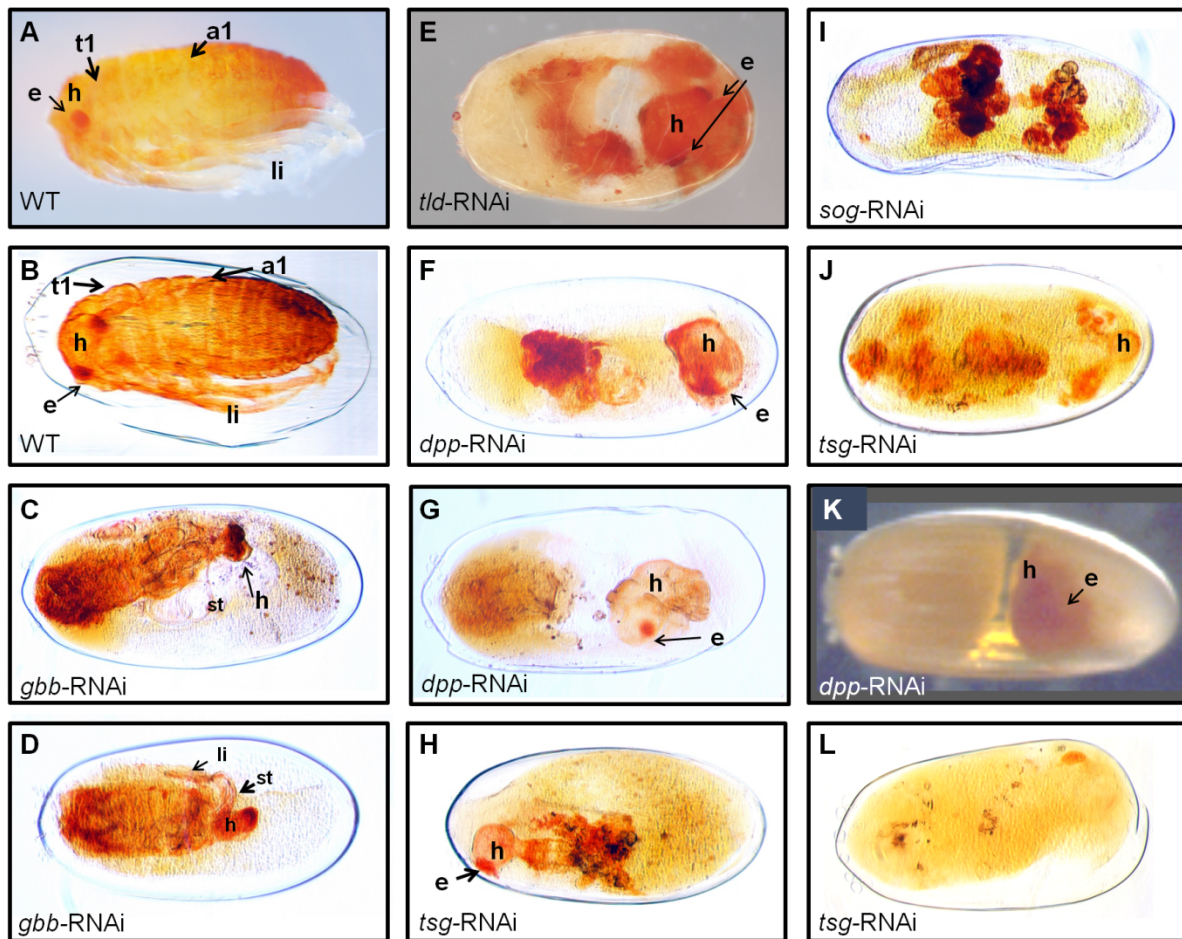


Figure 3-1: End stage phenotypes caused by disruption of BMP signaling

Anterior of the egg is to the left. All embryos were fixed with formaldehyde and, except for the ones shown in A, E and K, subsequently stored in BBBA to make the yolk optically clear (2.2.3.1; 2.2.4). Images A and B display wild type embryos shortly before hatching, C-F display embryos presumed to be everted. F, G and H show *dpp*-RNAi (F, G) and *tsg*-RNAi (H) knockdown embryos exhibiting weaker phenotypes. The typical *sog*- and *tsg*-RNAi phenotypes exhibited still a compact body (I), or were fragmented (J). K depicts the most abundant *dpp*-

RNAi phenotype. L shows an example of an end stage phenotype with only small pigmented fragments remaining. The knocked down gene is indicated in the left bottom corner of each panel. Abbreviations: a1: first abdominal segment, BBBA: mixture of benzyl benzoate and benzyl alcohol, e: eye; h: head, li: limb(s), st: stylets, t1: first thoracic segment, WT: wild type.

The above described constriction, which separated the anterior embryonic part and yolk from the more posterior part, was also frequently observed in most of the *BMPsc* knockdown phenotypes (Figure 3-1 K). It was present in almost all (> 90%) *dpp*-RNAi embryos, while it was observed in about 30% of *tsg*- and *sog*-RNAi embryos. Only in *gbb*-RNAi and *sax*-RNAi embryos was this constriction not found (Figure 3-2; *sax*-RNAi embryos are only shown in section 3.3.3.4). *gbb* knockdown embryos were (partially) everted as inside-out, *i.e.* inner organs were exposed to the yolk, while limbs were enclosed by the body cuticle (Figure 3-1 C, D). Exposed stylets, mouth parts that are usually stored in bilateral pockets within the head, served as hallmark for this phenotype (Figure 3-1 C, D; Panfilio et al. 2006). Sometimes not all limbs were included in the body, indicating that at least some *gbb*-RNAi embryos were only partially everted (Figure 3-1 D). It seemed that weak *dpp*-, *tld*-, *sog*- and *tsg*-RNAi end stage phenotypes were also (partially) everted, as they exhibited a smaller body with no visible limbs embedded not in yellow yolk but in a white mass, which might consist of organ tissue as well as yolk (data not shown; Figure 3-1 E, F). These features were described before as being typical for *zen*-RNAi embryos, which are all completely everted (Panfilio et al. 2006). Frequently, it was impossible to determine whether the end stage phenotypes of *tsg* and *sog* knockdown embryos were everted, as they commonly exhibited only a very thin, convoluted, tube-shaped, often partially fragmented embryo without any appendages (Figure 3-1 I, J).

Nevertheless, the previously mentioned inversion of the embryonic AP axis relative to the egg axis as well as the observed (partial) eversion phenotypes are both indicative for a failure in katatrepsis, the embryonic movement required to re-align the embryonic and egg axes after they became inverted relative to each other during anatrepis (1.1.2).

3.1.2 Knockdown of *decapentaplegic* impairs germ band formation

The morphology of the investigated knockdown embryos was also analyzed at anatrepsis and germ band stages. Knockdown of *dpp* led to a delayed and abnormal anatrepsis of the embryo. Typically, embryonic tissue accumulated first at the posterior pole and invaginated slightly delayed (compared to wild type) and in an unorganized fashion into the yolk. During invagination, a group of cells appeared to precede the bulk of the embryonic tissue, thereby losing contact to the remaining embryo (Figure 3-2 E, F, G). They might be primordial germ cells, which are formed at the yolk facing side of the indentation during late blastoderm stages and are attached to the posterior end of young germ bands in wild type embryos (Ewen-Campen et al. 2013). In germ band stages often only the head appeared to consist of compact tissue while the remaining body tissue appeared to be less dense rather suggesting it to be a loose grouping of cells than an organized structure (Figure 3-2 G). Sometimes the body (except for the head) seemed to be already degraded in the analyzed germ band embryos (3 to 4 dpf), which was consistent with identifying only the head in the majority (~80%) of *dpp*-RNAi end stage phenotypes (Figure 3-2 H; Figure 3-1 K).

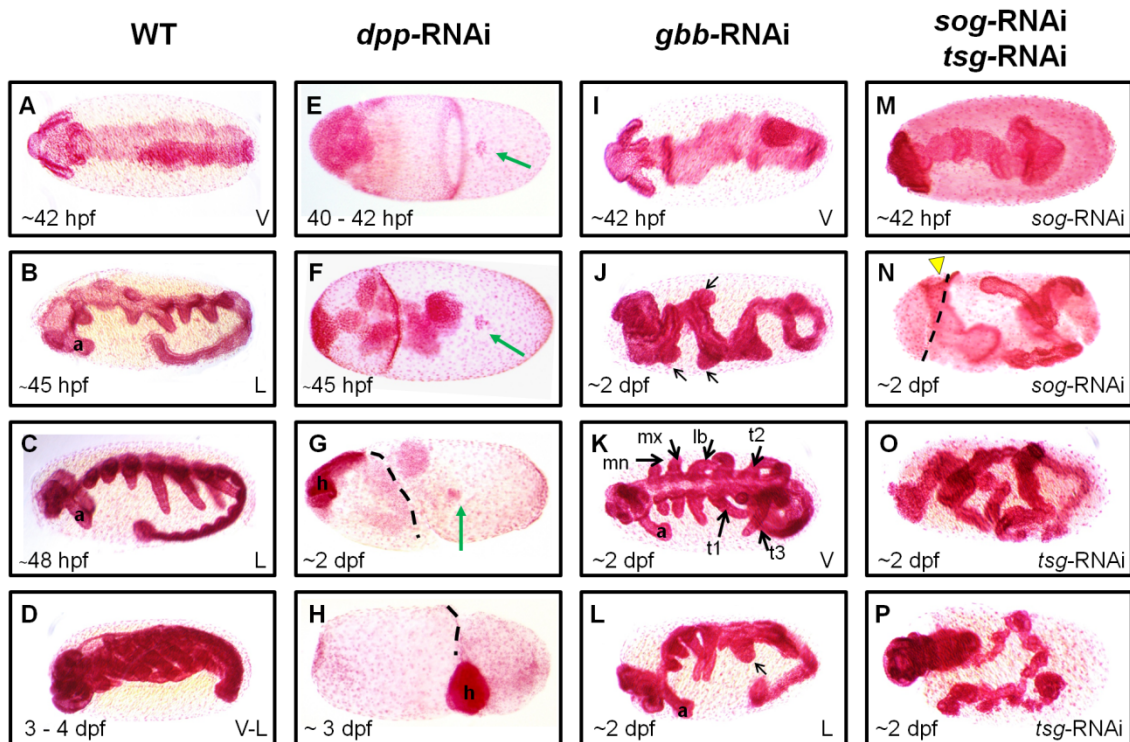


Figure 3-2: Morphological perturbations upon disrupted BMP signaling

The anterior of the embryo is to the left and embryo-ventral is down in lateral views (orientations are indicated in the right bottom corner, if they could be determined). In the left column are WT embryos, shown at successive developmental stages: shortly after anatrepsis (~42 hpf; A), early appendage bud development (~45 hpf; B), advanced appendage development (~48 hpf; C) and shortly before katatrepsis (3 to 4 dpf; D). *dpp*-RNAi

embryos (E-H) formed first accumulations of tissue at the posterior of the eggs (E: the posterior of the egg is at the left) before they formed thin, heavily twisted (F, G) germ bands, which exhibited often widely spaced nuclei (G), and later in development only heads (H). In addition, they were marked by the presence of a group of cells, separated from the remaining germ band (highlighted by green arrows). *gbb*-RNAi embryos (I-L) were misarranged (I-L) and exhibited malformed limbs (highlighted by black arrows without further labels) (J-K). *sog*-RNAi (M-N) and *tsg*-RNAi (O-P) germ bands became thin, long and very twisted and convoluted during germ band elongation (N-P). Constrictions separating the egg into two halves are highlighted by dashed lines in G, H and N (but are also present in F and P, and one is forming in E). The yellow arrowhead in N points towards the invagination site. The approximate age of the embryos is displayed in the left bottom corner. Abbreviations: a: antenna, dpf: days post fertilization, h: head, hpf: hours post fertilization, L: lateral, lb: labial segment, mn: mandibular segment, mx: maxillary segment, tx: thoracic segment x, V: ventral, V-L: ventral-lateral, WT: wild type.

3.1.3 Defective germ band elongation upon impaired BMP signaling

The typical end stage phenotype of *sog*- and *tsg*-RNAi embryos became apparent from anatrepsis onwards. Already during this process the arrangement of the germ band, sometimes even of the invagination site, started to deviate from the wild type. The embryos became longer, thinner and more convoluted during germ band elongation (Figure 3-2 compare A-D with M-P; data not shown). Such a malformation of the germ band was also observed in those *dpp*-RNAi embryos still exhibiting a compact body (Figure 3-2 F). Even *gbb*-RNAi embryos were often slightly misarranged, although only the abdomen of these embryos appeared to be thinner; this part of the embryo was also more strongly twisted than the anterior part (Figure 3-2 I-L). While limbs presumably only formed in weak knockdown phenotypes of *dpp*-, *sog*- and *tsg*-RNAi embryos, they were present in probably all *gbb*-RNAi embryos. However, these limbs were often malformed, misarranged and/or fused, with the more posterior limbs appearing to be more severely affected. Fusion of the limb buds was assumed if these were broader, shorter and only present on one side of the longitudinal body axis (Figure 3-2 J-L).

In summary, disruption of BMP signaling interferes with normal embryogenesis at various points, including morphogenetic movements, germ band formation and limb development.

3.2 BMP signaling appears not to be involved in body segmentation

BMP signaling was reported to influence not only DV patterning but also AP patterning in some vertebrate species (Schier & Talbot 2005; Dale et al. 1992). For example, *bmp2*-depleted, dorsalized zebrafish embryos lack not only ventral but also posterior tissue (Kishimoto et al. 1997). In order to test whether BMP signaling might also influence AP patterning of *O. fasciatus*, segmentation of wild type and several *BMPsc* knockdown embryos was compared. Therefore, Engrailed (En) was monitored by immunohistochemical staining. En is a conserved segmental marker in insects, expressed in the posterior compartment of most segments (Angelini & Kaufman 2005; Liu & Kaufman 2004; Patel et al. 1989). Six En-expressing segments, corresponding to the gnathal and thoracic regions of *O. fasciatus*, are established during the blastoderm stages (Liu & Kaufman 2004). The 11 abdominal segments (of which 10 express En) arise from the posterior growth zone; *i.e.* they can only be detected after the initiation of anatrepsis (Liu & Kaufman 2004).

Up to 13 of 16 En stripes were detected in germ band stage embryos with defective BMP signaling (Figure 3-3 compare A, A' with B-E). It is likely that the lack of the remaining En stripes is due to the age of the embryo, *i.e.* that the respective segments are not formed thus far, or that they were just not detected. The latter might be due to a variable distance of the germ band to the egg surface along the AP axis, as this is known to influence the rate of the color reaction and is particularly relevant after RNAi for several *BMPscs*, especially after *sog*- and *tsg*-RNAi (Figure 3-3 B, C, E). The En stripes appeared to be approximately evenly spaced along the longitudinal body axis in *gbb*-RNAi embryos (Figure 3-3 D). In contrast, *sog*- and *tsg*-RNAi embryos exhibited broader, fuzzier and more widely spaced En stripes in the anterior compared to the abdominal part of the germ band (Figure 3-3 B, C, E). This, together with the observation of heads of all *BMPsc* knockdown embryos being malformed, suggested defects in anterior segment formation. The abnormal morphology of the heads in the analyzed knockdown embryos often became manifested as a smaller size and absent, a reduced number, or malformed head appendages (Figure 3-2 J-K, N-P; Figure 3-3 B, C, E). However, the observed head defects became often only apparent as development progressed. Thus, the heads of young *gbb*-RNAi germ band embryos were still similar in size to wild type embryos (Figure 3-2 I), while they were smaller in later germ band stages (Figure 3-2 J, K). Therefore, the observed abnormalities in head morphology might be, at least partially, secondary effects.

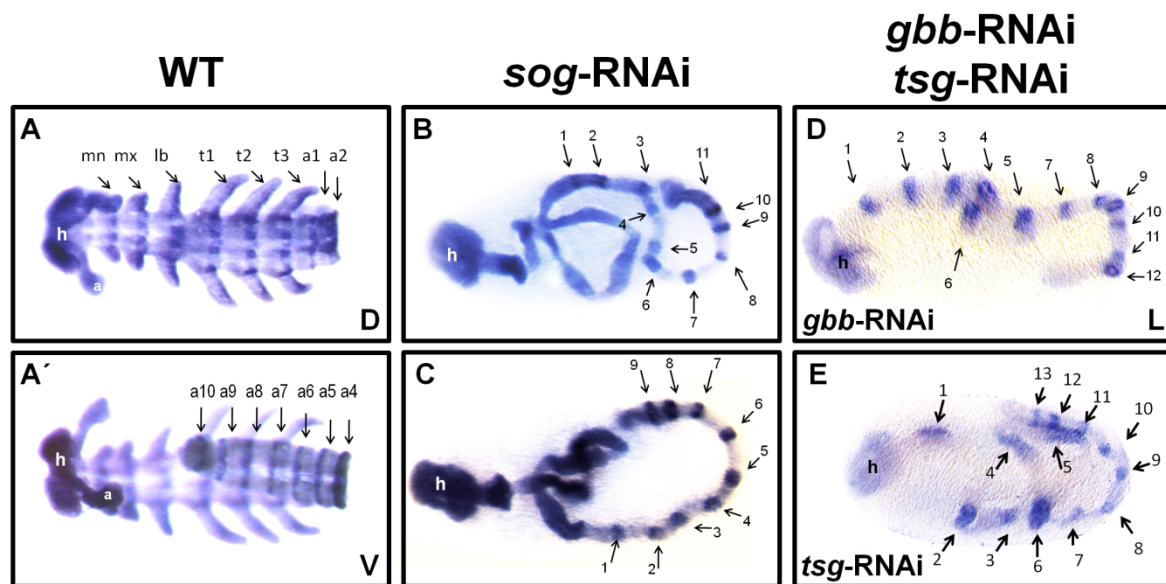


Figure 3-3: Segment number is probably not influenced by BMP signaling

Embryos are orientated with the anterior to the left, and in lateral views with the ventral side down. The view is indicated in the right bottom corner if it was possible to determine. The pictured embryos are between 42 hpf and 50 hpf old. The embryos were stained to detect an En antibody. WT embryos (A, A') express En in 16 segments. 11 or 9 En stripes were detected in the pictured *sog*-RNAi embryos in B and C, respectively. 12 En stripes were detected in the imaged *gbb*-RNAi embryo (D) and 13 in the pictured *tsg*-RNAi embryo (E). The arrows point towards the En stripes. Two views of the same embryo are shown in A and A'. This antibody staining experiment was performed four times. No specific staining was detected in the negative control embryos. Abbreviations: a: antenna, ax: abdominal segment x, En: Engrailed, h: head, hpf: hours post fertilization, L: lateral, lb: labial segment, mn: mandibular segment, mx: maxillary segment, tx: thoracic segment x, V: ventral, WT: wild type.

Furthermore, proper head segmentation was also indicated by wild type-like expression of En during the blastoderm stage. During this stage, mainly four, in one case also all, of six En-expressing segments could be monitored in *gbb*-, *sog*-, and *tsg*-RNAi knockdown embryos (Figure 3-4 B-D; data not shown). Blastoderm *en* expression has been reported to be only detectable shortly before and during anatrepsis and to be of different strength in the distinct blastoderm domains (Liu & Kaufman 2004). Therefore, it is likely that the absence of one or two blastoderm En stripe(s), in most investigated embryos, was rather due to technical issues (stage of fixed embryos and termination of the color reaction) than to a lack of segments. This point of view was supported by the presence of maxillary, mandibular, labial as well as thoracic limb buds (although they were often abnormal) in most *gbb*-RNAi embryos (Figure 3-2 K).

In summary, BMP signaling seemed not to be required for the establishment of segments, although it might influence AP patterning in the head anlage.

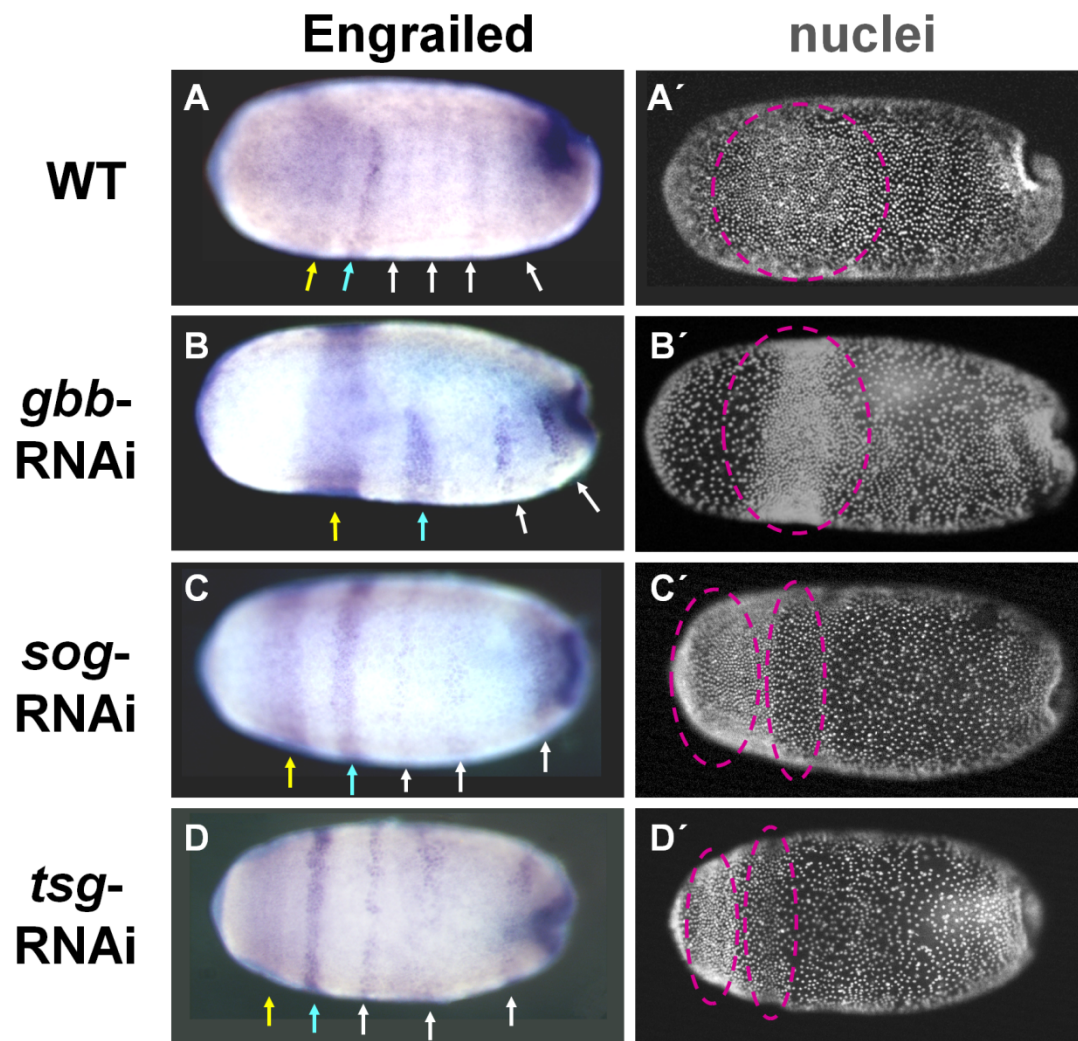


Figure 3-4: Segment number is not altered in blastoderm embryos with disrupted BMP signaling

Anterior of the egg is to the left. The view is always lateral with embryo-ventral down if it could be determined (was possible in A-B). The pictured embryos were about 40 hpf old (at the beginning of anatrepsis). The embryos were stained to detect an En antibody (A-D) and with a SYTOX-green nuclear counterstain (A'-D'). The pictured wild type embryo exhibits four (white and yellow arrows) or five (yellow arrow points to a potentially unspecifically stained domain) of the six blastoderm En stripes (A) and more densely packed cells (pink dashed oval) in the lateral region (A'). The pictured *gbb*-RNAi embryo (B, B') exhibited three to four En stripes (B), and the shown *sog*-RNAi (C, C'), as well as the pictured *tsg*-RNAi embryo (D, D'), four to five En stripes (C, D). All shown knockdown embryos exhibited cell accumulations (pink dashed ovals) in one or more transversal stripe(s). The yellow arrows point towards a possibly unspecifically stained domain (it is broader and less defined than the other stained stripes, and the region corresponds to an area of high cell-density that is often unspecifically stained (Sachs 2009)). The blue arrow points to an En domain, which might correspond to the same segment. This antibody staining experiment was performed four times. No specific staining was detected in the negative control embryos. Abbreviations: En: Engrailed, hpf: hours post fertilization, WT: wild type.

3.3 BMP signaling plays a major role in DV patterning of *Oncopeltus fasciatus*

The probably most conserved function of BMP signaling is its participation in DV patterning (Lall & Patel 2001). One aspect of the En expression pattern already indicated that BMP signaling is required for DV patterning in *O. fasciatus*. Wild type blastoderm embryos express En very strongly in the lateral region, weaker on the ventral side and not in the dorsal region (Figure 3-4 A; Liu & Kaufman 2004). The En expression pattern in *gbb*-RNAi embryos still resembled the wild type one, although the most anterior, possibly unspecifically stained domain appeared to be expanded around the complete circumference (Figure 3-4 B). However, *dpp*-, *sog*-, and *tsg*-RNAi embryos displayed En stripes uniformly expressed around the egg circumference (Figure 3-4 C, D; data not shown). This difference in the En expression pattern was reflected in a different distribution of nuclei in wild type and *BMPsc* knockdown embryos. Nuclei of wild type embryos start to condense in the lateral region of the embryo at the initiation of gastrulation (Figure 1-3 C, D; Figure 3-4 A'; Figure 7-1 A). It seemed that in embryos with disrupted BMP signaling this accumulation of nuclei rather happened in transversal stripes around the complete circumference (Figure 3-4 B', C', D'; Figure 7-1 B). While *gbb*-RNAi embryos exhibited one stripe of closely packed nuclei that still showed DV asymmetry, as it was thicker in the lateral and ventral region compared to the dorsal region, one or more completely DV symmetric stripes were present in *dpp*-, *sog*- and *tsg*-RNAi embryos (Figure 3-4 B', C', D'; Figure 7-1 B). The loss or reduction of DV asymmetry concerning En expression and nuclei distribution indicated that DV polarity of these embryos was reduced or absent.

3.3.1 BMP signaling and DV marker expression in wild type embryos

3.3.1.1 BMP signaling activity is dynamic in *Oncopeltus fasciatus* blastoderm stage embryos

Within insects BMP signaling appears to be especially important for the establishment of dorsal fates. To this end a gradient of nuclear pMad with peak levels at the dorsal side is established in all insects analyzed so far (van der Zee et al. 2006; Goltsev et al. 2007; Rafiqi et al. 2008; Ferguson & Anderson 1992a; Dorfman & Shilo 2001; Özüak 2014). However, the shape and dynamics of this gradient appear to vary across species. For example, in *D. melanogaster* a smooth, but clear pMad gradient, spanning the dorsal 40% of the blastoderm embryo, is transformed into a step-like gradient with extremely high activity only in a thin

longitudinal stripe along the dorsal-most region during the blastoderm stage (Raftery & Sutherland 2003; Dorfman & Shilo 2001; Sutherland et al. 2003). In contrast, the short germ beetle *Tribolium castaneum* establishes a rather smooth and flat nuclear pMad gradient during the blastoderm stage: it spans about 50% of the egg circumference at the anterior, the region of the serosa anlage, and narrows towards the posterior to cover only the dorsal 20% of the egg circumference and broadens again around the posterior pole (van der Zee et al. 2006).

The pMad gradient of *O. fasciatus* is very flat and encompasses the whole egg circumference in early blastoderm stages (~26 hours post fertilization (hpf)), although the signal is clearly weaker in the ventral 50% (Figure 3-5 A, D, G). This asymmetry becomes enhanced with progressing development: pMad can no longer be detected in the ventral half of differentiated blastoderm stage embryos (~30 hpf, posterior indentation is already visible)⁴. Simultaneously, the levels of nuclear pMad become enhanced in the dorsal 50% of the egg, with highest levels in a small transversal stripe dorsally adjacent to the future invagination site (Figure 3-5 B, E, H)⁵. At the beginning of anatrepsis, detectable pMad becomes restricted to the dorsal 40% of the egg circumference. In addition to the posterior domain, which is meanwhile invaginated into the yolk, pMad levels are also slightly elevated in two transversal stripes as well as a connecting lateral stripe in the anterior of the egg (Figure 3-5 C, F, I).

⁴ Blastoderm embryos during gastrulation (*i.e.* when they formed a posterior indentation) are referred to as differentiated or late blastoderm stage embryos (~29-40 hpf).

⁵ In addition, pMad levels appeared to be slightly reduced in some differentiated blastoderm embryos, but as this is variable within this stage it was neglected (during the analysis of phenotypes).

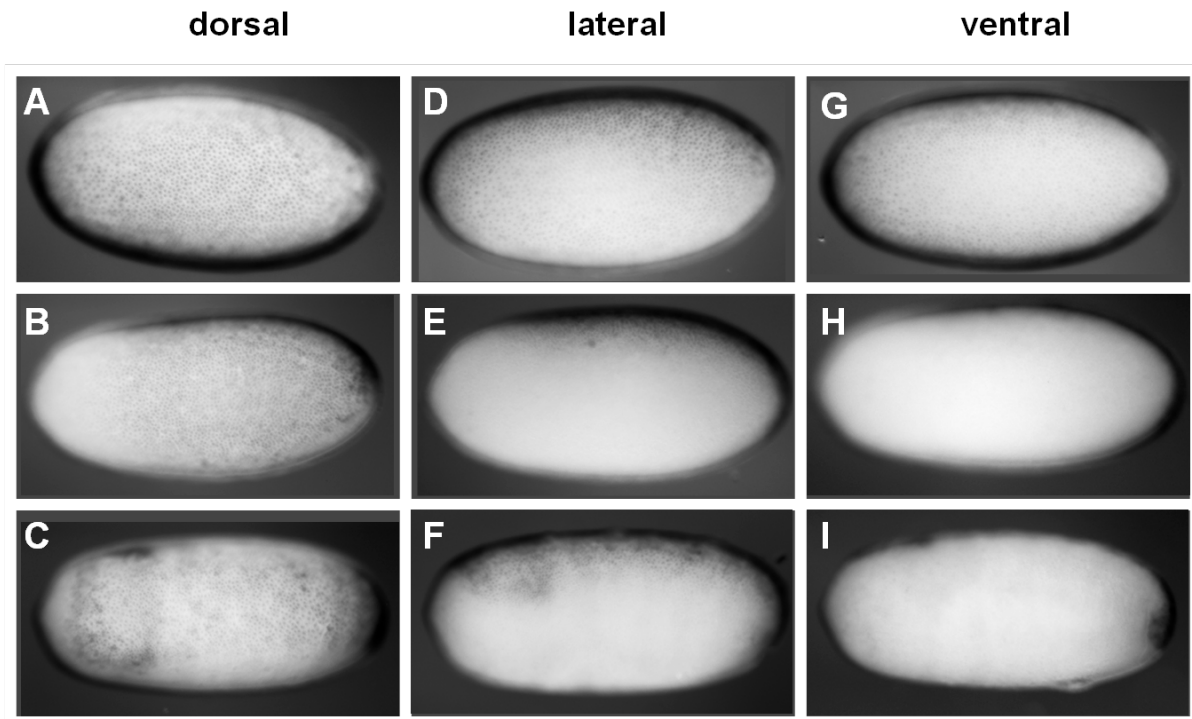


Figure 3-5: pMad distribution in young embryos

Anterior of the egg is to the left. The ventral side is down in lateral views (center column). pMad can be detected in a shallow gradient around 26 hpf (A, D, G) with higher levels on the dorsal (A) compared to the ventral side (G). This asymmetry enhances and around 30 hpf pMad is no longer detectable in the ventral 50% of the egg circumference (B, E, H). At the beginning of anatrepsis (C, F, I) detectable pMad is restricted to the dorsal 40% of the egg circumference (C). pMad was detected by an immunohistochemical staining. Abbreviation: hpf: hours post fertilization.

3.3.1.2 Expression patterns of BMP signaling components in *Oncopeltus fasciatus*

As shown in the previous section, it was possible to demonstrate that BMP signaling activity is stronger in the dorsal, compared to the ventral, region of *O. fasciatus* blastoderm embryos. In addition, the BMP signaling activity gradient changes from a smooth gradient to a rather step-like gradient, similar to *D. melanogaster*, although the domain of high BMP signaling activity is much broader than in *D. melanogaster* (Sutherland et al. 2003; Dorfman & Shilo 2001). However, it remained elusive how this gradient is set up. In *D. melanogaster* expression of the BMP ligand encoding gene *dpp* is restricted to the dorsal region during the blastoderm stage (Jackson & Hoffmann 1994). Also the expression of other components of the BMP signaling pathway, e.g. *tld* and *tsg*, is restricted to the dorsal ectoderm anlage in *D. melanogaster* blastoderm embryos (Shimell et al. 1991; Mason et al. 1994). In contrast, in *O. fasciatus* most of the analyzed BMP signaling components showed no localized expression pattern in blastoderm stage embryos around 26 hpf. It seems that *put*, *sax*, *tld* and *gbb* are

approximately uniformly expressed at low levels at this time (Figure 3-6 C, E-G). *dpp* and *tsg* expression could not be detected by *in situ* hybridization at this stage (Figure 3-6 A, D). The only component of the BMP signaling pathway that was found to have a localized expression at this time of development was *sog* (Figure 3-7 B, F, J). It is expressed at very high levels in the ventral 40% of the posterior 75% of the blastoderm at 26 hpf (Figure 3-7 F). Expression of *sog* becomes enhanced at its dorsal borders and adjacent to its former anterior border an additional domain of weak expression is formed during the differentiated blastoderm stage (Figure 3-7 J). At this time *dpp* expression is detectable in a small transversal stripe just dorsal to the posterior indentation (while *tsg*, *put*, *sax*, *tld* and *gbb* are still approximately uniformly expressed) (Figure 3-6 B, C, E-G; Angelini & Kaufman 2005). During anatrepsis *sog* expression flanks the internalizing mesoderm, *i.e.* it forms a stripe along the midline in the invaginated part of the embryo (data not shown). After anatrepsis localized *sog* expression was no longer detected. In conclusion, expression patterns of *BMPscs* do mainly not reflect the activity pattern of the BMP signaling pathway.

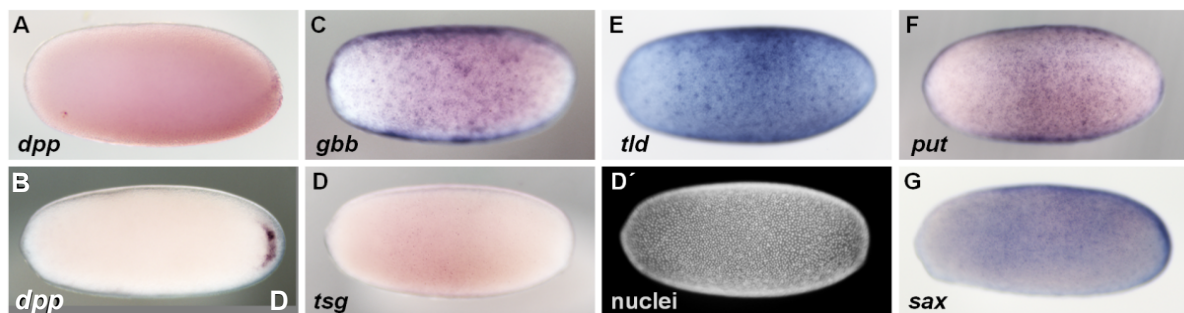


Figure 3-6: Transcripts of BMP signaling components are often not localized during the blastoderm stage Anterior of the egg is to the left. The view is indicated in the right bottom corner, if it was possible to determine. *dpp* expression could not be detected between 26 hpf and 28 hpf (A), but is present in a stripe dorsal to the future invagination site in late blastoderm stages (B). No blastoderm expression of *tsg* (D) could be detected. *gbb* (C), *tld* (E), *put* (F) and *sax* (G) are approximately uniformly expressed during the blastoderm stage. Expression was monitored by ISH. D' displays a nuclear counterstaining of the embryo shown in D. Abbreviations: D: dorsal, hpf: hours post fertilization, ISH: *in situ* hybridization.

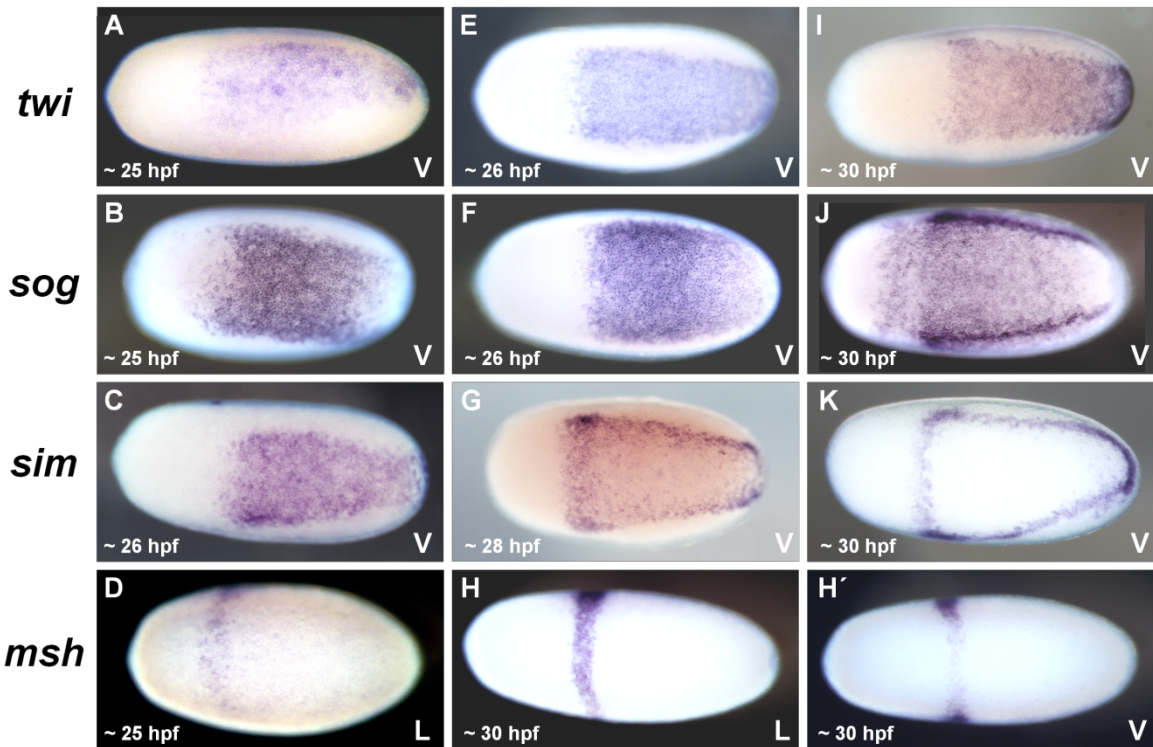


Figure 3-7: Expression of DV markers during the blastoderm stage

Anterior of the egg is to the left. The view is indicated in the right bottom corner. *twi* (A, E, I) starts to be weakly expressed in the ventral 20-30% of the egg circumference of the posterior 75% around 25 hpf (A, embryo is slightly tilted to the lateral side). The expression borders refine and the expression level increases during the next hour(s) (E). Around 30 hpf *twi* starts to be more strongly expressed close to the posterior pole (I). *sog* is expressed in the ventral 40% of the posterior 75% of the egg circumference from 25 hpf onwards (B). *sog* expression refines within the next hour (F) and becomes upregulated at the lateral borders in blastoderm embryos older than 29 hpf (J). Additionally a more anterior domain forms at this stage (J). Expression of *sim* is detectable in the ventral 20-30% of the egg circumference of the posterior 75% around 26 hpf (C), then becomes cleared from the center of its domain (G) until it is only detectable in a ventral, triangle-shaped domain from 29 hpf onwards (K). Transcripts of *msh* are first weakly detected in an anterior, dorsal, transversal stripe, encompassing 50-70% of the egg circumference (D). The expression of *msh* expands around the complete circumference around 29 hpf (H, H'), but is weaker and thinner in the ventral 30% (H'). Expression was monitored by ISH. The approximate age of the pictured embryos is shown in the left bottom corner of each panel. Two views of the same embryo are shown in H and H'. Abbreviations: hpf: hours post fertilization, ISH: *in situ* hybridization, L: lateral, V: ventral.

3.3.1.3 Expression patterns of DV marker genes in *Oncopeltus fasciatus*

In order to understand the role of BMP signaling during DV patterning, the expression of DV marker genes was analyzed in several *BMPsc*-RNAi embryos. Those markers are not expressed in (most of) the anterior 25% of the blastoderm embryo, which also contains the anterior (pregnathal) head anlage (Birkan et al. 2011; Weisbrod et al. 2013; Figure 3-7).

Nevertheless, preliminary data suggested that the DV position of anterior head markers is influenced by BMP signaling (data not shown; 4.2). A subset of DV marker genes might also be not expressed in the pregnathal head anlage in some other insects. For example, *twi* seems not to be expressed in this region in *Nasonia vitripennis* (Buchta et al. 2013). It is known that AP patterning in this area differs from that of the rest of the germ rudiment and is therefore referred to as terminal patterning (Weisbrod et al. 2013). It is conceivable that this also applies to the DV patterning system within the pregnathal head anlage. For simplification the posterior 75% of the blastoderm was considered to represent the complete germ rudiment. Several genes already showed a clearly defined expression pattern in the ventral embryonic region during the blastoderm stage.

One of them is *twi*, which encodes a basic helix loop helix (bHLH) transcription factor with a conserved role in mesoderm specification within insects (Drechsler 2007; Sachs 2009; Buchta et al. 2013; Goltsev et al. 2007; Leptin 1991; Thisse et al. 1987). It starts to be expressed in the ventral 20 to 30% of the germ rudiment from about 25 hpf onwards (Figure 3-7 A). The expression levels, as well as the precision of the borders, become enhanced during the next two hours (Figure 3-7 E). Around 30 hpf the expression is very strong close to the posterior and becomes gradually diminished towards the anterior. Close to the anterior border of its domain, however, *twi* expression is slightly stronger again (Figure 3-7 I; compare also with anatrepsis stage in Figure 3-10 B). During the germ band stage *twi* expression is first maintained in the complete, now internalized, mesoderm, which becomes triangle-shaped in each segment (Figure 3-8 A, D). At approximately 48 hpf, when limb development is already advanced, it becomes restricted to the muscle mesoderm within the limbs (Figure 3-8 G).

sog, whose expression is described in detail in 3.3.1.2 and shown in Figure 3-7 B, F, J, served as a further ventral marker.

Sim is a bHLH transcription factor, which is involved in development of the ventral nerve cord in *D. melanogaster* (Zelzer et al. 1997; Sonnenfeld et al. 1997; Nambu et al. 1990; Nambu et al. 1991). The expression of *sim* resembles *twi* expression between 26 hpf and 29 hpf, *i.e.* during this period it is expressed in the ventral 20 to 30% of the germ rudiment (Figure 3-7 C). Afterwards the expression becomes cleared from the *twi* expression domain and becomes restricted to a thin transversal stripe presumably within the head, and two longitudinal stripes flanking the *twi* domain, probably corresponding to prospective mesectoderm (Figure 3-7 G, K). During the germ band stage it is still present in the ventral-most area of the neuroectoderm, which now corresponds to the ventral midline (Figure 3-8 J).

Genes expressed in the dorsal region of embryos from holometabolous insect species are often not expressed in a similar way in *O. fasciatus*. For example, *u-shaped* (*ush*) is expressed in the dorsal ectoderm anlage in *D. melanogaster* but is not, or weakly and uniformly, expressed in *O. fasciatus* during the blastoderm stage (Fossett et al. 2000; data not shown). An exception is the *muscle specific homeobox* (*msh*) gene, also referred to as *Drop* (*Dr*). It encodes a homeodomain containing transcription factor, which is required for the specification of muscle progenitors in *D. melanogaster* (Jagla et al. 1999; Nose et al. 1998).

Expression of *msh* starts between 24.5 hpf and 27 hpf in *O. fasciatus*. Transcripts of *msh* were first detected in a transversal stripe, presumably located within the head, encompassing the dorsal 50% to 70% of the egg circumference (Figure 3-7 D). The expression level becomes elevated in later blastoderm stages. *msh* is then detectable at high levels in the dorsal 70% of the egg circumference, and at low levels, in a more narrow stripe, in the ventral 30% of the egg circumference (Figure 3-7 H, H'). During the germ band stage *msh* is expressed in a segmental fashion within the dorsal neuroectoderm as well as in the limb muscle mesoderm. Furthermore, it is expressed in the head lobes and antennae (Figure 3-8 C, F).

Several DV marker genes are only appropriate for *O. fasciatus* germ band stage embryos. Among them is *perlecan* (*pcan*), encoding a proteoglycan, *i.e.* an extracellular matrix (ECM) component, which is expressed in two stripes directly flanking the ventral midline in germ band stage embryos (Friedrich et al. 2000; Figure 3-8 B, E).

The high mobility group box (HMBG) transcription factor encoding gene *sox21b* is expressed adjacent and dorsal to *pcan*. The expression of *sox21b* bifurcates in the head and ends in a broad head lobe expression. In addition, it is broadly expressed in the growth zone (Figure 3-8 H; Bowles et al. 2000).

The gene *SoxNeuro* (*SoxN*) encodes a HMBG transcription factor, which is involved in nervous system development in *D. melanogaster*, and is expressed in two rather broad longitudinal stripes, partially overlapping with *msh* in *O. fasciatus*. It is additionally expressed in the head lobes as well as in the growth zone (Figure 3-8 K; data not shown; Buescher et al. 2002).

The secreted heparan sulfate binding protein encoding gene *pentagone* (*pent*) is expressed in segmental dots dorsal to the neuroectodermal *msh* expression domain, *i.e.* presumably in the dorsal, embryonic ectoderm (Vuilleumier et al. 2010; Figure 3-8 I, L). Furthermore, it is expressed in the base of the antennae and in the mandibular segment (Figure 3-8 I, L).

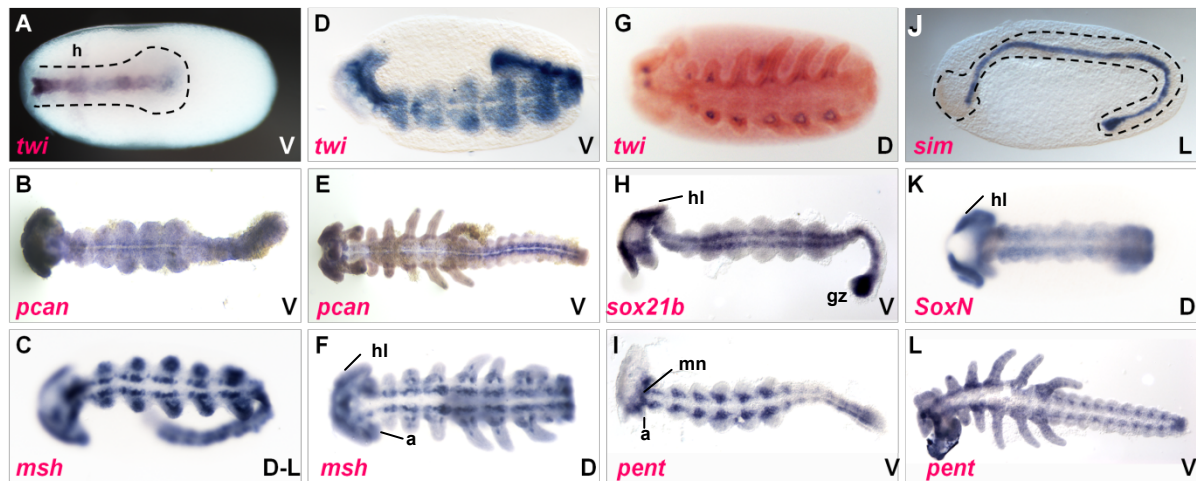


Figure 3-8: Expression of DV markers during the germ band stage

Anterior of the embryo is to the left. The ventral side is down in lateral orientations. The view is indicated in the right bottom corner. *twi* is expressed in the mesoderm during (A) and after anatrepsis (D) until its expression becomes restricted to the muscle mesoderm around 45-48 hpf (G). *sim* is expressed along the ventral midline in germ band stage embryos (J). *pcan* (B, E), *sox21b* (H) and *SoxN* (K) are expressed in two longitudinal stripes flanking the ventral midline during the germ band stage. Expression of *msh* is present in segmental domains within the dorsal neuroectoderm as well as in the muscle mesoderm in germ bands (C, F). *pent* is detected in segmental domains within the ectoderm during the germ band stage (I, L). Expression was monitored by ISH. The dashed lines approximately follow the outline of the germ band (A, J). The approximate position of the not-yet-invaginated head is marked by an h (A). Abbreviations: a: antenna, D: dorsal, D-L: dorsal-lateral, gz: growth zone, hl: head lobe, h: head, hpf: hours post fertilization, ISH: *in situ* hybridization, L: lateral, mn: mandibular segment, V: ventral.

3.3.2 BMP ligands have distinct roles in DV patterning of *Oncopeltus fasciatus*

3.3.2.1 Depletion of the BMP ligand Decapentaplegic leads to strongly ventralized embryos

In animals using BMP signaling for DV patterning, strong phenotypes can be usually obtained by knocking down the ligand encoding gene *dpp/bmp2/4* (van der Zee et al. 2006; Irish & Gelbart 1987; Wharton et al. 1993; Hammerschmidt et al. 1996; Özüak 2014). The depletion of *dpp* in *D. melanogaster*, or of *bmp2* in *Danio rerio*, prevents all BMP signaling activity during DV patterning (Little & Mullins 2009; Dorfman & Shilo 2001; Sutherland et al. 2003). Therefore, it was a reasonable starting point for this study. Indeed, pMad, and thus BMP signaling activity, was absent or strongly reduced in *Of-dpp*-RNAi embryos (Figure 3-9 compare A with B and C). Residual BMP signaling activity was observed in 48% of the

investigated embryos and was assumed to be due to an incomplete knockdown (51 embryos were investigated (N= 51); Figure 3-9 C, C').

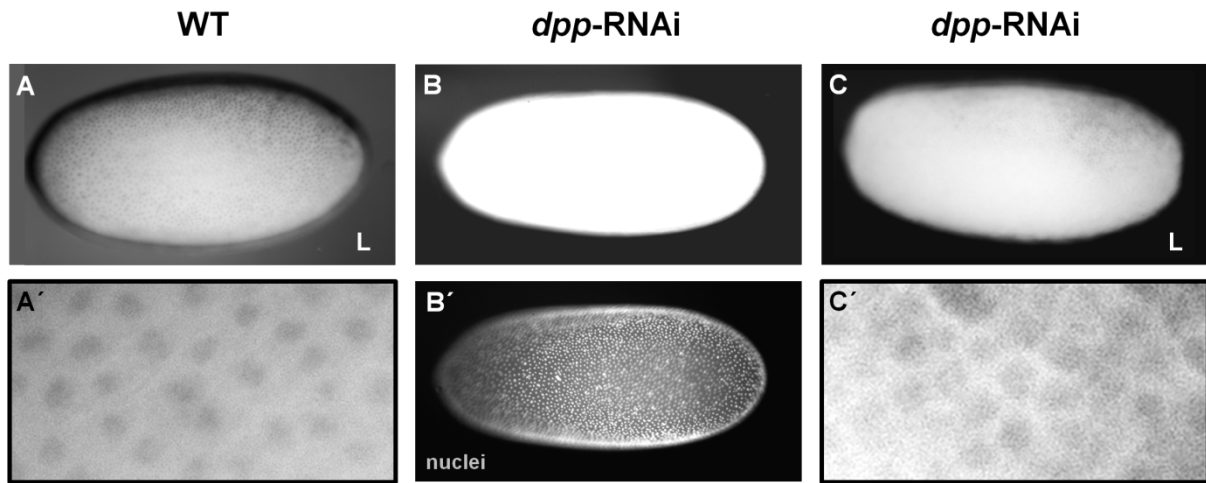


Figure 3-9: *dpp* is required for BMP signaling activity

Anterior of the egg is to the left. The ventral side is down in lateral views. The orientation is indicated in the right bottom corner, if it was possible to determine. Compared to WT (A, A'), pMad was absent (B) or strongly reduced (C) in *dpp*-RNAi embryos. pMad was detected by an immunohistochemical staining. A' and C' show about ten times magnified views from the embryos pictured in A and C, respectively. These are provided as evidence for a nuclear localization and thus specificity of the staining. B' displays a nuclear counterstaining of the embryo shown in B. Abbreviations: L: lateral.

To test if BMP signaling would exert any influence on ventral fates *twi*, *sog* and *sim* expression was monitored in *dpp*-RNAi embryos. *twi* and *sog* appeared to be expanded around the whole circumference in strong knockdown embryos (Table 3-1; Figure 3-10 compare A, B with I, J and C with K). This is consistent with a previous report of expanded *twi* expression upon *dpp* depletion in *O. fasciatus* (Sachs 2009). The early (26 hpf to 29 hpf) *sim*⁶ expression was expanded around the whole circumference, similar to *twi* and *sog* expression, in strong *dpp*-RNAi (Figure 3-10 compare E and M; Table 3-1). However, during the differentiated blastoderm stage the lateral, mesectodermal *sim* expression domain appeared to be lost, while the anterior, ventral domain expanded around the whole circumference in strong *dpp*-RNAi embryos (Figure 3-10 compare F and N; Table 3-2).

In addition to ventral markers, the expression of *msh* was monitored in blastoderm stages. Depletion of *dpp* caused a strong reduction in size and intensity, or even a complete loss of *msh* expression also in late blastoderm stages (Figure 3-10 compare G, H with O, P; Table 3-3).

⁶ During the blastoderm stage it is distinguished between early (26 hpf to 29 hpf) *sim* expression, which is similar to *twi*, and late (>29 hpf) *sim* expression, which no longer overlaps with *twi* expression.

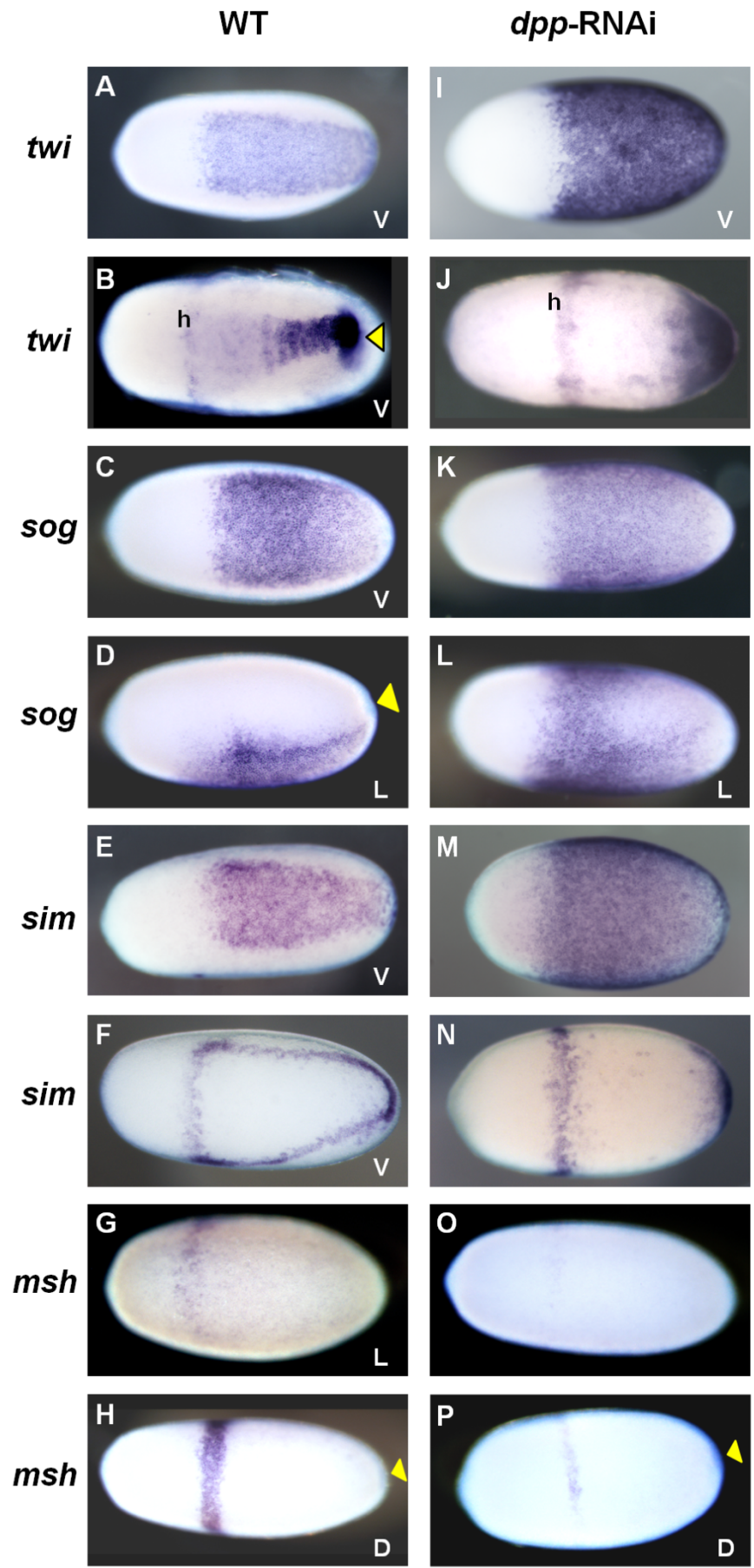


Figure 3-10: *dpp*-RNAi embryos are ventralized

Anterior of the egg is to the left. The ventral side is down in lateral orientations. The view is indicated in the right bottom corner, if it was possible to determine. The expression of *twi* (A, B, I, J), *sog* (C, D, K, L), and the ventrally located expression of *sim* (E, M) was expanded in *dpp*-RNAi embryos (I-M) compared to WT (A-E). The lateral domain of *sim* (N) and a part (P) or the complete *msh* expression domain (O) was lost upon *dpp* knockdown (compare with WT pictured in F-H). Expression was monitored by ISH in blastoderm (A, C-I, K-P; 26-35 hpf) and anatrepsis (B, J) stage embryos. The approximate position of the head is highlighted by an h in anatrepsis stage embryos (B, J). Yellow arrowheads point towards posterior indentations or invagination sites. Abbreviations: D: dorsal, h: head, hpf: hours post fertilization, ISH: *in situ* hybridization, L: lateral, V: ventral, WT: wild type.

Table 3-1: Ventral marker expression is expanded in *dpp*-RNAi blastoderm stage embryos

Expression of the ventral markers *twi*, *sog* and *sim* (only in embryos younger than 29 hpf when *sim* expression completely overlaps *twi* expression) were monitored by ISH in *dpp*-RNAi blastoderm stage embryos. It was completely expanded around the circumference in 73% of the embryos (first and second data column from left), either equally expressed in the entire domain (first data column from left), or with weaker expression levels on one side (central data column). 27% of the investigated blastoderm embryos exhibited only a complete expansion of the anterior part of the domain (right-most column). The number of investigated embryos is given in parentheses: shown as ratio of positive embryos to total sample size. Abbreviations: hpf: hours post fertilization, ISH: *in situ* hybridization.

	Complete expansion, no DV asymmetry	Complete expansion, with DV asymmetry	Only anterior completely expanded
<i>twi</i>	71% (22/31)	29% (9/31)	-
<i>sog</i>	17% (5/29)	14% (4/29)	69% (20/29)
<i>sim</i> (26-29 hpf)	50% (7/14)	50% (7/14)	-
sum	46% (34/74)	27% (20/74)	27% (20/74)

Table 3-2: *sim* expression in late blastoderm and anatrepsis stages of *dpp* knockdown embryos

Expression of *sim* was monitored by ISH in late blastoderm stage *dpp*-RNAi embryos. The ventral, anterior domain of *sim* expression was completely expanded around the circumference in 70% of the embryos (left and central column), either equally expressed in the entire domain (left column), or with weaker expression level on one side (central column). 30% of the investigated blastoderm embryos exhibited *sim* expression along the entire length of the germ rudiment in 50% of the egg circumference, while they exhibited only the transversal, anterior *sim* domain in the other half of the egg circumference (right column). The number of investigated embryos is given in parentheses: shown as ratio of positive embryos to total sample size. Abbreviations: ISH: *in situ* hybridization.

anterior stripe completely expanded, no DV asymmetry	anterior stripe completely expanded, with DV asymmetry	anterior stripe (50%), filled triangle (50%)
60% (24/40)	10% (4/40)	30% (12/40)

Table 3-3: *msh* expression is reduced in late blastoderm and anatrepsis stage *dpp*-RNAi embryos

Expression of *msh* was monitored by ISH in late blastoderm stage *dpp*-RNAi embryos. It was completely absent in 29% of the investigated embryos (left-most column), and reduced in levels as well as in domain size in 54% of the investigated embryos (central columns), either only encompassing less than 50% (second column from left), or between 50 and 70% (third column from left) of the egg circumference. One time the expression level was found to be reduced but equal in a wild type-shaped domain (right-most column). The number of investigated embryos is given in parentheses: shown as ratio of positive embryos to total sample size. Abbreviations: ISH: *in situ* hybridization.

No expression	Weak expression spanning <50%	Weak expression, spanning 50-70%	weak expression all around
29% (4/14)	29% (4/14)	36% (5/14)	7% (1/14)

Expression of *twi* persisted in the entire germ band (now including all present head tissue) except for the presumed germ cells in strong *dpp*-RNAi embryos (Figure 3-11 F; Table 3-4). Consistent with this was the almost complete absence of expression of the ectoderm⁷ markers *sim*, *SoxN*, *msh*⁸ and *pent* in strong *dpp*-RNAi embryos (Figure 3-11 G, H, P, I, J, N, R; Table 3-5). However, the expression of *SoxN* was not abolished in the growth zone, although it was only detectable in embryos exhibiting still a compact, intact germ band, and sometimes *msh* expression was observed in a ring-shaped domain in the head (Figure 3-11 P, I; Table 3-5). It might be that the expression in these domains is not dependent on DV patterning.

Hence, it seemed that strong *dpp* knockdown embryos are completely ventralized and consist (almost) only of mesoderm during the blastoderm as well as the germ band stage.

⁷ In this study ectoderm is used as general term for dorsal and ventral ectoderm.

⁸ In *BMPsc* knockdown embryos without limbs and/or absence of *twi* expression, *msh* served as a ectodermal marker although it is also expressed in the muscle mesoderm (within the limbs) in wild type.

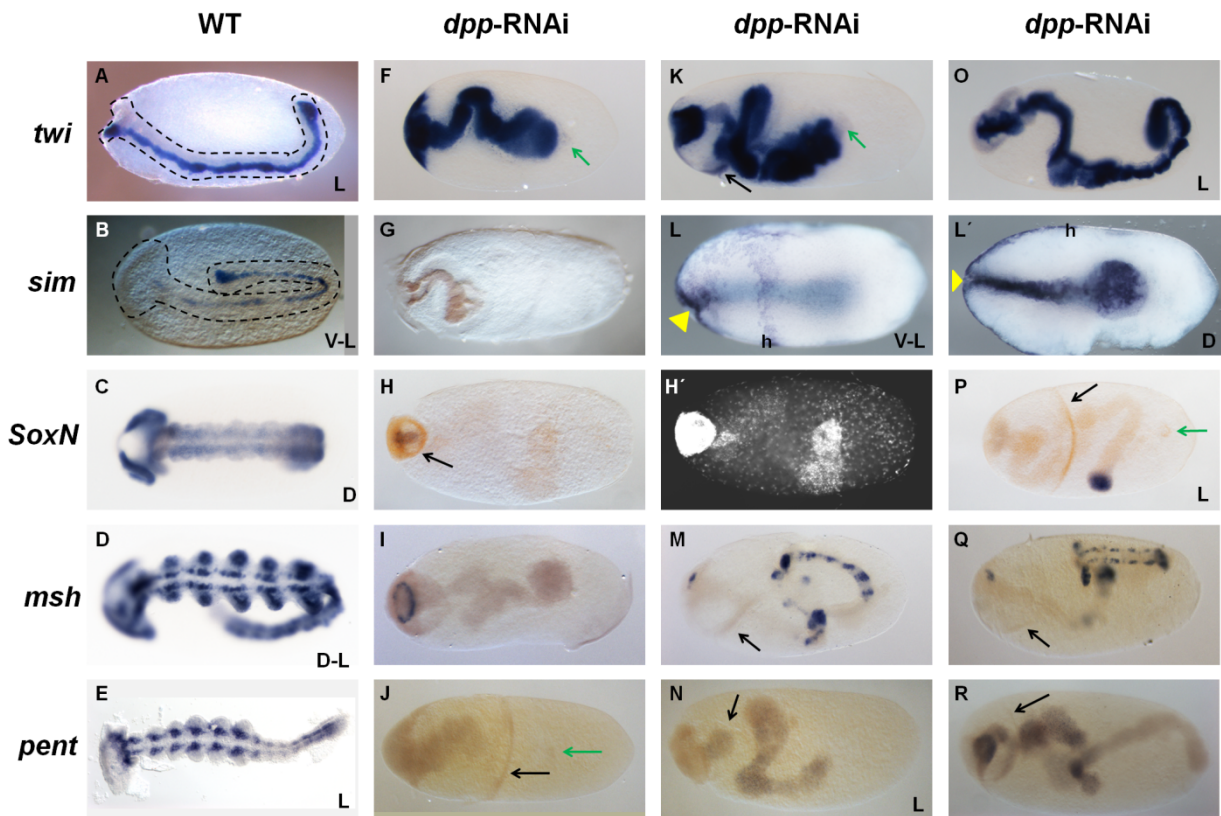


Figure 3-11: *dpp*-RNAi germ band stage embryos are ventralized

Anterior of the embryo is to the left. The ventral side is down in lateral orientations. The view is indicated in the right bottom corner if it was possible to determine. Compared to WT (A) expression of *twi* was completely (F, K) or partially (O) expanded around the egg circumference in *dpp*-RNAi germ band embryos. Except for terminal domains the expression of *sim* (second row from top), *SoxN* (third row from top), *msh* (fourth row from top) and *pent* (bottom row) was lost in most *dpp* knockdown germ band stage embryos (G, H, I, J, N, P, R). Presumed weaker *dpp* knockdown embryos exhibited a partially expanded *sim* expression domain during anatrepsis (L, L') compared to WT (B). In addition, they exhibited dorsally fused (M) or WT-like (Q) ectodermal *msh* expression in their abdomens (compare to WT pictured in D). Expression was monitored by ISH. The approximate position of the head is highlighted by an h in anatrepsis stage embryos (L, L'). Yellow arrowheads point towards posterior invagination sites in L and L'. Black arrows highlight ectopic constrictions, green arrows point to the presumed germ cells of *dpp*-RNAi embryos. Dashed lines approximately follow the outline of the germ band in A and B. The same embryo is shown with intact surface (L) and partially prepped germ band (L'). H' displays a nuclear counterstaining of the embryo shown in H. Abbreviations: D: dorsal, D-L: dorsal-lateral, h: head, ISH: *in situ* hybridization, L: lateral, V-L: ventral-lateral, WT: wild type.

Table 3-4: *twi* expression is expanded in germ band and anatrepsis stage *dpp*-RNAi embryos

Expression of *twi* was monitored by ISH and found in the whole germ band (except the group of separated cells) in 85% of the *dpp*-RNAi germ band and anatrepsis stage embryos (left and central column). In 52% of these (which are 44% of all investigated) embryos *twi* expression appeared to be weak in the maxillary region (central column). 15% of the investigated *dpp*-RNAi germ bands exhibited *twi* expression only in the ventral 50% (right column). The number of investigated embryos is given in parentheses: shown as ratio of positive embryos to total sample size. Abbreviations: ISH: *in situ* hybridization.

complete expansion	Reduced staining in maxillary region	Expanded to 50%
41% (11/27)	44% (12/27)	15% (4/27)

3.3.2.2 The anterior is more sensitive to *dpp* knockdown than the posterior

Embryos with a weak *dpp* knockdown appeared to consist of mesoderm and neuroectoderm (Figure 3-11 L, L', O, M, Q). This was demonstrated by monitoring the expression of *sim* in weak *dpp* knockdown embryos. In these embryos *sim* was expressed in an anterior transversal stripe in the ventral half, whereas it was uniformly expressed in the dorsal half at the onset of gastrulation (Figure 3-11 L; data not shown). This resulted in a broad dorsal expression of *sim* during the germ band stage (Figure 3-11 L').

Analyses of expression patterns of further DV markers not only confirmed weak *dpp* knockdown embryos to be partially ventralized, but revealed a different degree of ventralization along the AP axis in these embryos. In a weakening phenotypic series, blastoderm stage expression of *twi* and *sog* became first weaker in the dorsal region, then retracted from the thorax of the embryo, while it still completely encompassed the head region (data not shown; Figure 3-10 L). The weakest observed blastoderm *dpp* knockdown embryos exhibited a partial expansion of *sog* and *twi* expression along the complete AP axis (data not shown). The germ band stage expression of *twi* was first cleared or weakened close to/in the maxillary segment; with further attenuation of the knockdown effect, it additionally retracted from the dorsal region (Figure 3-11 K, O; Table 3-4). Differences along the longitudinal body axis were most obvious regarding *msh* expression. The expression of *msh* was only detectable in the abdomen, while it was lost in the anterior in germ band stage embryos with a weak *dpp* knockdown. This abdominal *msh* expression was dorsally fused (*i.e.*, expressed in the dorsal region of the germ band,) or wild type-resembling depending on the strength of the knockdown (Figure 3-11 M, Q; Table 3-5).

In summary, the head and thorax appeared to be more sensitive to a *dpp* knockdown than the abdomen.

Table 3-5: Expression of ectodermal markers is reduced in germ band *dpp*-RNAi embryos

Expression of *sim*, *pcan*, *sox21b*, *SoxN*, *msh* and *pent* was monitored by ISH in *dpp*-RNAi germ band stage embryos and found to be completely absent (first data column from left), sometimes with exception of their terminal domains (central columns), in 83% of the investigated embryos. Expression was exclusively detected in the abdomen (further described in this section) in 17% of the investigated *dpp*-RNAi germ band stage embryos (right-most column). The number of investigated embryos is given in parentheses: shown as ratio of positive embryos to total sample size. Abbreviations: ISH: *in situ* hybridization.

	No expression	Except for the head	Except for a posterior domain	Expression in the abdomen
<i>sim</i>	100% (2/2)	-	-	-
<i>pcan</i>	82% (9/11)	-	-	18% (2/11)
<i>sox21b</i>	85% (11/13)	-	-	15% (2/13)
<i>SoxN</i>	100% (18/18)	-	17% (3/18)	-
<i>msh</i>	65% (15/23)	22% (5/23)	-	35% (8/23)
<i>pent</i>	84% (21/25)	-	-	16% (4/25)
sum	83% (76/92)			17% (16/92)

3.3.2.3 Knockdown of *glass bottom boat* leads to lateralization

Full BMP signaling activity requires BMP heterodimers during DV patterning in several bilaterians (Schmid et al. 2000; Little & Mullins 2009; Wang & Ferguson 2005; Saina et al. 2009; Reversade & De Robertis 2005). BMP heterodimers often consist of one BMP2/4 ligand and one ligand of the BMP5/6/7/8 group (Guo & Wu 2012; Little & Mullins 2009). While several representatives of both groups are present in vertebrates, *D. melanogaster* possesses only one homolog of *BMP2/4*, which is *dpp*, and two homologs of BMP5/6/7/8, termed *screw* (*scw*) and *gbb* (Newfeld et al. 1999; Miyazono et al. 2005).

Thus far only transcripts of two BMP ligands, Dpp and Gbb, were found in *O. fasciatus* (Angelini & Kaufman 2005; Sachs 2011; 2.2.8). The knockdown of *gbb* revealed that, like *dpp*, it is required for DV patterning. However, the *gbb* knockdown phenotype remarkably differed from that of *dpp*-RNAi embryos. BMP signaling activity was not significantly reduced, but the gradient appeared to be flattened, *i.e.* the difference in pMad levels on the ventral and dorsal side frequently seemed to be lower than in wild type (Figure 3-12; Table 3-6). The pMad distribution was quite variable in *gbb* knockdown embryos, thus in some embryos the pMad gradient appeared to be very similar to wild type, while in others the DV asymmetry was clearly reduced (Figure 3-12; Table 3-6). pMad was still detected in

the ventral half of *gbb*-RNAi embryos in most late blastoderm stages, while this was impossible to detect in wild type embryos (Figure 3-12 compare D with E; Table 3-6).

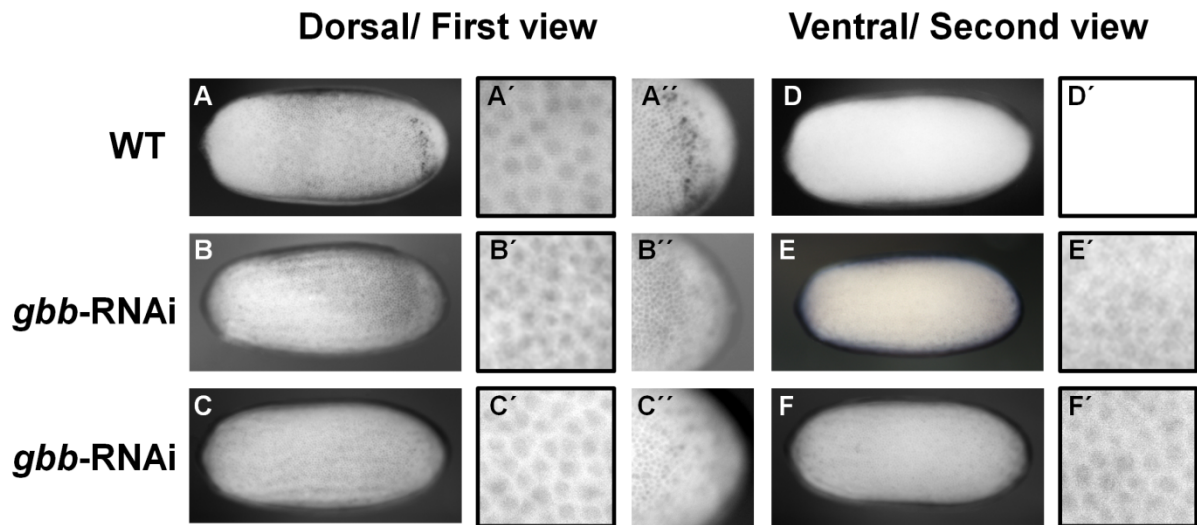


Figure 3-12: pMad distribution is impaired by *gbb*-RNAi

Anterior of the egg is to the left. pMad distribution exhibits stronger DV asymmetry in WT (A, A', A'', D, D') compared to *gbb*-RNAi embryos (B-C'', E-F'). Around 30 hpf pMad is no longer detectable on the ventral side in WT (D, D'), while this was still possible in *gbb*-RNAi embryos (E, E'). The degree of residual pMad DV asymmetry varied and was often clear (B, E), but rarely it was also not detectable (C, F). pMad was detected by an immunohistochemical staining. In one row different views and magnifications of one embryo are shown. . Either a dorsal and ventral view or, if the staining exhibited no DV asymmetry, from two opposing sides. A', B', C', D', E' and F' show ten times magnified views from the embryo pictures in A, B, C, D, E and F, respectively. A'', B'' and C'' display magnifications of the posterior poles of embryo-pictures shown in A, B and C, respectively. Abbreviations: DV: dorsal-ventral, hpf: hours post fertilization, WT: wild type.

Table 3-6: *gbb*-RNAi causes a flattened pMad gradient

Distribution of pMad was similar to wild type in 44% of the investigated *gbb*-RNAi embryos (first data column from left) of which 88% (39% of all, 71% of investigated uniform blastoderm stage embryos) were rather young blastoderm stage embryos (~26-29 hpf). 54% of the investigated *gbb*-RNAi embryos (central data column) exhibited a clearly reduced DV asymmetry of pMad distribution compared to wild type, *i.e.* pMad was detected in the ventral nuclei during late blastoderm stages, or at least in 80% of the egg circumference in anatrepsis stage embryos. 3% of the investigated embryos exhibited no detectable DV asymmetry of pMad (right-most column). Black bars separate the uniform blastoderm (26-29 hpf), differentiated blastoderm and anatrepsis stage embryos. The last three rows of the differentiated blastoderm section specify posterior defects of the embryos in the top row of this section: it was distinguished between enhancement of pMad around the posterior pole comparable to wild type (fifth row from top), its absence (sixth row from top), or a weakening instead of enhancement of pMad close to the posterior pole (seventh row from top). The frequency of the phenotype indicated in the top row is given relative to the sum of all 39 *gbb*-RNAi embryos in which pMad distribution was investigated and, in squared brackets, to the sum of the embryos analyzed in the respective stage. The number of investigated embryos is given in parentheses: shown as ratio of positive embryos to total sample size. Abbreviations: diff bl: differentiated blastoderm stage, DV: dorsal-ventral, hpf: hours post fertilization, WT: wild type.

	WT-like DV asymmetry	Weaker DV asymmetry	No DV asymmetry
sum	44% (17/39)	54% (21/39)	3% (1/39)
Blastoderm ~26-29 hpf [only 26-29 hpf regarded]	39% (15/39) [71% (15/21)]	13% (5/39) [24% (5/21)]	3% (1/39) [5% (1/21)]
Differentiated blastoderm [only diff bl regarded]	5% (2/39) [13% (2/15)]	33% (13/39) [87% (13/15)]	-
With posterior enhancement [only diff bl regarded]	-	[7% (1/15)]	-
Without posterior enhancement [only diff bl regarded]	[13% (2/15)]	[40% (6/15)]	-
Posterior weakening [only diff bl regarded]	-	[40% (6/15)]	-
Anatrepsis [only anatrepsis stage regarded]	-	8% (3/39) [100% (3/3)]	-

Consistent with this difference in pMad distribution between *dpp* and *gbb* knockdown embryos are the different consequences of both knockdowns for the embryonic fate map. The expression of *twi* as well as *sim* was either completely absent or strongly reduced in levels in *gbb*-RNAi blastoderm embryos between 26 hpf and 29 hpf (Figure 3-13 compare A with H,

O, compare E with L; Table 3-7). Interestingly, the drastic reduction in levels of early (26 hpf to 29 hpf) *sim* and *twi* expression was found to be accompanied by a dorsal expansion of the expression domain, encompassing about 40% to 70% of the egg circumference, if expression was still detectable (Figure 3-13 H, L; Table 3-7). During late blastoderm and anatrepsis stages, *sim* was still expressed in this domain, albeit with clearly higher expression levels (Figure 3-13 compare F with Q, M, M'; N=27). The expression levels were usually similar to wild type at these stages, except for rare cases that exhibited slightly reduced *sim* expression levels (11%, N=27; Figure 3-13 Q). In contrast, the levels of *sog* expression never appeared to be significantly altered in *gbb*-RNAi blastoderm stage embryos. Instead, the degree of dorsal expansion of *sog* expression was variable. It was typically only partially expanded in the complete germ rudiment, encompassing 50% to 70% of the egg circumference (95%, N=43; Figure 3-13 compare C, D with J, K, K'; Table 3-8). However, occasionally (5%, N=43) the anterior part of the *sog* expression domain was completely expanded around the circumference (Figure 3-13 P; Table 3-8). Consistent with this, in 90% (N=10) of the investigated embryos the ventral domain of *msh* was expanded, at the expense of the dorsal domain, to encompass approximately 60% of the egg circumference, while in 10% (N=10) the DV asymmetry of *msh* was entirely lost (Figure 3-13 compare G with N, N'; data not shown).

All these results suggest that *gbb*-RNAi embryos are lateralized, with an expansion of neuroectoderm and mesectoderm at the expense of the mesoderm and the dorsal ectoderm. Embryos with an almost complete expansion of *sog* might have lost the complete dorsal ectoderm, while it might have been only reduced in embryos with a less drastic expansion of *sog* (Figure 3-13 J, P). Similarly, the complete loss of early *sim* and *twi* expression indicated a total absence of the mesoderm, while the expansion of early *sim* and *twi*, accompanied by a strong reduction in levels, could reflect an expansion of the *sim* and *twi* expression border region in 26 hpf to 29 hpf old blastoderm stages (Figure 3-13 H, L, O). Hence, the quality of the lateralization was variable in *gbb* knockdown embryos.

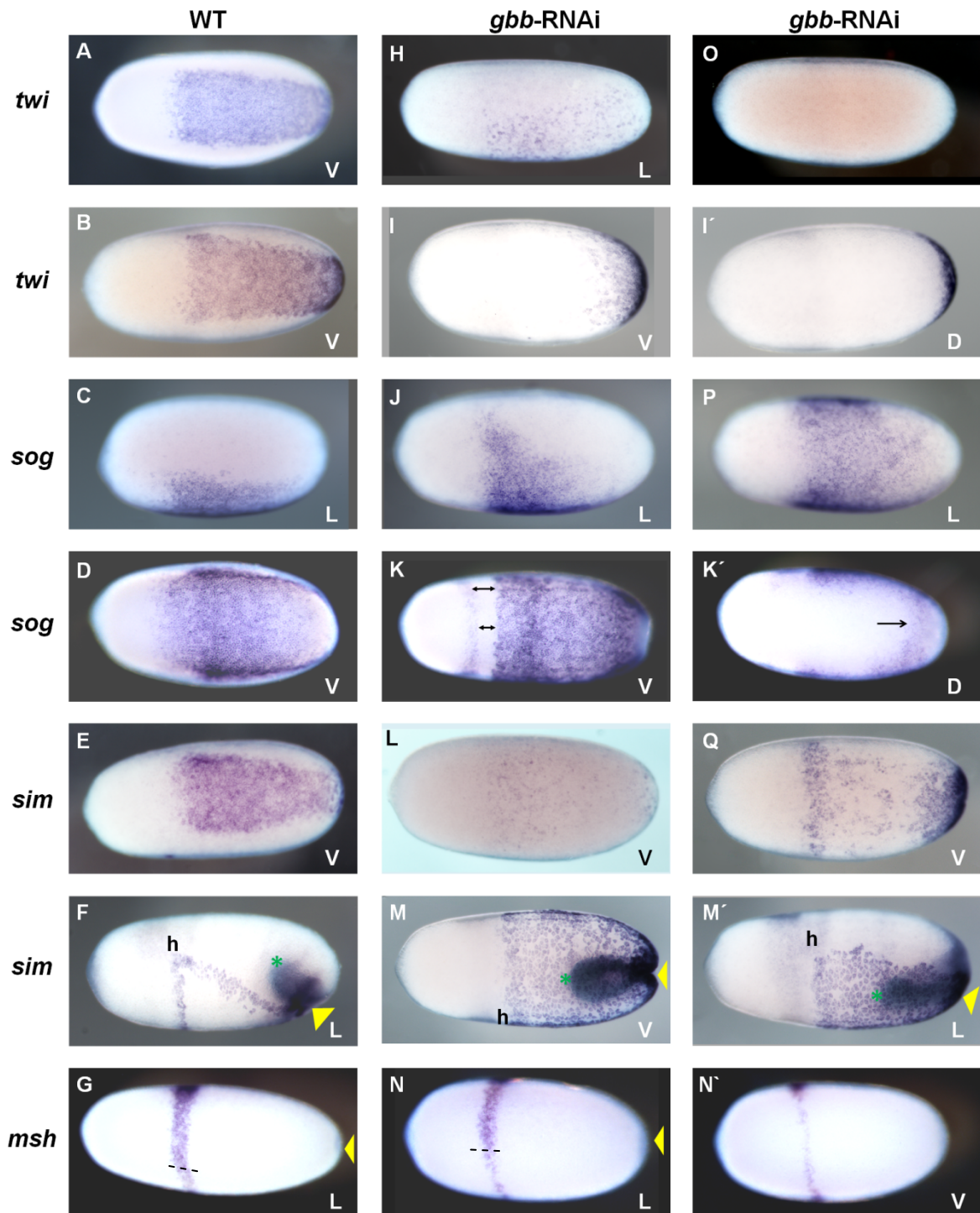


Figure 3-13: Expression of DV marker genes is altered in *gbb*-RNAi blastoderm embryos

Anterior of the egg is to the left. The ventral side is down in lateral orientations. The view is indicated in the right bottom corner. Compared to WT (A-E) the expression of *twi* (A, H, O) and *sim* (E, L) was absent (O) or strongly reduced in levels but expanded in domain size (H, L) in 26-29 hpf old *gbb*-RNAi embryos. In older blastoderm embryos (>29 hpf) *twi* expression was expanded around the posterior pole in *gbb*-RNAi embryos (I, I' compared to WT shown in B). While the expression of *sim* is excluded from the *twi* domain in late blastoderm and anatrepsis WT embryos (F) it persisted in this region in late blastoderm (Q) and anatrepsis stage (M, M') *gbb*-RNAi embryos. The expression of *sog* was expanded in *gbb*-RNAi embryos (J-K', P) compared to WT (C, D). In late blastoderm *gbb*-RNAi embryos it was often completely expanded only close to the posterior pole

(highlighted by the arrow in K') and the anterior domain was separated from the remaining expression domain and its dorsal ends were tilted anterior ward (K compare arrow width). The ventral expression domain of *msh* was slightly expanded in *gbb*-RNAi (N, N') relative to WT (G) embryos. The approximate position of the head is highlighted by an h in anatrepsis stage embryos (F, M, M'). The expression patterns were monitored by ISH. Yellow arrowheads point towards posterior invagination sites. Green asterisks mark the position of the posterior end of the germ rudiment within the yolk. The dashed line marks the approximate border between the dorsal and ventral *msh* domain in G and N. Abbreviations: D: dorsal, h: head, hpf: hours post fertilization, ISH: *in situ* hybridization, L: lateral, V: ventral, WT: wild type.

Table 3-7: mesodermal marker expression is reduced in uniform blastoderm *gbb*-RNAi embryos

Expression of *twi* and *sim* was monitored by ISH in *gbb*-RNAi 26-29 hpf old blastoderm embryos and found to be absent (first data column from left) in 63% of the investigated embryos, or strongly reduced in 37% of the investigated embryos, with (right-most column) or without (central data column) a dorsal-ventral expansion of the domain to about 40 to 70% of the egg circumference. The numbers of investigated embryos are given in parentheses: shown as ratio of positive embryos to total sample size. Abbreviations: hpf: hours post fertilization, ISH: *in situ* hybridization.

	No expression	Strongly reduced expression levels, Normal domain size	Strongly reduced expression levels, Expanded domain (40-70%)
<i>twi</i>	70% (45/64)	5% (3/64)	25% (16/64)
<i>sim</i>	-	57% (4/7)	43% (3/7)
sum	63% (45/71)	10% (7/71)	27% (19/71)

Table 3-8: *sog* expression is expanded in blastoderm stages of *gbb*-RNAi

Expression of *sog* was monitored by ISH in *gbb*-RNAi blastoderm stage embryos and found to be completely expanded in the anterior region of the germ rudiment (first data column from left) or partially expanded in the complete germ rudiment (second data column from left). The 12 investigated *gbb*-RNAi blastoderm stage embryos, older than 29 hpf (bottom row) were further specified: it was distinguished whether they exhibited a separated anterior domain (right-most column) and whether the dorsal ends of this anterior domain were bent towards anterior (right-most column: squared brackets) and whether they also exhibited a complete expansion only close to the posterior pole (third data column from left). The frequency of the phenotype indicated in the top row is given relative to the sum of embryos analyzed in the respective stage. The number of investigated embryos is given in parentheses: shown as ratio of positive embryos to total sample size. Abbreviations: hpf: hours post fertilization, ISH: *in situ* hybridization.

	Strong expansion (anteriorly completely)	Partial expansion (50-70%)	Complete expansion around the posterior pole	Anterior domain separated [& oblique]
26-29 hpf	7% (2/31)	94% (29/31)	-	-
29 hpf +	-	100% (12/12)	42% (5/12)	100% (12/12) [42% (5/12)]

3.3.2.4 The consequences of *gbb* knockdown differ along the AP axis

The phenotype of *gbb*-RNAi embryos changed with progressing development. While in blastoderm embryos from 26 hpf to 29 hpf lateralization was observed along the complete AP axis (3.3.2.3), this appeared not to apply to late blastoderm embryos. These exhibited expression of *twi*, which was expanded around the complete circumference and elevated in levels compared to wild type, but only in a region very close to the posterior pole (100%, N=35). In contrast, *twi* levels were still reduced (43%, N=35) or absent (57%, N=35) and never expanded around the complete circumference in more anterior regions of those embryos (Figure 3-13 I, I'; data not shown).

Consistent with this was a reduction of pMad around the posterior pole in most late blastoderm stage *gbb*-RNAi embryos (87%, N=15; Table 3-6; Figure 3-12 compare A'' with B''). Thus, the enhancement of BMP signaling activity, which is present dorsal to the posterior indentation around 30 hpf in wild type, was either lacking (47%, N=15; Table 3-6; data not shown), or the pMad levels around the posterior pole appeared to be even weaker than in the more anterior dorsal region (Figure 3-12 B''; 40%, N=15; Table 3-6).

In addition, the expression of *sog* was also often expanded around the posterior pole in late blastoderm stages (Figure 3-13 K'; Table 3-8). A further peculiarity of late blastoderm *sog* expression was that the anterior domain was thinner than in wild type, separated from the remaining domain, and its ends were tilted towards the anterior pole (Figure 3-13 K; Table 3-8).

The observed differences along the AP axis became also frequently apparent during the germ band stage. Thus, only *sim* expression was equally expanded along the complete AP axis in all investigated *gbb* knockdown embryos (Figure 3-14 compare B with E, H, K; N=8), although it might have been separated into two domains in rare cases (Figure 3-14 K). In contrast, *msh* expression was only seldom fused dorsally along the complete AP axis (Figure 3-14 compare C with I, I'; Table 3-9). In most analyzed *gbb*-RNAi germ band embryos the two neuroectodermal *msh* domains were only fused in the abdomen of the embryo, while *msh* expression was often similar to wild type in the anterior part (Figure 3-14 F; Table 3-9). The morphology also frequently was more wild type-like in the anterior compared to the posterior part (Figure 3-14 F; Figure 3-2 J-L; 3.1.3). The most prominent differences along the AP axis were found for germ band stage *twi* expression: although *twi* expression was detected along the complete length of the embryo, it differed not only in levels and domain size but also in the pattern along the AP axis: in the anterior part of the embryo (~ head and thorax) *twi* expression was strongest at its dorsal margins and sometimes even split into two domains (as

expression in center of the *twi* domain was very weak or lost), while *twi* was broadly expressed at homogenous high levels in the abdomen (Figure 3-14 compare A with D, G, J; Table 3-9). It appeared that there was no strict border between the two parts, but that *twi* expression became rather gradually, albeit not smoothly, stronger towards the abdomen (Figure 3-14 D). Hence, in most *gbb*-RNAi embryos the posterior became ventralized, while the anterior remained lateralized, albeit tending to (partially) regain mesodermal fate from anatrepsis stages onwards.

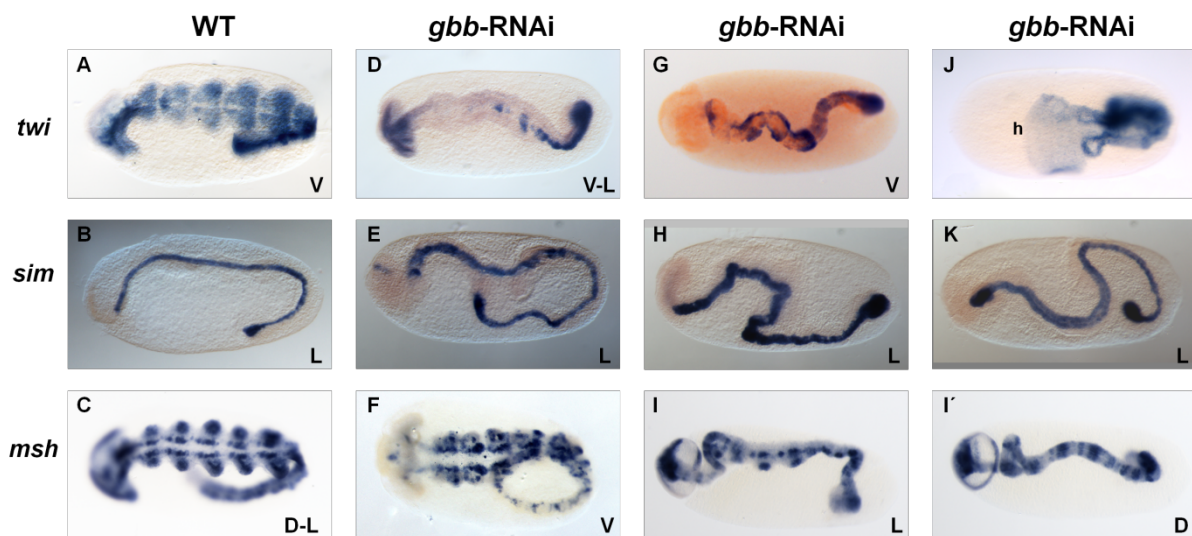


Figure 3-14: Expression of DV marker genes is altered in *gbb*-RNAi germ band embryos

Anterior of the embryo is to the left. The ventral side is down in lateral orientations. The view is indicated in the right bottom corner (uncertain for embryo pictured in J). Compared to WT (A) expression of *twi* was reduced (G, J) or almost absent (D) in the anterior part of *gbb*-RNAi germ band (D, G) and anatrepsis (J) embryos. In addition, *twi* expression was usually stronger at the lateral margins than in the central part of its domain from which it was sometimes completely absent in the anterior part of these knockdown embryos (D, G, J). In contrast, it was expanded in the abdomen of the same embryos (D, G, J). The expression of *sim* was expanded in *gbb*-RNAi germ band stage embryos (E, H, K) compared to WT (B). The expression of *msh* was often similar to WT (C) in the anterior of *gbb*-RNAi germ band embryos, while it was dorsally fused in the abdomen (F); rarely it was fused on the dorsal side in the complete *gbb*-RNAi germ band embryo (I, I'). Expression was monitored by ISH. The approximate position of the not-yet-invaginated head is highlighted by an h in anatrepsis stage embryos (J). Germ band stage embryos were 42 hpf to 50 hpf old. Abbreviations: D: dorsal, D-L: dorsal-lateral, DV: dorsal-ventral, h: head, hpf: hours post fertilization, ISH: *in situ* hybridization, L: lateral, V: ventral, V-L: ventral-lateral, WT: wild type.

Table 3-9: Expression of DV marker genes exhibits differences along the AP axis in *gbb*-RNAi germ band stage embryos

Expression of *twi*, *pcan*, *sox21b*, *msh* and *pent* was monitored by ISH in *gbb*-RNAi germ band stage embryos and found to exhibit differences along the AP axis in 64% of the investigated embryos (second to tenth row from top): in the anterior part of the germ band (approximately corresponding to head and thorax) the expression was, in difference to WT, stronger at the dorsal margins of the expression domain, or even only present in this region, compared to the central part of the expression domain (third row from top). Other embryos exhibited a dorsally shifted expression domain (fourth row from top), or a WT-like expression (fifth row from top) in the anterior part of the germ band. The same embryos were distinguished with regard to their posterior expression patterns (sixth to ninth row from top): embryos exhibited expanded expression domains, compared to WT (sixth row from top), or wild type-resembling expression (seventh row from top), or dorsal fusion of in WT separated domains (eighth row from top), or the expression was lost in the abdomen (ninth row from top). 37% of the investigated *gbb*-RNAi germ band stage embryos did not exhibit differences with regard to expression patterns along the AP axis (twelfth to fifteenth row from top). The frequency of the phenotype indicated in the top row is given relative to the sum of all analyzed embryos. The number of investigated embryos is given in parentheses: shown as ratio of positive embryos to total sample size. Abbreviations: AP: anterior posterior, DV: dorsal-ventral, ISH: *in situ* hybridization, mdl: midline, WT: wild type.

		<i>twi</i>	<i>pcan</i>	<i>sox21b</i>	<i>msh</i>	<i>pent</i>	
A N T E R I O R	No expression	-	-	-	-	-	1
	Weaker expression, margins stronger/split domain	94% (29/31)	-	-	-	-	2
	Shifted dorsally	-	-	-	26% (3+2/19)	-	3
	Wild type-like expression	-	-	-	47% (9/19)	46% (6/13)	4
P O S T E R I O R	<i>Expanded expression in the abdomen</i>	74% (23/31)	-	-	-	-	5
	<i>Wild type-like expression in the abdomen</i>	19% (6/31)	-	-	-	-	6
	<i>Dorsally fused expression in the abdomen</i>	-	-	-	63% (12/19)	-	7
	<i>No expression in the abdomen</i>	-	-	-	11% (2/19)	46% (6/13)	8
Sum (differences along AP axis)		94% (29/31)	0% (0/3)	0% (0/8)	74% (14/19)	46% (6/13)	9
64% (49/74) exhibited differences along the AP axis, 37% (25/74) exhibited no differences along the AP axis							10
Wild type like [larger distance to mdl]		3% (1/31)	[100% (3/3)]	100% (8/8)	21% (4/19)	54% (7/13)	11
Split domain		3% (1/31)			-		12
Dorsally fused expression		-			5% (1/19)		13
Sum (equal along AP axis)		6% (2/31)	100% (3/3)	100% (8/8)	26% (5/19)	54% (7/13)	14
							15

3.3.3 BMP receptors are required for a proper BMP signal transduction

3.3.3.1 Knockdown of *punt* causes a *dpp* knockdown-resembling DV phenotype

BMP type II receptors are essential for BMP signal transduction (Miyazono et al. 2005). Only one type II BMP receptor, termed Punt (Put), is required during blastoderm DV patterning in *D. melanogaster* (Little & Mullins 2006). Hence, loss of *put* or *dpp* causes similar DV phenotypes in *D. melanogaster* (Letsou et al. 1995).

One presumed ortholog of *put* was found in *O. fasciatus* (2.2.8). The knockdown of *Of-put* via parental RNAi (pRNAi) resulted in reduced fertility as well as strong ventralization, similar to the knockdown of *dpp*. Thus, *twi* was expanded in *put*-RNAi embryos (Figure 3-15 compare A, B with C, D), albeit mainly not around the complete egg circumference (64%, N=14; Figure 3-15 D). This confirmed the DV phenotype of *dpp*-RNAi embryos to be specific to disrupted TGF β signaling. In addition, it suggests *Of-put* to be the only BMP type II receptor that participates in blastoderm DV patterning.

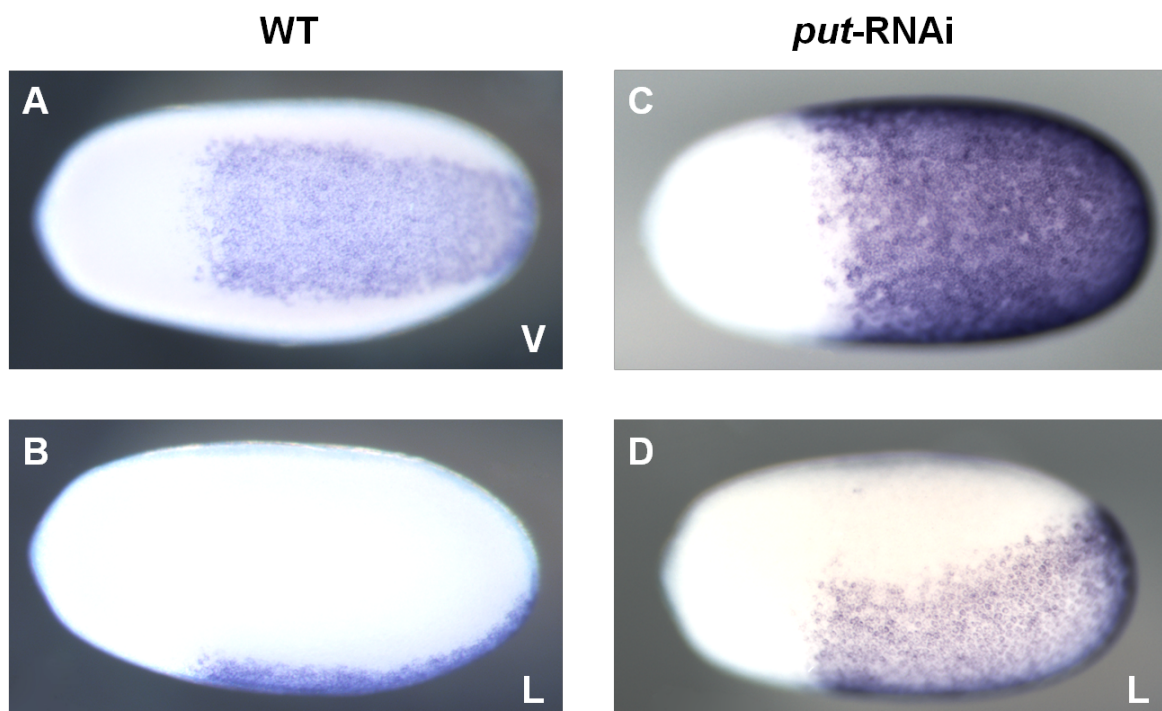


Figure 3-15: *put*-RNAi embryos are ventralized

Anterior of the egg is to the left. The ventral side is down in lateral orientations (B, D). The view is indicated in the right bottom corner, if it was possible to determine. The expression of *twi* was completely (C) or partially (D) expanded around the egg circumference in *put*-RNAi embryos (compared with WT pictured in A, B). Expression was monitored by ISH. Abbreviations: ISH: *in situ* hybridization, L: lateral, V: ventral, WT: wild type.

3.3.3.2 Knockdown of *thickveins* causes ventralization

The tetrameric BMP receptor complexes consist of both type I and type II BMP receptors (Miyazono et al. 2005). BMP type I receptors are responsible for the specificity of BMP signaling regarding ligands as well as for the interaction with intracellular adaptors (Miyazono et al. 2005; Little & Mullins 2006). *D. melanogaster* possesses two BMP type I receptors, Saxophone (Sax) and Thickveins (Tkv), which are involved in DV patterning (Little & Mullins, 2006). Tkv was reported to preferentially bind Dpp (Neul & Ferguson 1998; Nguyen et al. 1998). The depletion of *tkv* leads in *D. melanogaster* to a DV phenotype resembling that caused by loss of *dpp*, indicating a complete prevention of BMP signaling activity (Nellen et al. 1994).

Unfortunately, the pRNAi mediated knockdown of *tkv* led to a massive impairment of fertility in *O. fasciatus*. Therefore, it was hardly possible to collect fertilized eggs from the injected females. However, the DV fate map of embryos from one egg batch could be analyzed. These embryos all exhibited a partially ventralized fate map, *i.e.* *twi* and early *sim* were both dorsally expanded and encompassed approximately 60% of the egg circumference (data not shown; Figure 3-16). It is conceivable that the sterility effect prevented obtaining of complete knockdown embryos. Hence, *tkv* is required for proper BMP signaling during DV patterning and its depletion might even entirely prevent BMP signaling activity in *O. fasciatus*.

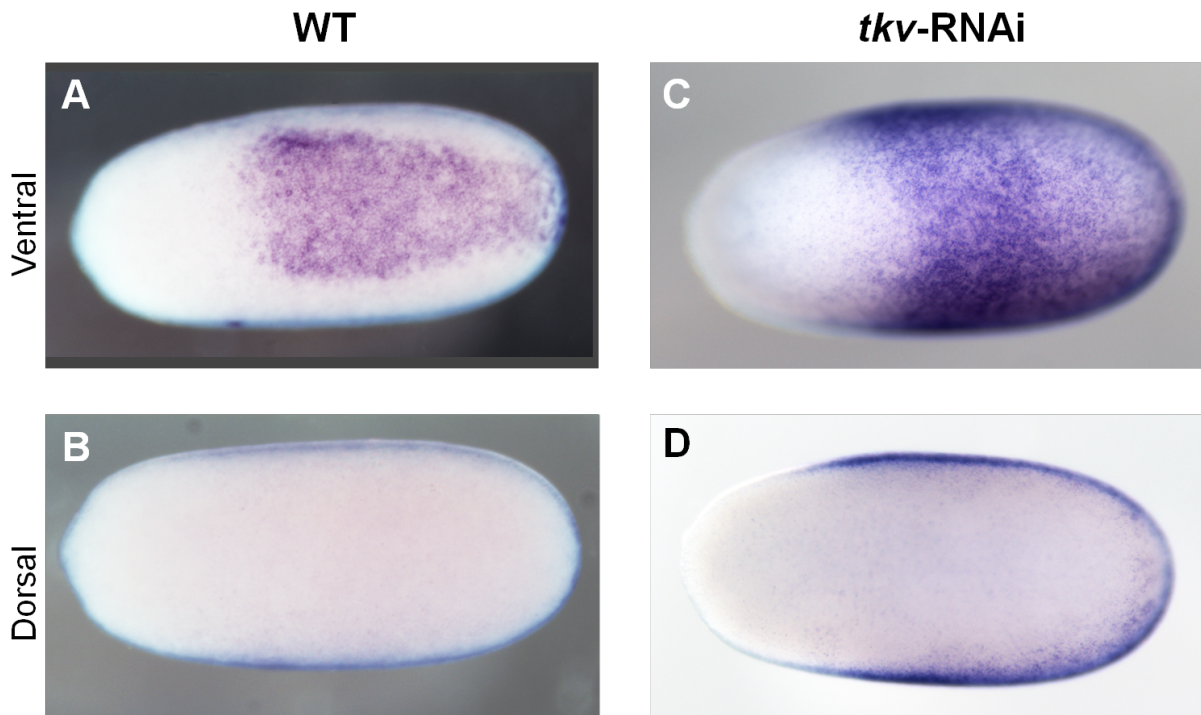


Figure 3-16: *tkv*-RNAi embryos are ventralized

Anterior of the egg is to the left. The view is indicated at the left side. The expression of *sim* was expanded in *tkv*-RNAi embryos (C, D) compared to WT (A, B). Two different views of the same embryo are shown in A, B and C, D, respectively. Expression was monitored by ISH. Abbreviations: ISH: *in situ* hybridization, WT: wild type.

3.3.3.3 Knockdown of *saxophone* causes ventralization

In addition to *Of-tkv*, a presumed ortholog of *sax* was identified in *O. fasciatus* (2.2.8). The depletion of *sax* resulted in ventralized embryos. *twi* (100%, N=32), *sog* (100%, N=16) and early *sim* (100%, N=34) expression was expanded in *sax*-RNAi blastoderm embryos (Figure 3-17 compare A-C with E-G'; data not shown; N=82). Sometimes *sog* expression was completely expanded in the anterior region of the germ rudiment (although the expression in the dorsal region was clearly weaker compared to ventral) (31%, N=16; Figure 3-17 F, F'). However, *sax*-RNAi embryos were, at least mainly, partially ventralized as *twi* (100%, N=32) and early *sim* (100%, N=34) expression always and *sog* (69%, N=16) expression usually encompassed only 50 to 70% of the egg circumference (Figure 3-17 E, E', G, G'; data not shown). Consistent with this was a shift of the lateral, mesectodermal domain of *sim* towards the dorsal side (this domain was typically found in the middle of the egg circumference) accompanied by a dorsal expansion of the ventral, anterior *sim* domain in late blastoderm stage *sax*-RNAi embryos (100%, N=14; Figure 3-17 compare D with H, H'). In contrast to *sog* and *twi* expression, the lateral, mesectodermal *sim* expression appeared to be not, or only very slightly, expanded (100%, N=14; Figure 3-17 H'). These results indicate that *sax*-RNAi blastoderm stage embryos are ventralized, with expanded mesoderm and neuroectoderm, except for the mesectodermal region, at the expense of the prospective dorsal ectoderm.

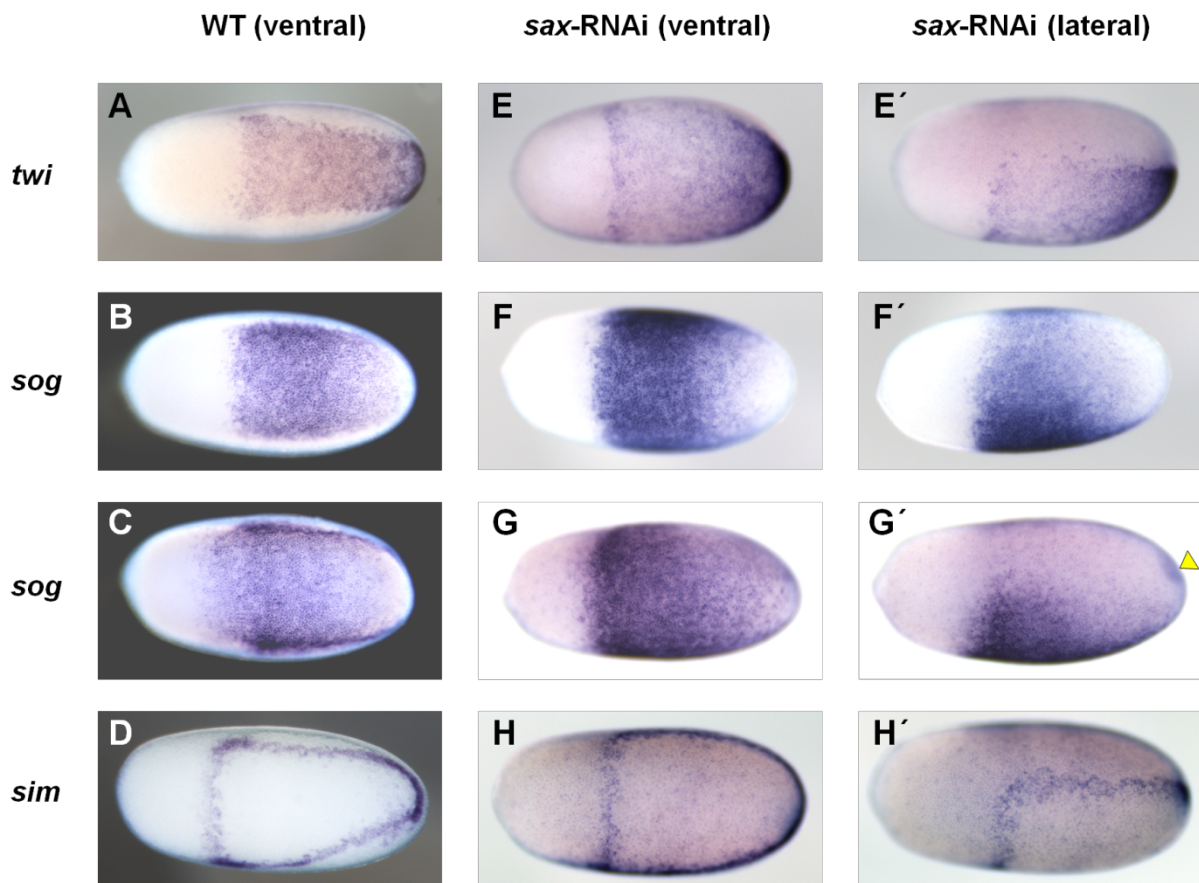


Figure 3-17: *sax*-RNAi blastoderm embryos are ventralized

Anterior of the egg is to the left. The ventral side is down in lateral orientations (right column). The central column displays ventral views of the embryos shown in the right column. The view is indicated on top of the columns. The expression of *twi* (A, E, E') and *sog* (B, C, F-G'), and the ventral, anterior expression domain of *sim* (D, H, H') was expanded in *sax*-RNAi embryos (E-H') compared to WT (A-D). The lateral, mesectodermal domain of *sim* was dorsally shifted upon knockdown of *sax* (H, H'). Expression was monitored by ISH. A yellow arrowhead points towards the posterior indentation in G'. Abbreviations: ISH: *in situ* hybridization, WT: wild type.

3.3.3.4 Partial recovery of DV marker expression in *sax*-RNAi germ band stage embryos

Since it seems that the DV phenotypes differ sometimes between the blastoderm and the germ band stage embryos, the expression of DV markers was also monitored in *sax*-RNAi germ band stage embryos. Surprisingly, expression of *twi* and other DV marker genes appeared to be quite similar to wild type at this stage, despite an abnormal morphology (95%, N=39; Figure 3-18). Thus, for example, *twi* expression seemed not to be (Figure 3-18 compare A with E), or to be maybe slightly (compare Figure 3-8 G with Figure 3-18 I) expanded (100%, N=11). Furthermore, *sim* expression was mainly indistinguishable from wild type (92%, N=13; Figure 3-18 compare B with F). Even in one severely morphologically disturbed

embryo, which consisted only of a heavily convoluted, thin tube and a malformed head, *sim* expression was still localized to the midline, although it was less defined and appeared to be spotty (Figure 3-18 J). The expression of *pcan* showed minor perturbations, since the two longitudinal stripes were in parts of the embryo transformed into rings (33%, N=3; Figure 3-18 compare C with K), or appeared to be wild type-like in germ band stage *sax*-RNAi embryos (67%, N=3; Figure 3-18 G). Similarly, no significant differences between wild type (Figure 3-18 D; Figure 3-8 C, F) and *sax*-RNAi embryos (Figure 3-18 H, L) were observed regarding ectodermal *msh* expression during germ band stages (100%, N=12). These results suggested that *sax* knockdown embryos reconstituted normal DV patterning during germ band stages. Indeed, about 55% of the knockdown embryos hatched. However, approximately 40% of *sax*-RNAi embryos developed an eversion end stage phenotype, resembling *gbb*-RNAi (~15%; Figure 3-1 C, D) or weak *dpp*-RNAi (~25%; Figure 3-1 F) embryos. Furthermore, the morphology of most *sax*-RNAi germ band stage embryos appeared to be severely affected. The morphological defects comprised shifted invagination sites (Figure 3-18 E), an unorganized arrangement of the germ band, especially the abdomen (Figure 3-18 E, G, I, J, L), disordered or lacking appendages and appendage buds (Figure 3-18 I, L), head malformations (Figure 3-18 E, J, K, L) and (compared to wild type) thinner germ bands (Figure 3-18 E-G, J-L). Therefore, a complete recovery of DV patterning to the wild type state in *sax*-RNAi germ band stage embryos was unlikely to apply to all of the investigated *sax*-RNAi embryos. Furthermore, dorsal fates, which could not be monitored, could have been more severely affected than ventral fates in *sax*-RNAi embryos. It is conceivable that only embryos with an incomplete knockdown could recover to wild type state. Additionally, one has to consider that it is more difficult to compare expression patterns in germ band stages than in blastoderm stages, especially if the morphology of the germ bands is not equal. Therefore, slight differences in expression patterns might not have been discovered in *sax*-RNAi germ band stages.

In summary, the DV pattern of *sax*-RNAi embryos might become more similar to wild type during the transition from blastoderm to germ band stages.

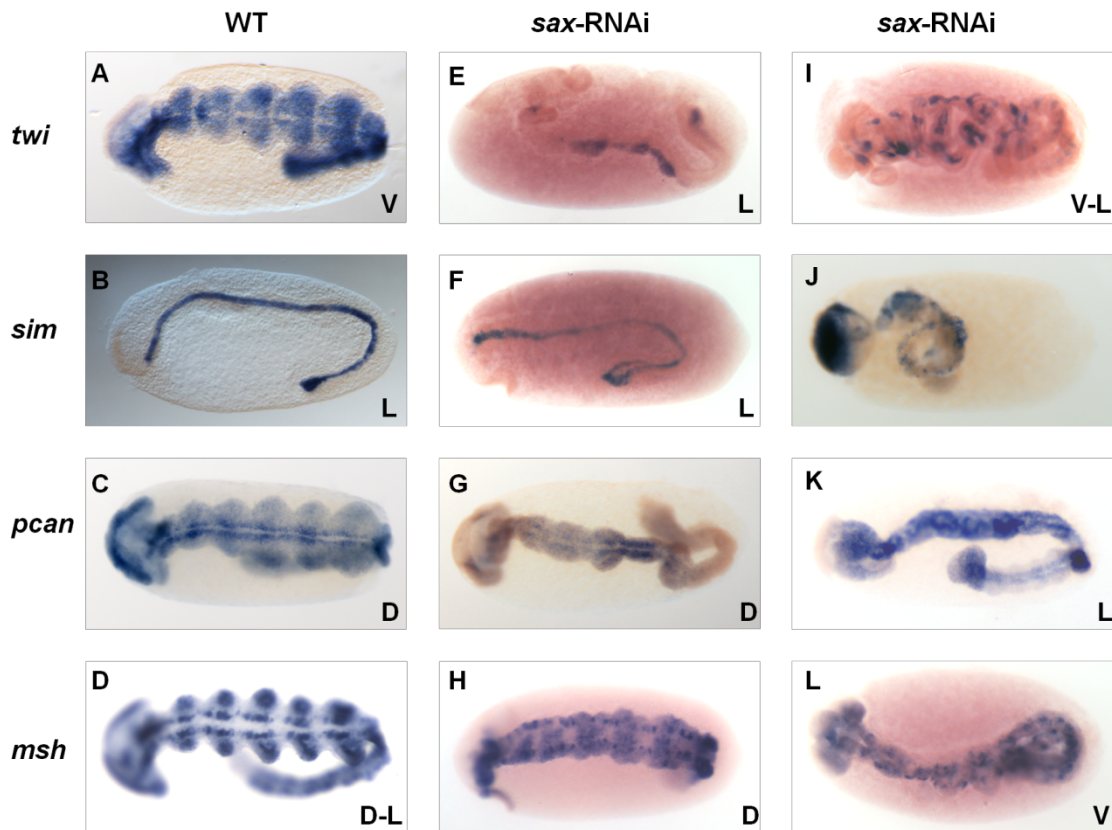


Figure 3-18: partial recovery of DV marker expression in *sax*-RNAi germ band embryos

Anterior of the embryo is to the left. The ventral side is down in lateral orientations. The view is indicated in the right bottom corner. The expression of *twi* (top row), *sim* (second row from top), *pcan* (third row from top) and *msh* (bottom row) was similar in *sax*-RNAi (E-L) and WT (A-D) germ band stage embryos. Expression was monitored by ISH. Germ band stage embryos were 42 hpf to 50 hpf old. Abbreviations: D: dorsal, D-L: dorsal-lateral, hpf: hours post fertilization, ISH: *in situ* hybridization, L: lateral, V: ventral, V-L: ventral-lateral, WT: wild type.

3.3.4 Extracellular modulators strongly influence BMP signaling activity during DV patterning

3.3.4.1 Ventral fates require protection from BMP signaling by Twisted gastrulation and Short gastrulation

The expression patterns of *BMPscs* and the location of BMP signaling activity frequently exhibit remarkable differences during DV patterning (van der Zee et al. 2006; Lapraz et al. 2009; Kuo & Weisblat 2011). For example, the expression of some BMP signaling components is restricted to dorsal areas of the germ rudiment in *D. melanogaster* (Jackson & Hoffmann 1994; Shimell et al. 1991; Mason et al. 1994). Thus, *dpp* is uniformly expressed in

the dorsal region (Jackson & Hoffmann 1994; Arora et al. 1994). Nevertheless, BMP signaling activity is not only restricted to the dorsal 40% of the egg circumference, but forms a steep gradient with extremely high activity only in a very narrow stripe along the dorsal midline (Dorfman & Shilo 2001). These observations can be explained by the action of extracellular BMP modulators. One, which seems to be especially important for the localization of BMP signaling activity, is Short gastrulation (Sog). In contrast to *dpp* the localization of *sog* expression is decisive for the BMP signaling activity pattern (van der Zee et al. 2006; Goltsev et al. 2007; Lapraz et al. 2009; Lynch et al. 2006; Saina et al. 2009). For instance, ectopic *sog* expression can induce the formation of a second DV axis in *Xenopus* embryos (Sasai et al. 1994). Sog is a powerful BMP antagonist in many animals (van der Zee et al. 2006; Lapraz et al. 2009; Little & Mullins 2006; Lowe et al. 2006; Akiyama-Oda & Oda 2006; Francois et al. 1994; Biehs et al. 1996; Schmidt et al. 1995). It prevents BMP signaling by ligand sequestering (Little & Mullins 2006; Marqués et al. 1997; Piccolo et al. 1996; Ross et al. 2001; Shimmi & O'Connor 2003; Xie & Fisher 2005). BMP signaling is completely inhibited in the region of *sog* expression and is strongly impaired in adjacent areas, as Sog is a mobile, diffusible, secreted protein (Marqués et al. 1997; Piccolo et al. 1996; Sasai et al. 1994). For the efficient binding of BMP ligands, it needs to form complexes with Tsg (Shimmi & O'Connor 2003; Ross et al. 2001).

Expression of *sog* is ventrally localized in *O. fasciatus* blastoderm stage embryos (Figure 3-7 B, F, J). Therefore, a knockdown of *sog* or *tsg* should cause ventrally elevated BMP signaling activity.

Indeed, all investigated *tsg* and *sog* knockdown embryos exhibited elevated ventral pMad levels (Figure 3-19; Figure 3-20; Table 3-10). In addition, the dorsal, posterior domain of high pMad levels present in late blastoderm wild type embryos is not formed in the same manner in *sog*-RNAi and *tsg*-RNAi embryos (Figure 3-19 compare A'' with G'' and H''; Figure 3-20 compare A'' with B''). Furthermore, the DV asymmetry of pMad distribution was strongly reduced after *tsg*-RNAi and was not detectable in 49% (N=72) and only slightly developed in 51% (N=72) of the investigated embryos (Figure 3-20; Table 3-10). However, a clear DV asymmetry of pMad was still detectable in 55% (N=112) of the analyzed *sog*-RNAi embryos, although it was clearly reduced compared to wild type and always also detectable on the ventral side (Figure 3-19 compare A, F with B, G and D, I with E, J; Table 3-10). This observed DV asymmetry is likely due to an incomplete *sog* knockdown, as even in most (85%, N=32) offspring from females injected with almost 40 µg of *sog* dsRNA (4 to 80-fold more dsRNA than injected for other experiments), weak *sog* expression was still ventrally

detected by *in situ* hybridization (Figure 3-21 F). The failure to produce a complete *sog* knockdown might reflect the high expression levels of *sog*. In all *in situ* hybridization experiments the first visible signal in blastoderm stage wild type embryos was that of *sog* probes. For example, it developed always about five times faster than that of *twi* probes during blastoderm stages.

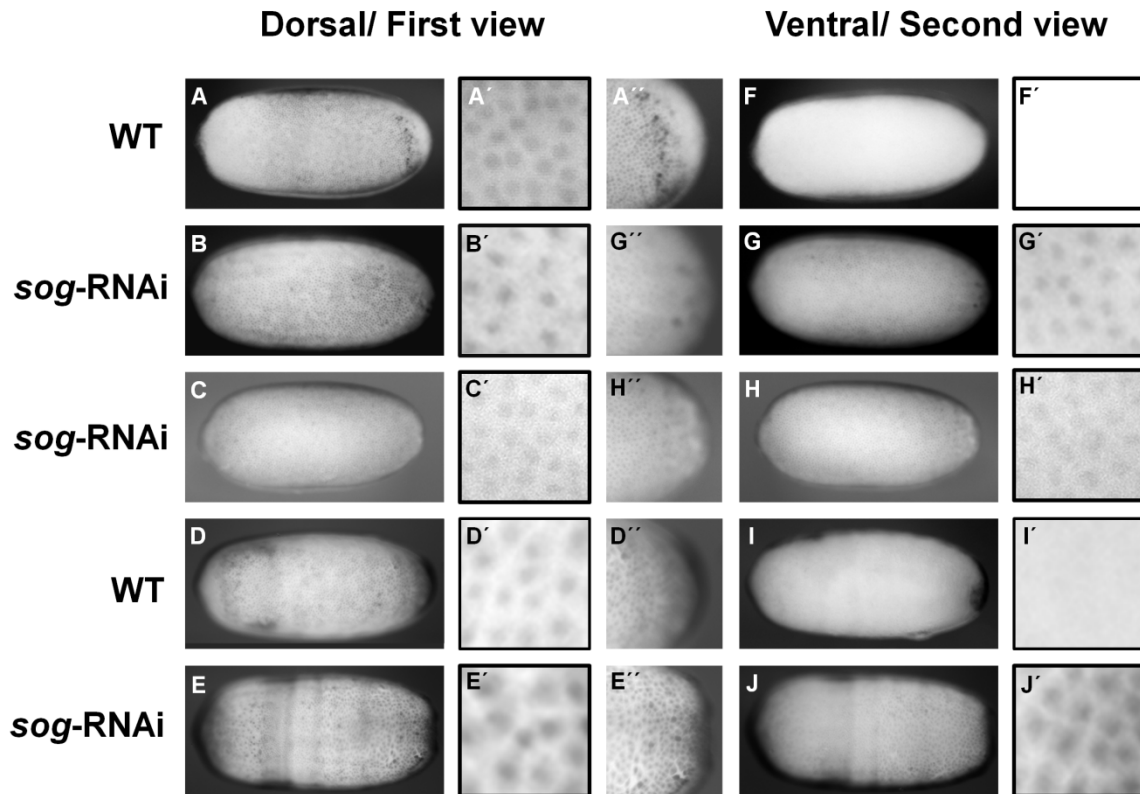


Figure 3-19: pMad gradient formation is disrupted in *sog*-RNAi embryos

Anterior of the egg is to the left. pMad distribution exhibits stronger DV asymmetry in WT (A, A', A'', D, D', D'', F, F', I, I') compared to *sog*-RNAi embryos (B-C', E-E'', G-H'', J-J'). Around 30 hpf pMad is no longer detectable on the ventral side in WT (F, F'), while this is still possible in *sog*-RNAi embryos (G, G'), although pMad distribution was often clearly asymmetric (B, G, E, J) and only rarely completely symmetric (C, H). In addition, the dorsal, posterior domain of high pMad levels present in late blastoderm stages in WT (A, A'') is not formed in the same manner in *sog*-RNAi embryos: only a few speckled spots of enhanced pMad levels close to the posterior pole were observed in these embryos (G, G'', H, H''). At the beginning of anatrepsis pMad was still detected on the ventral side in *sog* knockdown embryos (J, J'), while it is in WT only detected in the dorsal 40% of the egg circumference at this stage (D-D'', I, I'). pMad was detected by an immunohistochemical staining. In one row different views and magnifications of one embryo are shown. Either a dorsal and ventral view or, if the staining exhibited no DV asymmetry, from two opposing sides. A', B', C', D', E', F', G', H', I' and J' show about ten times magnified views from the embryos pictured in A, B, C, D, E, F, G, H, I and J, respectively. A'', D'', E'', G'', and H'' display magnifications of the posterior poles of the embryos shown in A, D, E, G and H, respectively. Abbreviations: DV: dorsal-ventral, hpf: hours post fertilization, WT: wild type.

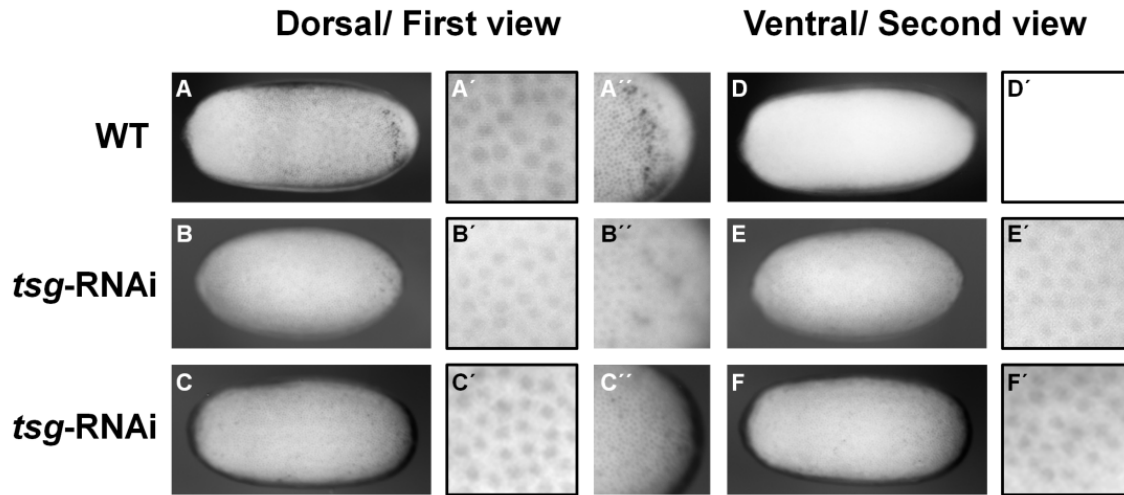


Figure 3-20: pMad gradient formation is disrupted in *tsg*-RNAi embryos

Anterior of the egg is to the left. pMad distribution lacks DV polarity in most *tsg*-RNAi embryos (B-C'', E-F'') (compare with WT (A, A', A'', D, D')). In addition, the dorsal-posterior domain of high pMad levels present in late blastoderm stages in WT (A, A'') is not formed in the same manner in *tsg*-RNAi embryos: only a few speckled spots of enhanced pMad levels close to the posterior pole were observed in these embryos (B, B''). pMad was detected by an immunohistochemical staining. In one row different views and magnifications of one embryo are shown. Either a dorsal and ventral view or, if the staining exhibited no DV asymmetry, from two opposing sides. A', B', C', D', E' and F' show about ten times magnified views from the embryos pictured in A, B, C, D, E and F, respectively. A'', B'' and C'' display magnifications of the posterior poles of embryos shown in A, B and C, respectively. Abbreviations: DV: dorsal-ventral, WT: wild type.

Table 3-10: Localization of BMP signaling activity requires *sog* and *tsg*

The dorsal-ventral (DV) asymmetry of pMad distribution was reduced in *sog*-RNAi and *tsg*-RNAi embryos. It was distinguished whether pMad asymmetry was still clearly detectable (second row from top), or only very slightly visible (third row from top), or whether it was completely symmetric distributed along the DV axis (bottom row). The frequency of phenotypes is given relative to all investigated embryos with one knockdown phenotype. The number of investigated embryos is given in parentheses: shown as ratio of positive embryos to total sample size.

	<i>sog</i>-RNAi	<i>tsg</i>-RNAi
clear DV asymmetry	55% (62/112)	-
slight DV asymmetry	41% (46/112)	51% (37/72)
no DV asymmetry	4% (4/112)	48% (35/72)

As demonstrated in 3.3.2.1, 3.3.3.1, 3.3.3.2 and 3.3.3.3 reduction of BMP signaling activity causes expansion of ventral fates in *O. fasciatus*. Monitoring of ventral marker gene expression in *tsg*- and *sog*-RNAi embryos should reveal consequences of elevated BMP signaling activity on ventral fates.

The expression of *twi* (100%, N=127) and *sim* (100%, N=55) was lost in *sog*-RNAi and *tsg*-RNAi embryos during the blastoderm stage (Figure 3-21 compare A with E and C with G; Figure 3-22 compare A with E and C with G). Exempted from this was a posterior domain of *sim*, which forms shortly after the onset of gastrulation, presumably independent of DV patterning (Figure 3-22 G). The expression of *sog* appeared to be lost as well upon depletion of *tsg* (100%, N=58), confirming the loss of the ventral anlagen (Figure 3-22 compare B with F). Consistent with this was an expansion of the dorsal *msh* domain around the complete circumference in all investigated late blastoderm *tsg*-RNAi embryos (100%, N=16), with 50% (N=16) of them even exhibiting no detectable DV asymmetry at all (Figure 3-22 compare D with H, I; data not shown). In contrast, *msh* expression in *sog*-RNAi embryos was found to be reduced in expression levels (100%, N=14) and sometimes (14%, N=14) also in domain size during late blastoderm stages (Figure 3-21 compare D with H, H'; data not shown). Nevertheless, the afore described loss of expression of ventral and ventral-lateral markers clearly indicates a loss of the mesoderm and at least a part of the neuroectoderm in *tsg*- and *sog*-RNAi blastoderm embryos.

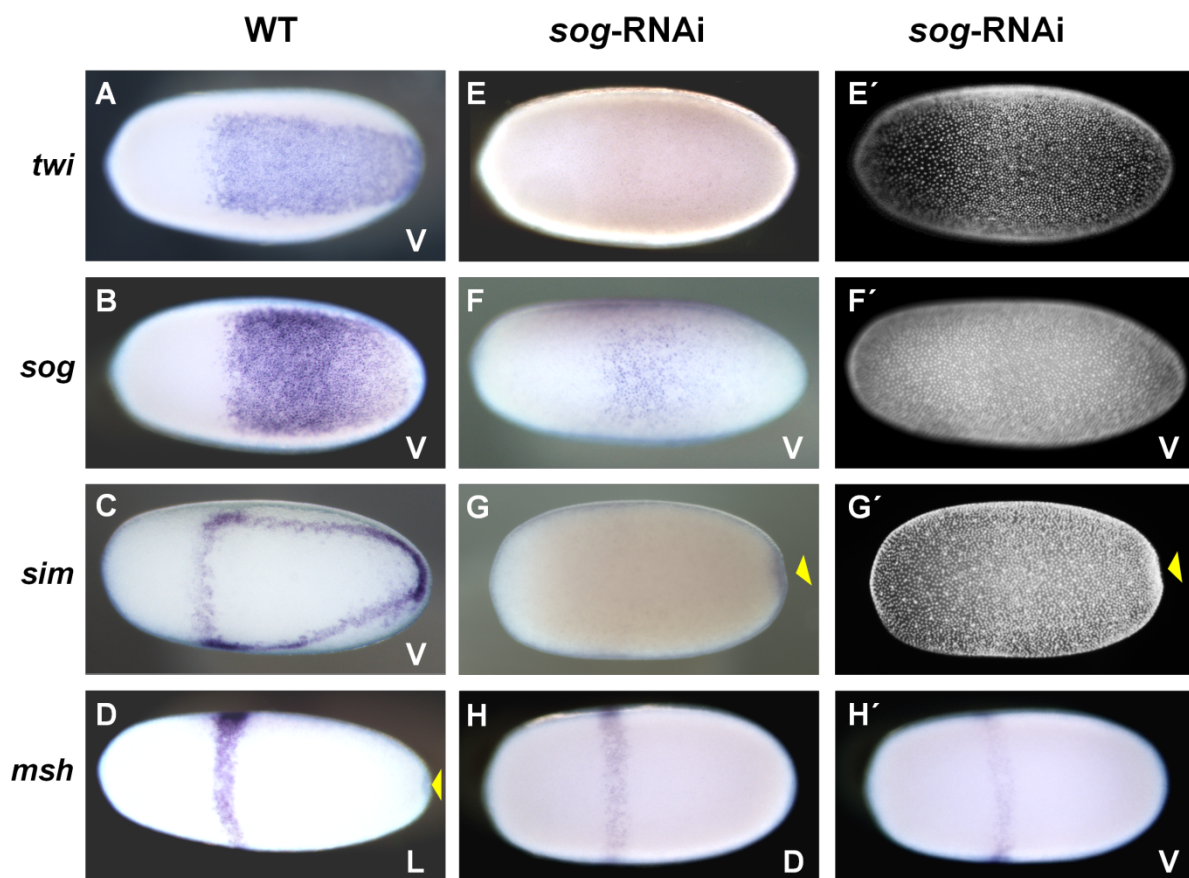


Figure 3-21: Ventral fates are lost upon a *sog* knockdown

Anterior of the egg is to the left. The view is indicated in the right bottom corner, if it was possible to determine. The expression of *twi* (A, E) and *sim* (C, G) was lost in *sog*-RNAi blastoderm stage embryos (E, G compare to

WT pictured in A, C). The expression of *sog* (B, F) and *msh* (D, H, H') was reduced in levels in *sog*-RNAi embryos (F, H, H') compared to WT (B, D). E', F' and G' display nuclear counterstaining of the embryos shown in E, F and G, respectively. H and H' show to different views of the same embryo. Expression was monitored by ISH. Yellow arrowheads point towards posterior indentations in G and G'. Abbreviations: D: dorsal, ISH: *in situ* hybridization, L: lateral, V: ventral, WT: wild type.

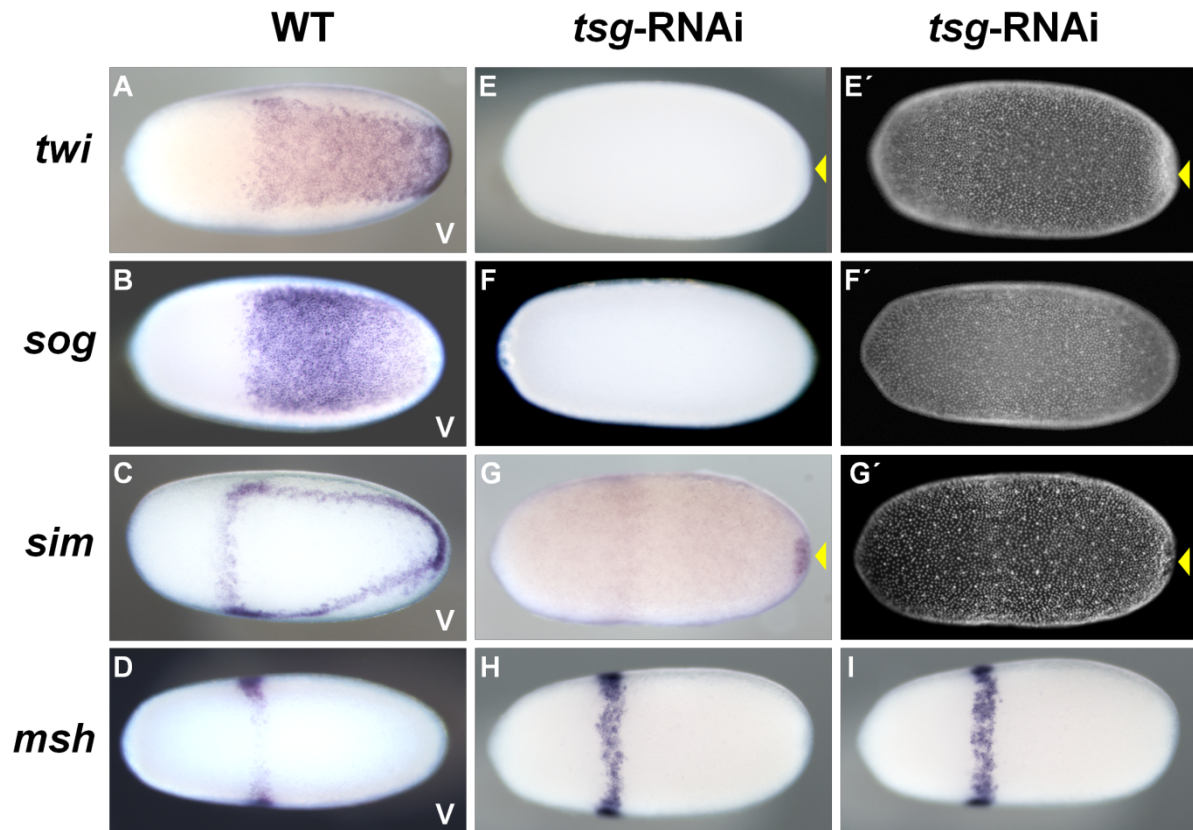


Figure 3-22: Ventral fates are lost upon a *tsg* knockdown

Anterior of the egg is to the left. The view is indicated in the right bottom corner, if it was possible to determine. The expression of *twi* (A, E), *sog* (B, F) and *sim* (except for the terminal domain C, G) was lost in *tsg*-RNAi blastoderm stage embryos (E, F, G). The dorsal expression domain of *msh* (D, H, I) was expanded, the ventral *msh* expression domain was lost in late blastoderm stage *tsg*-RNAi embryos (H, I) (compared with WT pictured in D). E', F' and G' display nuclear counterstaining of the embryos shown in E, F and G, respectively. H and I show to different views of the same embryo. Expression was monitored by ISH. Yellow arrowheads point towards posterior indentations in E, E', G and G'. Abbreviations: ISH: *in situ* hybridization, V: ventral, WT: wild type.

This was further confirmed by analysis of germ band stage *sog* and *tsg* knockdown embryos. Expression of the neuroectodermal markers *sim* (100%, N=54), *pcan* (100%, N=28) and *sox21b* (100%, N=11) was lost, except for the terminal domains (Figure 3-23 compare B with F, J; data not shown; Figure 3-24 compare B-D with H-J). In contrast, the ectodermal markers *msh* (83%, N=54) and *pent* (89%, N=44), which exhibit more dorsal expression domains in

wild type, often formed DV axis-surrounding, transversal stripes along the entire length of these knockdown embryos (Figure 3-23 compare C with G, K, and D with H, L; Figure 3-24 compare E with K, and F with L). Occasionally (13%, N=54), *msh* expression appeared to be absent or extremely reduced in *tsg*-RNAi (40%, N=15) and *sog*-RNAi (3%, N=39) germ band embryos, which was assumed to be a consequence of a stronger knockdown. Hence, *tsg*- and *sog*-RNAi germ band embryos might consist of ectodermal tubes, with different ectodermal identities arranged along the AP instead the DV axis.

Taking all the above described results together, it seems that depletion of *tsg* or *sog* causes not simply ventrally elevated BMP signaling activity, but rather a DV symmetric BMP signaling activity that results in the loss of ventral fates and DV polarity in *O. fasciatus* embryos.

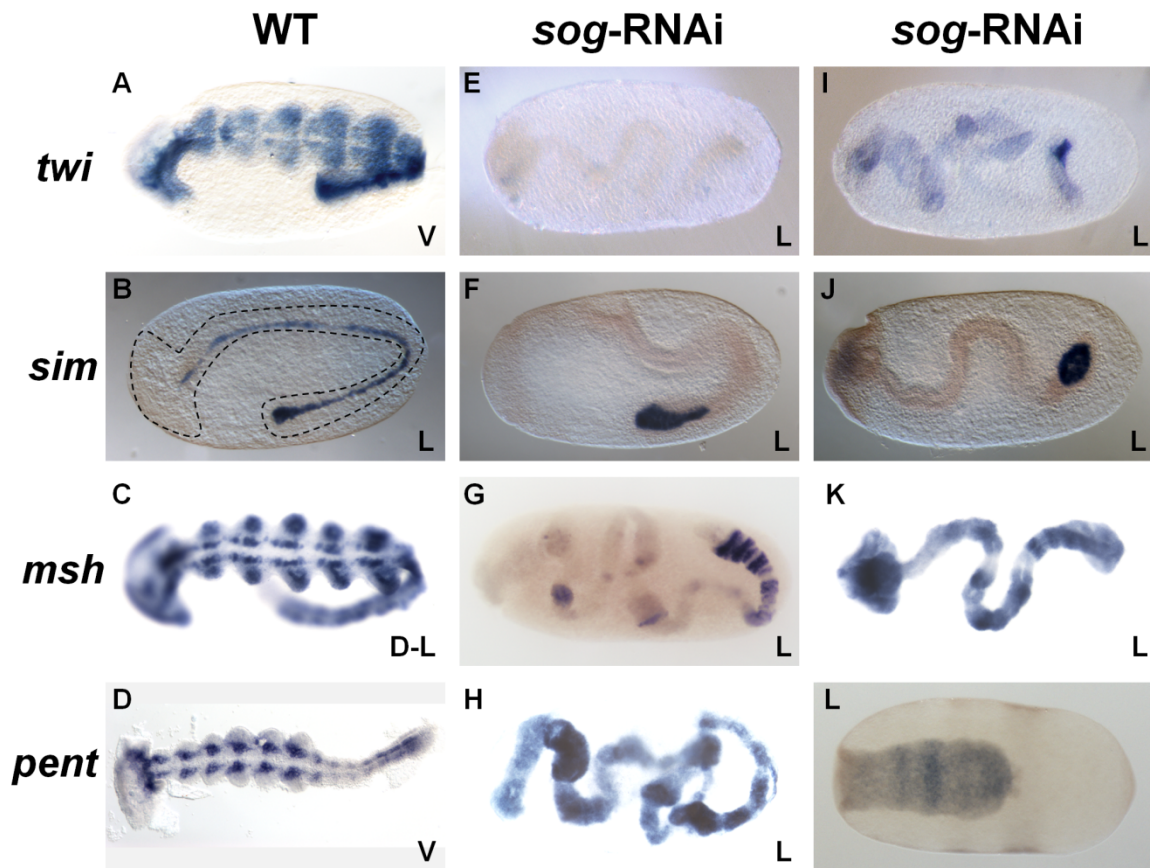


Figure 3-23: *sog*-RNAi germ bands mainly consist of ectoderm

Anterior of the embryo is to the left. The ventral side is down in lateral orientations, if dorsal and ventral could be distinguished. The view is indicated in the right bottom corner, if it was possible to determine. Expression of *twi* (top row) and *sim* (except for the terminal domain; second row from top) was lost (E, F, J), or restricted to the posterior of the germ band (I) in *sog*-RNAi embryos (compare to WT pictured in A and B). *msh* (third row from top) and *pent* (bottom row) were expressed in DV axis-surrounding, transversal stripes in *sog*-RNAi germ band (G, H, K) and anatrepsis (L) stage embryos. Germ band stage embryos were 42 hpf to 50 hpf old (A-K).

Dashed lines approximately follow the outline of the germ band in B. Abbreviations: D-L: dorsal-lateral, DV: dorsal-ventral, hpf: hours post fertilization, ISH: *in situ* hybridization, L: lateral, V: ventral, WT: wild type.

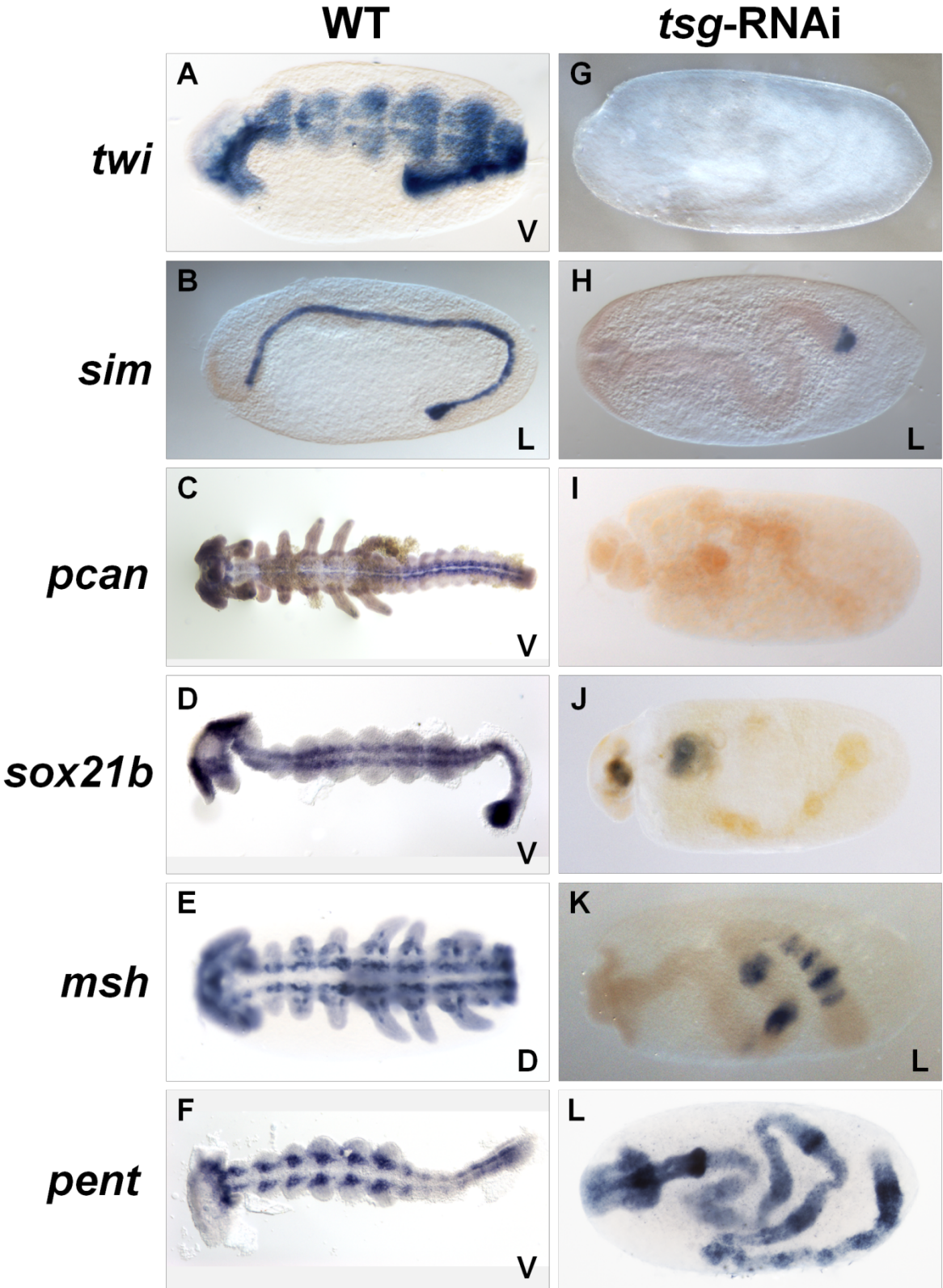


Figure 3-24: *tsg*-RNAi germ bands are ectodermal tubes

Anterior of the embryo is to the left. The ventral side is down in lateral orientations, if dorsal and ventral could be distinguished. The view is indicated in the right bottom corner, if it was possible to determine. Expression of *twi* (A, G), *sim* (except for the terminal domain; B, H), *pcan* (C, I) and *sox21b* (D, J) was lost in *tsg*-RNAi germ band stage embryos (G-J; staining in J is assumed to be background staining). *msh* (E, K) and *pent* (F, L) were expressed in DV axis-surrounding, transversal stripes in *tsg*-RNAi germ band stage embryos (K, L). Expression was monitored by ISH. Germ band stage embryos were 42 hpf to 50 hpf old. Abbreviations: D: dorsal, DV: dorsal-ventral, hpf: hours post fertilization, ISH: *in situ* hybridization, L: lateral, V: ventral, WT: wild type.

3.3.4.2 DV patterning of *sog* knockdown embryos is less impaired in the abdomen compared to the head and thorax

Consistent with the difficulty to completely knock down *sog*, a few *sog*-RNAi embryos showed residual DV polarity at the germ band stage (16%, N=75). *sog*-RNAi embryos, which were presumed to have a weaker phenotype, exhibited residual *twi* expression in the posterior tip of the germ band (Figure 3-23 I; 39%, N=18). In addition, some germ band embryos exhibited only transversal stripes of *pent* expression in the anterior region, while *pent* expression was restricted to the dorsal region of the germ rudiment within the abdomen (data not shown; 39%, N=13). Thus, the abdomen appeared to be less sensitive, or more resistant, to ectopic down regulation of *sog* than the anterior of the embryo.

3.3.4.3 *dpp* is epistatic to *sog*

Differences along the AP axis were also discovered upon *dpp-sog* double knockdown, which was performed to assure Sog to act upstream of Dpp. 56% (N=66) of the *dpp-sog* knockdown embryos were completely ventralized with *twi* (52%, N=56) and early *sim* (50%, N=2), or the ventral, anterior domain of late (29 hpf to 40 hpf) *sim* (88%, N=8) being expanded around the complete egg circumference in blastoderm stages (Figure 3-25 compare A with D; data not shown). Embryos with a presumed weaker knockdown (44%, N=66) were partially ventralized, *i.e.* *twi* (48%, N=56) and early *sim* (50%, N=2) expression were not completely expanded along the whole AP axis of the germ rudiment (Figure 3-25 compare B with E; data not shown). Furthermore, *sim* (13%, N=8) expression was restricted to the anterior, ventral domain only in one half of the germ rudiment, whereas it was uniformly expressed in the remaining germ rudiment during the differentiated blastoderm stage (Figure 3-25 compare C with F). Interestingly, partially ventralized *dpp-sog* knockdown embryos differed in one aspect to weak *dpp*-RNAi embryos: expression of *twi* not only tended to expand first in the

anterior part of its domain, but in addition also around the posterior pole in *dpp-sog* knockdown embryos (Figure 3-25 E). Aside from this feature *dpp-sog* knockdown embryos exhibited a DV phenotype indistinguishable from *dpp* knockdown embryos. Therefore, *dpp* seems to be epistatic to *sog* in *O. fasciatus*, which is consistent with Sog acting upstream of Dpp.

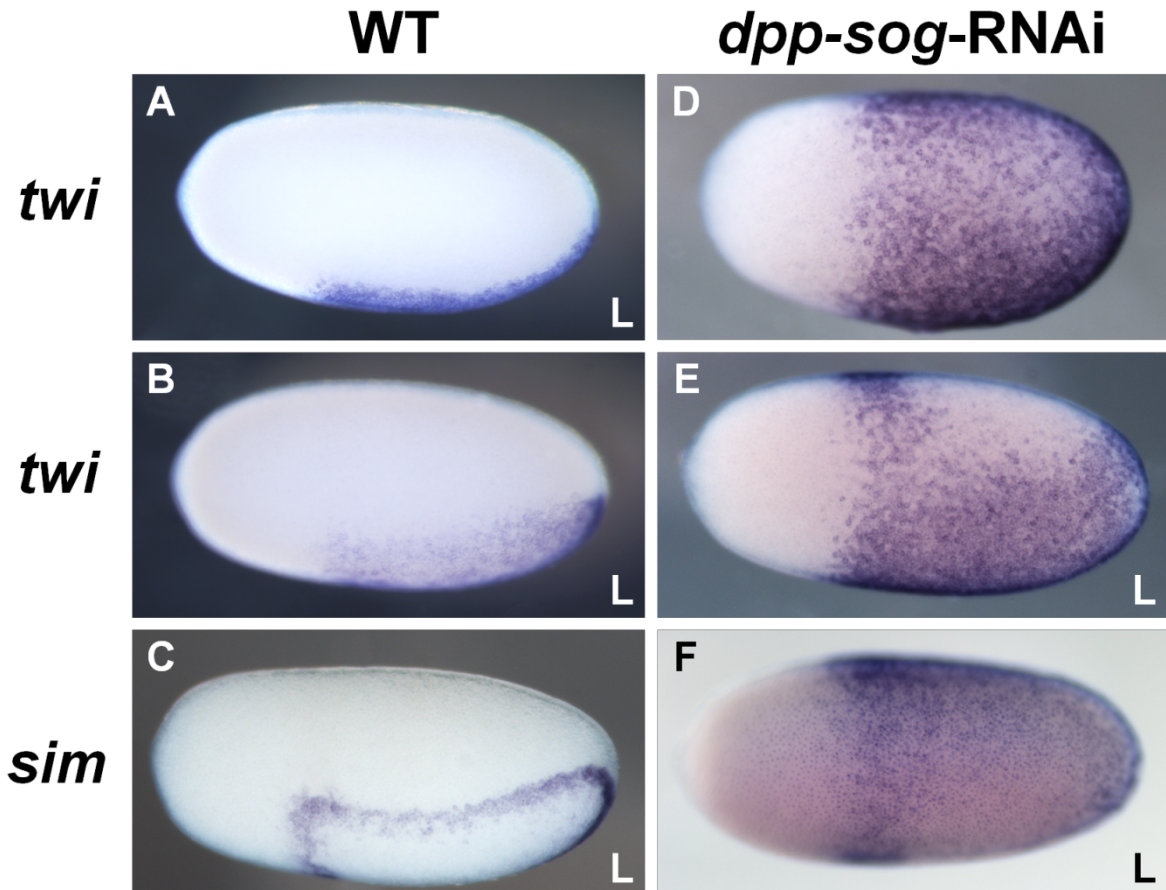


Figure 3-25: *dpp* is epistatic to *sog*

Anterior of the egg is to the left. The ventral side is down in lateral views (A-C, E-F). The orientation is indicated in the right bottom corner, if it was possible to determine. The expression of *twi* (A, B, D, E) was expanded in *dpp-sog*-RNAi embryos (D, E) compared to WT (A, B). Occasionally, late blastoderm *sim* was uniformly expressed in the presumed dorsal half of the germ rudiment, while the presumed ventral half exhibited only the anterior, ventral domain of *sim* expression (F compared to WT in C). Expression was monitored by ISH. Abbreviations: ISH: *in situ* hybridization, L: lateral, WT: wild type.

3.3.4.4 Sterility effects caused by loss of *dpp* and *tsg* are cumulative

The conserved function of Tsg as extracellular BMP modulator implies that it acts upstream of Dpp in *O. fasciatus* as well (Ben-zvi et al. 2008; Little & Mullins 2006; Nunes da Fonseca et al. 2010). In order to test if *dpp* is, as assumed, epistatic to *tsg*, a double knockdown of *dpp*

and *tsg* was performed. Unfortunately, the sterility effects of both knockdowns⁹ appeared to be additive, so that it was hardly possible to obtain any fertilized eggs from the injected females. Only two of the eight investigated embryos exhibited a *dpp* single knockdown phenotype, with *twi* expanded around the complete circumference (Figure 3-26 compare A with D). The other analyzed embryos showed indications of lateralization or dorsalization (Figure 3-26 compare B, C with E, F). It is likely that the sterility effect prevented collection of embryos with a complete *dpp-tsg* double knockdown and instead embryos with a single knockdown or an incomplete double knockdown were collected. Hence, to assure *dpp* to be epistatic to *tsg*, this double knockdown experiment should be repeated using embryonic RNAi instead of parental RNAi.

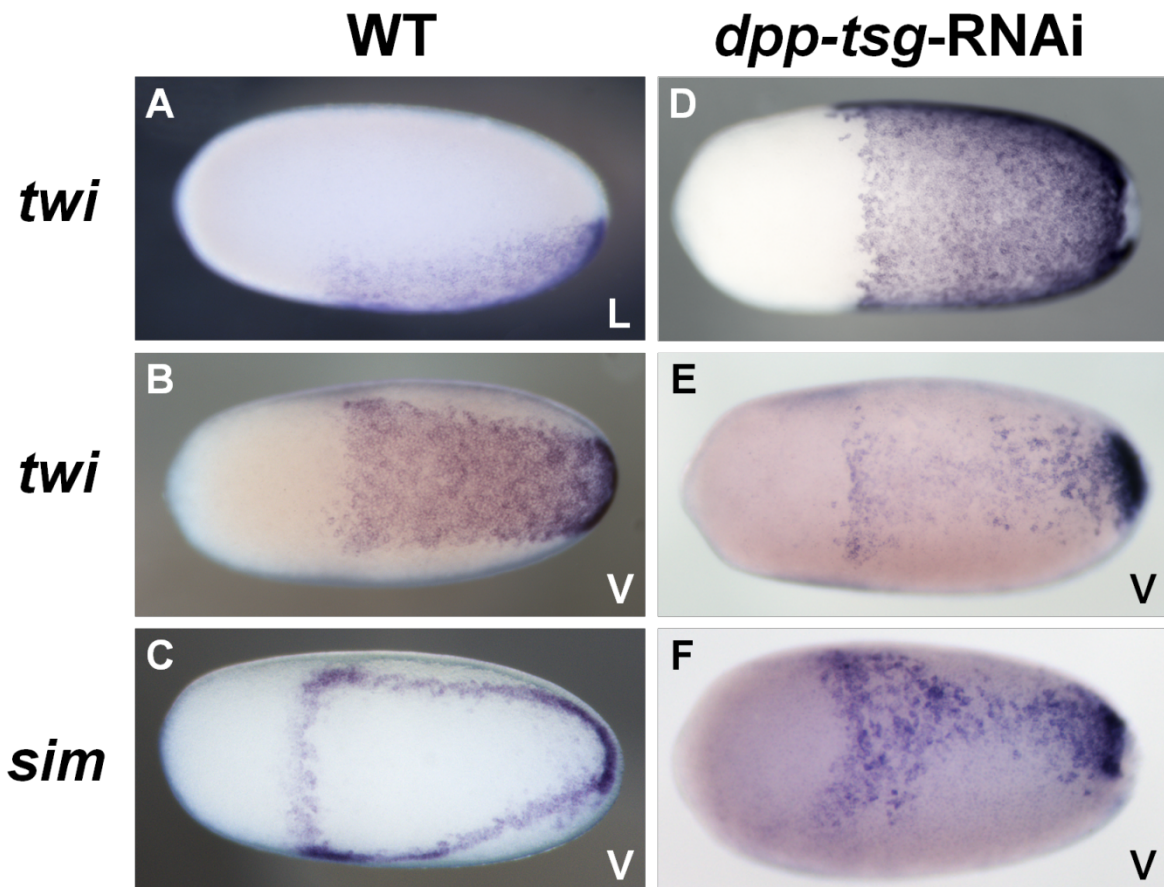


Figure 3-26. Expression of DV marker genes in *dpp-tsg* RNAi blastoderm stage embryos

Anterior of the egg is to the left. The ventral side is down in lateral aspects (A). The view is indicated in the right bottom corner, if it was possible to determine. The expression of *twi* (A, B, D, E) was occasionally completely expanded (D) and sometimes fuzzier and slightly reduced in size (E) in *dpp-tsg*-RNAi embryos (D, E) compared to WT (A, B). Expression of *sim* was sometimes detectable on the ventral side in late blastoderm stage *dpp-tsg*-

⁹ *BMPsc* knockdowns usually impaired the fertility, but in most cases it still was possible to collect enough eggs for a phenotypic analysis.

RNAi embryos (F), when it is already cleared from the ventral side, with exception of the anterior domain in WT (C). Expression was monitored by ISH. Abbreviations: ISH: *in situ* hybridization, L: lateral, V: ventral, WT: wild type.

3.3.4.5 Tolloid is essential for BMP signaling activity

Besides Sog and Tsg the function of another extracellular BMP modulator, termed Tolloid (Tld), was analyzed. Tld is a metalloprotease, which is reported to cleave Sog especially when it is in complexes with BMP ligands (Ben-zvi et al. 2008; Connors et al. 1999; Little & Mullins 2006; Marqués et al. 1997; Shimmi & O'Connor 2003). The knockdown of *tld* caused a *dpp*-RNAi-resembling phenotype in *O. fasciatus*. Affected embryos frequently exhibited (85%, N=67) expanded expression of *twi* (96%, N=23), *sog* (83%, N=24) and early *sim* (75%, N=20), along the complete DV axis during the blastoderm stage (Figure 3-27 compare A with D and B with E; data not shown). This indicated that strong *tld*-RNAi embryos consist only of mesoderm, which was confirmed by the loss of the lateral, mesectodermal expression domain of *sim* accompanied by an expansion of the anterior, ventral domain of *sim* in late blastoderm stages (100%, N=4; Figure 3-27 compare C with F). In addition, expression of *sim* (100%, N=13) and *msh* (100%, N=13) appeared to be absent, (except for some terminal staining) in *tld*-RNAi germ band stage embryos (data not shown). This similarity between *dpp* and *tld* knockdown embryos suggested Tld to be essential for BMP signaling activity, probably by preventing Sog overexpression.

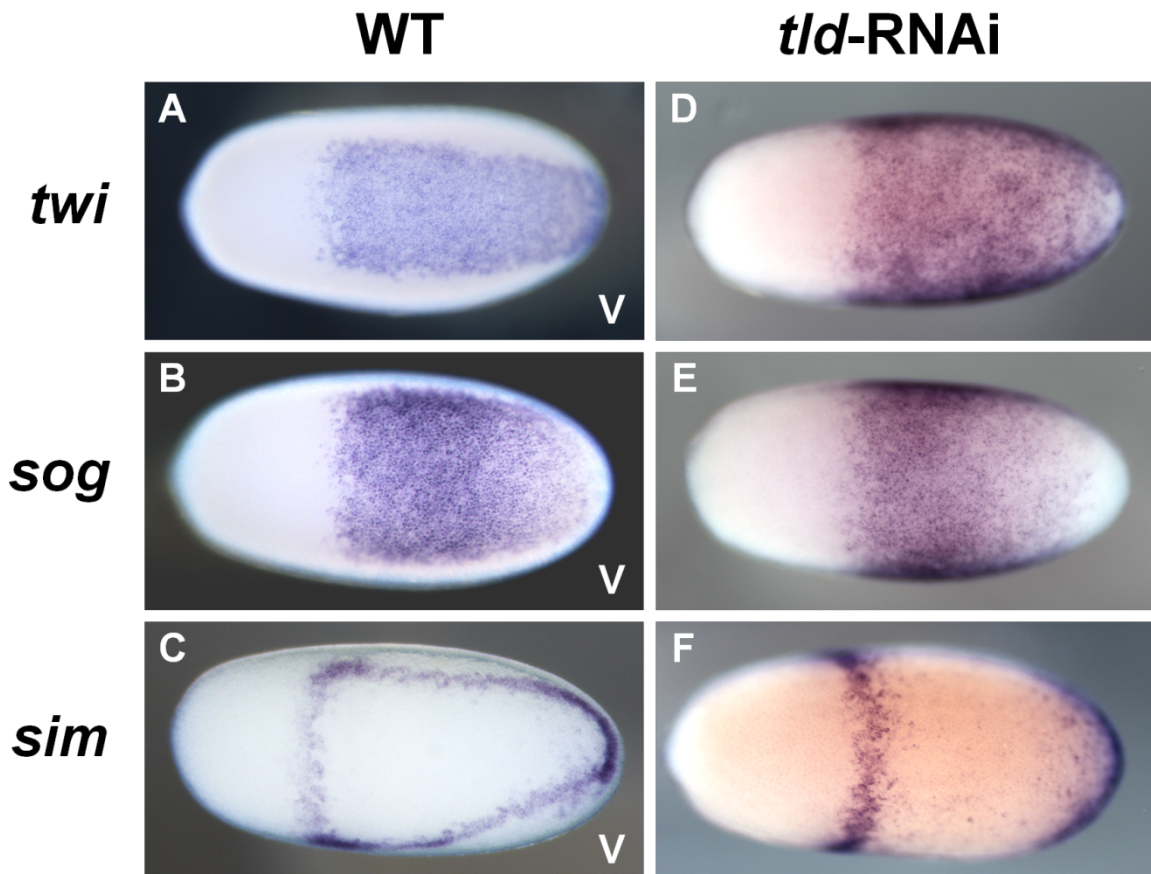


Figure 3-27: Tolloid might be required to prevent a Sog overexpression

Anterior of the egg is to the left. The view is ventral in A-C and was not possible to determine in D-F. The expression of *twi* (A, D), *sog* (B, E) and the anterior, ventral expression domain of *sim* (C, F) was expanded in *tld*-RNAi embryos (D-F) compared to WT (A-C). The lateral domain of *sim* was lost upon knockdown of *tld* (compare F with WT pictured in C). Expression was monitored by ISH. Abbreviations: ISH: *in situ* hybridization, V: ventral, WT: wild type.

3.3.5 Toll signaling is essential for DV polarity formation

3.3.5.1 The DV phenotype of *dpp* is epistatic to *Toll*

All the previously described results of this study indicated BMP signaling to be able to repress ventral fates. However, the Toll pathway is known to have a conserved and important role in patterning of ventral anlagen in insect embryos (Anderson et al. 1985; Belvin & Anderson 1996; Nunes da Fonseca et al. 2008; Buchta 2014). Indeed, my colleague Yen-Ta Chen, who is analyzing the role of Toll signaling in DV patterning of *O. fasciatus*, discovered that *sog* and *twi* expression are completely abolished (~50%), or strongly reduced (~50%) upon a *Toll* knockdown (unpublished data of Yen-Ta Chen). We wondered to what extent Toll signaling is responsible for the establishment of ventral fates in *O. fasciatus*. Therefore, we knocked

down simultaneously *Toll* and *dpp* and monitored expression of ventral marker genes. Unexpectedly, the *Toll-dpp* double knockdown phenotype strongly resembled the *dpp* single knockdown phenotype regarding DV patterning. *twi* (99%, N=79), *sog* (100%, N=43) and early *sim* (100%, N=4) were expanded around the whole circumference in 99% (N=126) of the investigated embryos (Figure 3-28 compare A, B with D, E; data not shown). In addition, the ventral, anterior domain of late blastoderm *sim* expression was expanded around the complete circumference, while the lateral domain was lost (100%, N=22) (Figure 3-28 compare C with F). In conclusion, *Toll-dpp* double knockdown embryos appeared to consist only of mesoderm, like *dpp* single knockdown embryos.

My colleague Yen-Ta Chen verified the double knockdown by semi-quantitative PCR (semi-qPCR) (unpublished data of Yen-Ta Chen). In addition, we observed some phenotypic deviations from *dpp* single knockdown embryos. Late blastoderm stage embryos with a *dpp* knockdown exhibited an anterior transversal stripe with high cell density, instead of the lateral cell aggregation present in wild type (Figure 6-1 compare A with B; Figure 1-2 C, D; Figure 3-4 A'). In contrast, this region of high cell density appeared to be absent or extremely faint in *Toll-dpp*-RNAi embryos. The cells appeared to be rather equally distributed along the DV axis and became gradually more widely spaced towards the anterior, except for the poles where the cells appeared to be more densely packed in late blastoderm stages of *Toll-dpp*-RNAi embryos (Figure 7-1 C). Second, the double knockdown embryos exhibited an AP phenotype (Table 3-11): the anterior expression border of *sog* (79%, N=43) and *twi* (71%, N=79) was often less defined (74%, N=122) and shifted anteriorly (43%, N=122), compared to wild type. Rarely *twi*, *sog* and early *sim* were expressed in the complete blastoderm (9%, N=126) (Figure 3-28 D, E; data not shown). Consistent with this was a shift of *sim* expression towards the anterior in late blastoderm stages, which was accompanied by the anterior *sim* domain becoming broader and less defined (Figure 3-28 compare C with F; Table 3-11). Such AP defects also became apparent in *Toll*-RNAi embryos by analyzing *msh* expression (unpublished data of Yen-Ta Chen). Hence, the AP defects of *Toll-dpp*-RNAi embryos are probably solely dependent on Toll signaling and their presence in the double knockdown embryos provided further evidence for the successful, simultaneous knockdown of both *Toll* and *dpp*.

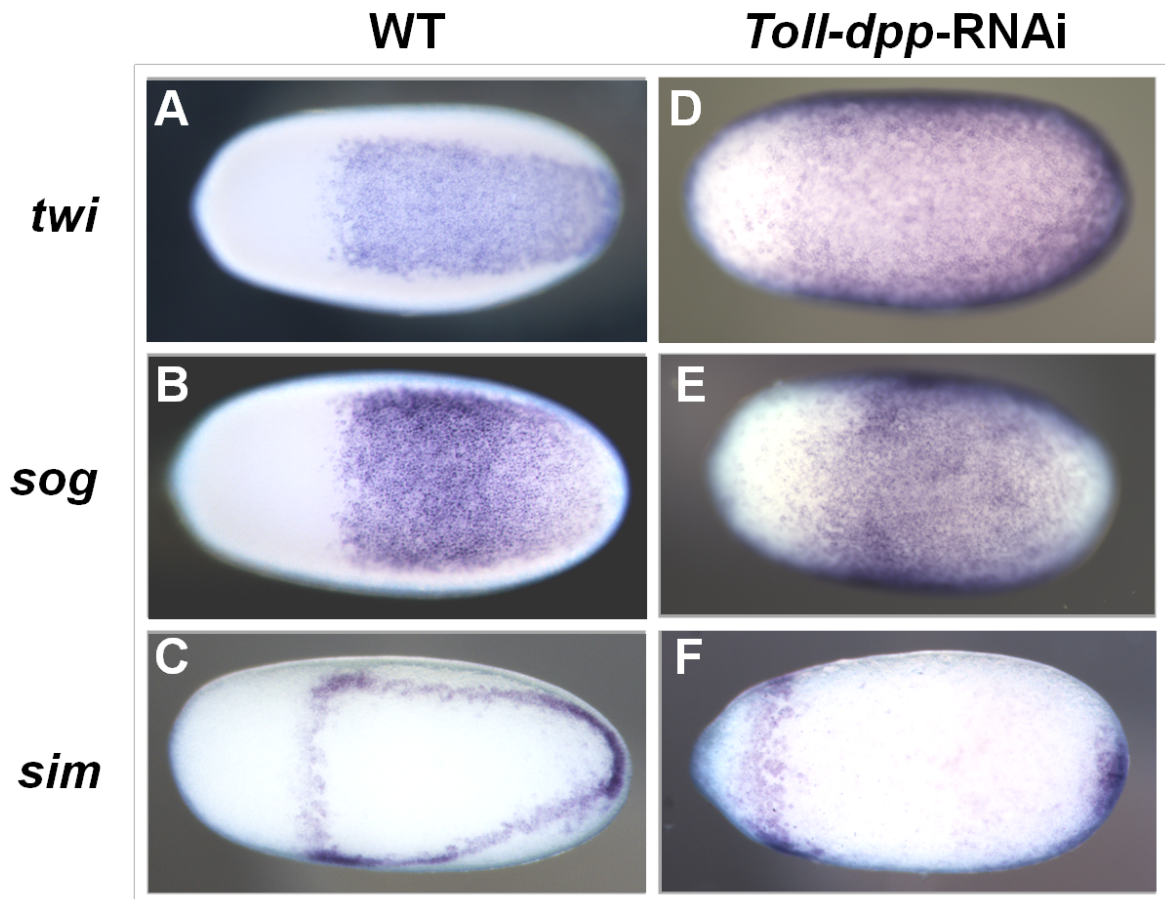


Figure 3-28: *Toll-dpp*-RNAi embryos are ventralized and exhibit AP defects

Anterior of the egg is to the left. The view is ventral in A-C and was not possible to determine in D-F. The expression of *twi* (A, D), *sog* (B, E) and the anterior, ventral expression domain of *sim* (C, F) was expanded in *Toll-dpp*-RNAi embryos (D-F) compared to WT (A-C). The lateral domain of *sim* was lost upon knockdown of *Toll-dpp* (compare F with WT pictured in C). The expression of *twi* (A, D), *sog* (B, E) and *sim* (C, F) was more undefined and shifted towards the anterior pole in *Toll-dpp*-RNAi (D-F) relative to WT embryos (A-C). Expression was monitored by ISH. Abbreviations: ISH: *in situ* hybridization, WT: wild type.

Table 3-11: *Toll-dpp*-RNAi embryos exhibit an AP patterning defect

Expression of the ventral markers *twi*, *sog* and *sim* was monitored by ISH in *Toll-dpp*-RNAi blastoderm stage embryos and found to be completely (first data column from left) or partially (second data column from left) expanded along the AP-axis in 51% of the analyzed embryos. Expansion of expression along the AP-axis was always accompanied by less defined, fuzzier AP-borders of the expression domain, compared to wild type. This feature was also observed without a significant anterior expansion of expression in 32% (third data column from left) of the investigated embryos. 17% of the investigated embryos showed no alteration of the expression pattern along the AP axis. The frequency of the phenotype indicated in the top row is given relative to the sum of *Toll-dpp*-RNAi embryos in which the expression of the respective gene (first column) was monitored, except for *sim* where early (26-29 hpf) blastoderm expression (fourth row) and late blastoderm expression (including early anatrepsis stages) was distinguished and the last row in which the frequency of phenotypes is given relative to all investigated embryos. The number of investigated embryos is given in parentheses: shown as ratio of positive embryos to total sample size. Abbreviations: hpf: hours post fertilization, ISH: *in situ* hybridization.

	Complete AP expansion	Weak AP expansion	Undefined border	No AP defect detected
<i>twi</i>	6% (5/79)	52% (41/79)	19% (15/79)	23% (18/79)
<i>sog</i>	5% (2/43)	26% (11/43)	54% (23/43)	16% (7/43)
early <i>sim</i>	100% (4/4)	-	-	-
late <i>sim</i>	54% (10/22)	12% (3/22)	35% (9/22)	-
sum	14% (21/148)	37% (55/148)	32% (47/148)	17% (25/148)

3.3.5.2 Toll is not required for the early activation of *sog*

A complete DV expansion of *sog* and *twi* occurred upon simultaneous depletion of *Toll* and *dpp* (Figure 3-28 D, E). This indicated that in contrast to *D. melanogaster* and *T. castaneum*, Toll signaling does not directly activate *twi* or *sog* in *O. fasciatus* (Jaźwińska et al. 1999; Stappert 2014). But why did the expression of *twi* and *sog* disappear in *Toll*-RNAi embryos? To shed light on this issue, we decided to analyze *Toll* knockdown embryos in more depth. First we wanted to evaluate the degree of DV asymmetry in blastoderm stages and therefore monitored pMad in *Toll*-RNAi embryos. We found pMad to be quite uniformly distributed in blastoderm stage *Toll* knockdown embryos: some completely lacked DV asymmetry while others retained only a slight, or rarely a clear but reduced, DV polarity (N=78, 32%, 56% and 12%, respectively; Figure 3-29 compare A and C with B and D; data not shown; Table 3-12). Hence, the absence or strong reduction of *sog* and *twi* could result from ventral BMP signaling activity. However, the reason for this ventral BMP signaling activity in *Toll* knockdown embryos remained unclear. Therefore, we decided to more carefully analyze *sog*

expression in wild type and *Toll* knockdown embryos. Indeed, we found *sog* expression to start already in very young blastoderm stages around 15 hpf to 18 hpf (Figure 3-30 A). It seemed that *sog* is first ubiquitously expressed in the complete blastoderm (Figure 3-30 A), then becomes restricted to the posterior 75% and is afterwards successively cleared from the dorsal 60% of the egg circumference while it is enhanced in the ventral region (Figure 3-30 B, C). Finally, *sog* is exclusively and strongly expressed in the ventral 40% of the germ rudiment from 25 hpf onwards (Figure 3-7 B). Interestingly, the early uniform expression of *sog* appeared unaltered in *Toll* knockdown embryos (Figure 3-30 D; N=16). Hence, it seems that the initial ubiquitous activation of *sog* is independent of *Toll* signaling, while *Toll* is required for the later, ventral *sog* expression.

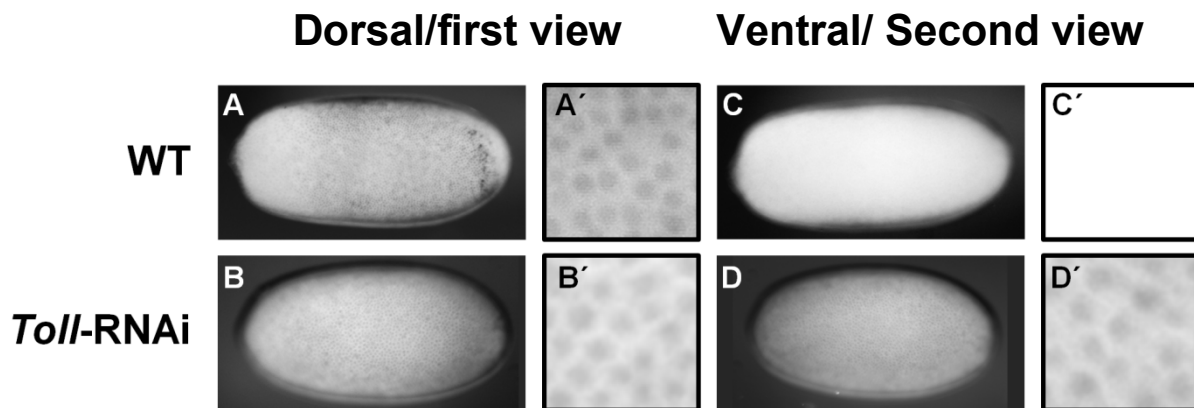


Figure 3-29: DV polarity is strongly impaired upon a *Toll* knockdown

Anterior of the egg is to the left. The asymmetry of pMad distribution observed in WT (A, A', C, C') was strongly reduced or absent in *Toll*-RNAi embryos (B, B', D, D'). pMad was detected by an immunohistochemical staining. In one row different views and magnifications of one embryo are shown. Either a dorsal and ventral view or, if the staining exhibited no DV asymmetry, from two opposing sides. A', B', C' and D' show about ten times magnified views from the embryo pictured in A, B, C and D, respectively. Abbreviations: DV: dorsal-ventral, WT: wild type.

Table 3-12: Localization of BMP signaling activity requires *Toll*

The DV asymmetry of pMad distribution was reduced in *Toll*-RNAi embryos. It was distinguished whether pMad asymmetry was still clearly detectable (second row from top), or only very slightly visible (third row from top), or whether it was completely symmetric distributed along the DV axis (bottom row). The frequency of phenotypes is given relative to all investigated embryos. The number of investigated embryos is given in parentheses: shown as ratio of positive embryos to total sample size. Abbreviations: DV: dorsal-ventral.

clear DV asymmetry	12% (9/78)
slight DV asymmetry	56% (44/78)
no DV asymmetry	32% (25/78)

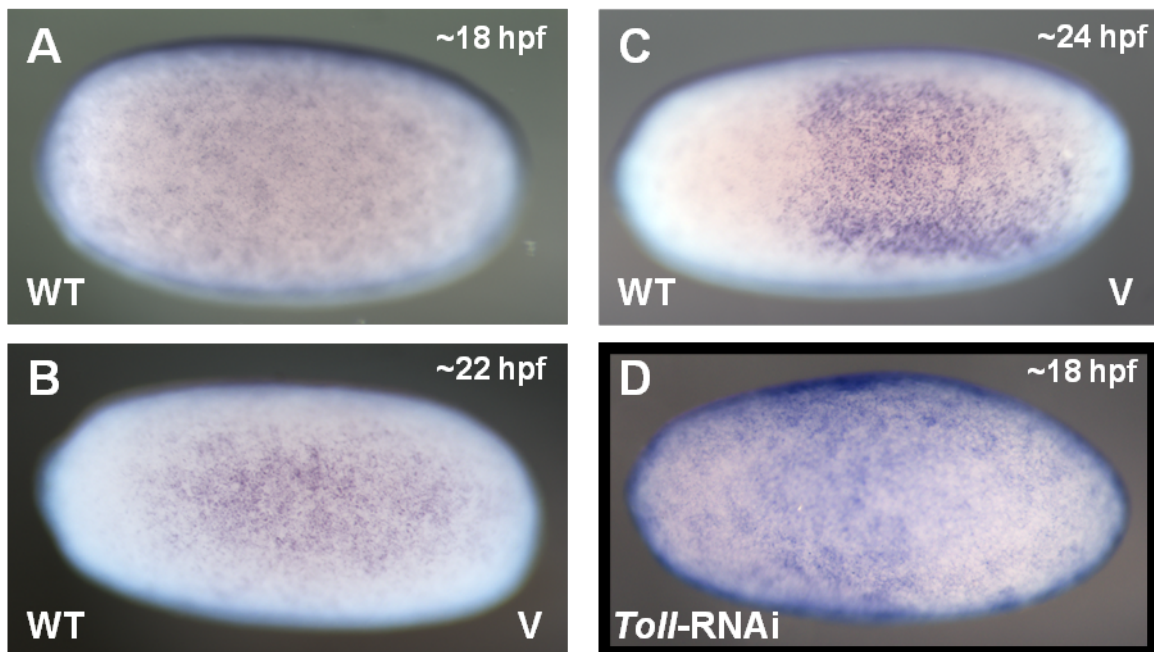


Figure 3-30: *sog* activation is initially independent of *Toll*

Anterior of the egg is to the left. The view is indicated in the right bottom corner, if it was possible to determine. The expression of *sog* starts uniformly around 18 hpf (A) and becomes enhanced in the ventral and diminished in the dorsal region from about 22 hpf onwards (B, C). The early ubiquitous expression was also detected in *Toll*-RNAi embryos (D). Expression was monitored by ISH. Abbreviations: hpf: hours post fertilization, ISH: *in situ* hybridization, V: ventral, WT: wild type.

4. Discussion

In the following I will first discuss the influence of BMP signaling on extraembryonic tissue formation and morphogenesis (4.1). Then a small excursus about interactions between the AP and the DV patterning system will follow (4.2). Afterwards I will deal with the role of Tsg and Sog (4.3, 4.4) and of BMP heterodimers (4.5-4.7) during DV patterning. This will include a discussion about DV patterning in the growth zone (4.5). Furthermore, the negative influence of BMP signaling on mesoderm formation (4.8) as well as on *sog* transcription (4.9) will be elucidated. Finally, the role of Toll in the DV patterning system of *O. fasciatus* (4.10) as well as its change in the course of evolution (4.11) will be discussed.

4.1 BMP signaling seems to be required for extraembryonic membrane function

BMP signaling is known to be most active on the non-neural side of the embryo, which is ventral in vertebrates and dorsal in invertebrates (Akiyama-Oda & Oda 2006; van der Zee et al. 2006; Ben-zvi et al. 2008; De Robertis & Kuroda 2004; Dorfman & Shilo 2001; Raftery & Sutherland 2003). In this study the dorsal-most anlage of insects will be referred to as dorsal ectoderm, as several insect species exhibit indications that this region is first discriminated from more ventral anlagen before it becomes subdivided into embryonic ectoderm, giving rise to dorsal epidermis, and extraembryonic ectoderm (Buchta et al. 2013; Goltsev et al. 2007; Rushlow et al. 1987). The extraembryonic, dorsal ectoderm contains the amnion anlage, or in long germ insects the future amnion and serosa. In higher cyclorrhaphan flies, which possess neither serosa nor amnion, this region gives rise to the amnioserosa (Schmidt-Ott 2000; Buchta et al. 2013; Goltsev et al. 2007; Rafiqi et al. 2012). The extraembryonic, dorsal ectoderm anlage usually needs to receive higher BMP signaling activity and is located more dorsally within the blastoderm than the dorsal, embryonic ectoderm (Buchta et al. 2013; Rafiqi et al. 2012; van der Zee et al. 2006; Goltsev et al. 2007).

The amnion anlage is assumed to be located dorsally in the germ rudiment in *O. fasciatus* as well (1.1.4; Figure 1-4). Consistent with this, highest BMP signaling levels, *i.e.* nuclear pMad, were found in this region (3.3.1.1; Figure 3-5). And although early extraembryonic markers are still not available in *O. fasciatus*, *BMPsc* knockdown phenotypes provided evidence for a contribution of BMP signaling to extraembryonic development, especially amnion specification.

BMPsc-RNAi embryos often exhibited disordered, heavily convoluted and, compared to wild type, much thinner and longer germ bands (3.1.3; Figure 3-2). The amnion is believed to provide mechanical protection to the germ band through the fluid filled chamber, termed the amniotic cavity, which forms between itself and the embryo (Panfilio 2008). The amniotic cavity could exert hydrostatic pressure that helps the embryo to maintain its position and prevents it from deleterious torsions of its body. On this assumption it is easily conceivable that a defective amnion and consequently a faulty amniotic cavity could lead to an uncontrolled extension and arrangement of the germ band in *O. fasciatus*. Indeed, irregularities in germ band retraction, extension and arrangement are associated with amnion or amnioserosa defects in insects (Arora & Nüsslein-Volhard 1992; Rafiqi et al. 2010; van der Zee et al. 2006; Weber 2006). For instance, the failure of germ band retraction in the scuttle fly *Megaselia abdita* upon the synchronous knockdown of *dorsocross* and *tail up* is suggested to be due to a reduction of the amnion (Rafiqi et al. 2010).

Therefore, the morphological defects described above, which appeared to occur in ventralized (e.g. *dpp*-RNAi embryos) as well as in lateralized/dorsalized (*tsg*- and *sog*-RNAi) embryos could indeed depend on amniotic defects in *O. fasciatus*. Consistent with this, these defects were absent or less pronounced in *gbb* knockdown embryos, which also exhibit a less impaired pMad gradient, compared to *tsg*-, *sog*-, and *dpp*-RNAi embryos (3.3.2.3; Figure 3-12; Table 3-6 compare with 3.3.2.1; 3.3.4.1; Figures 3-9, 3-19, 3-20; Table 3-10). Interestingly, the morphologically most affected region of the germ band was the abdomen in *gbb*-RNAi embryos (3.1.3; Figure 3-2 I-L). The abdomen of *gbb*-RNAi embryos might have received less BMP signaling activity than the remaining germ rudiment, as it is ventralized while head and thorax are lateralized (3.3.4.2; Figure 3-14; Table 3-9). Therefore, the amnion might be especially impaired in this region of *gbb*-RNAi germ bands, while it is probably more generally affected in *dpp*, *sog* and *tsg* knockdown embryos.

The (partial) eversion phenotype of *gbb*-RNAi embryos provides additional hints for defects in extraembryonic development. An eversion phenotype had been previously observed in *O. fasciatus* upon *zen*-RNAi and was shown to result from malfunction of the serosa. No katatrepsis takes place upon depletion of *zen*, i.e. the embryo is not pulled out of the yolk by the contracting serosa as in wild type (Panfilio 2009; Panfilio 2006; Figure 4-1 A-J).

Based on these observations it is inferred that katatrepsis did not occur in *gbb*-RNAi embryos. This applies to all investigated *BMPsc* knockdown embryos as the embryonic and the egg AP axis were still inverted to each other after embryogenesis (3.1.1; Figure 3-1). The failure of katatrepsis in *BMPsc* knockdown embryos is in line with amniotic defects as

katatrepsis requires intact extraembryonic membranes (Panfilio 2008). For example, the serosa needs to fuse with the amnion to pull the germ rudiment out of the yolk, which is impossible if the amnion is strongly reduced or lost (Panfilio 2008; Figure 4-2).

The absence of katatrepsis could be also (additionally) caused by serosa defects. However, it appears likely that at least a part of the serosa was specified in all *BMPsc* knockdown embryos: first the presumed position of its anlage implies that it is in part specified by the AP patterning system (1.1.4; Figure 1-4). In addition, the abnormal constrictions observed in *dpp-*, *tld-*, *tsg-* and *sog*-RNAi embryos could be caused by serosal tissue since they appeared to originate from tissue on the egg surface and in wild type the serosa also constricts during katatrepsis (Figure 4-2 A-D; Figure 4-1 B-D, G-I; Panfilio 2008; Panfilio et al. 2006). It seemed though that the timing and the direction of the constriction differed from wild type (Figure 4-2 A-D). Either mechanical or molecular signals that prevent premature constriction of the serosa might be missing in knockdown embryos with these ectopic constrictions. This could be due to cells secreting such signals not being specified, or due to a loss or strong reduction of the amnion.

This is also consistent with the higher frequency of this constriction in *dpp* compared to *tsg* and *sog* knockdown embryos. It could be that it is impossible to create a "serosa control area", or rather an amnion-serosa contact region, in strongly ventralized embryos, but that the respective region is sometimes formed in dorsalized or lateralized embryos (Figure 4-2 compare A-D with E-H). Presumably this region was unaffected in *gbb*-RNAi embryos as these did not exhibit the previously described ectopic constriction.

Based on the assumptions that these ectopic constrictions are due to an abnormal serosa, this provides further evidence that extraembryonic membrane defects exacerbate with increasing perturbations of the BMP signaling activity gradient. Therefore, the failure of katatrepsis after *gbb*-RNAi might not be caused by a loss or strong reduction of the amnion, like presumed for *dpp*- *sog*-, and *tsg*-RNAi embryos, but rather by more subtle amniotic defects. One possible explanation for this failure is elucidated in the following (and in Figure 4-1 K-O).

Although the amnion was not largely absent, it was defective and therefore less robust to mechanical stress. Hence, the amnion would rupture when it is pulled by the contracting serosa during katatrepsis. Consequently, the embryo would not be pulled out of the yolk and would remain its inverse orientation with respect to the egg axes.

In summary, the degree of pMad gradient (the readout of the BMP gradient) perturbation correlates with that of morphological aberrations indicative for extraembryonic

membrane defects. Hence, BMP signaling appears to be required for the proper formation of extraembryonic membranes in *O. fasciatus*, presumably via specification of the amnion and possibly also a part of the serosa.

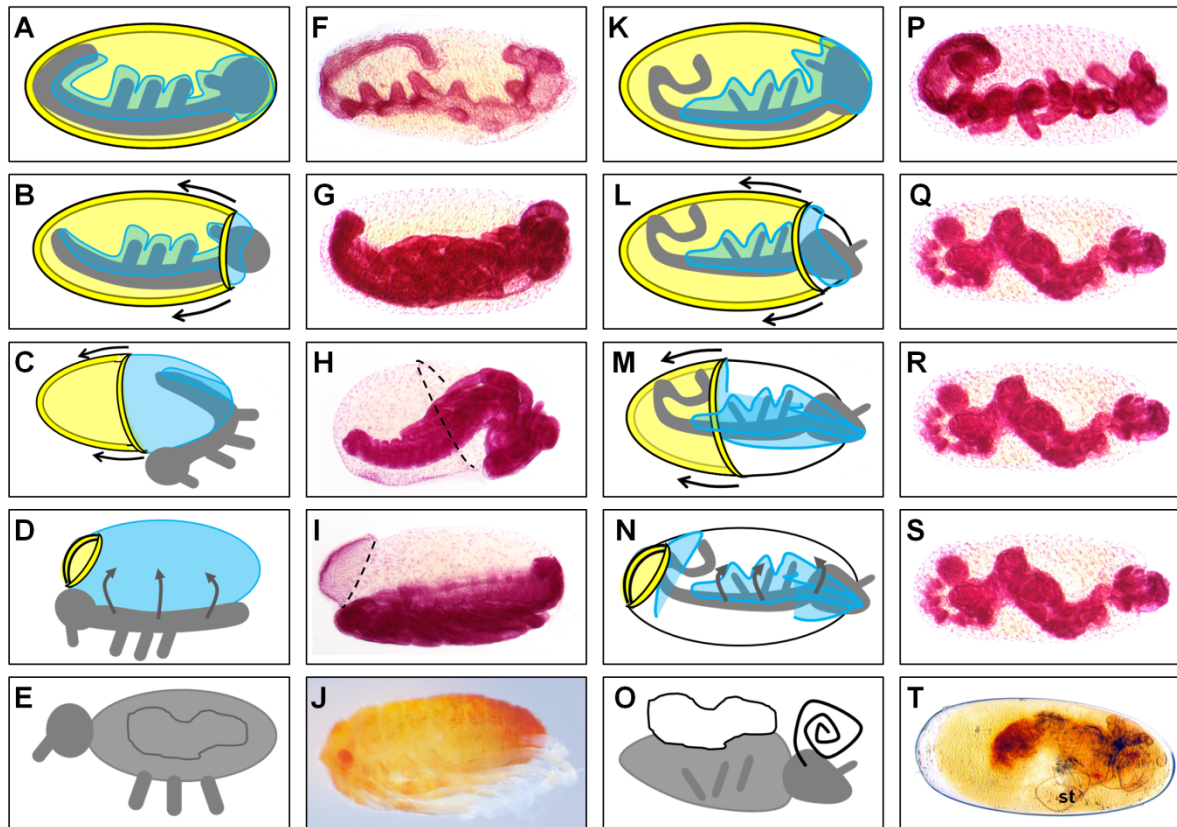


Figure 4-1: Failure of katasepsis in *gbb* knockdown embryos

Anterior of the egg is to the left. The view is always lateral with egg-ventral down. Wild type embryos exhibit an inverse orientation of the egg and the embryonic axes during germ band stages (A, F). Around mid-embryogenesis, after germ band retraction, katasepsis starts, the amnion (blue in A-D, K-N) and the serosa (yellow in A-D, K-N) fuse and rupture and the embryo (gray in A-E, K-O) is pulled out of the yolk (B-D, G-I). The embryonic and egg axes are congruent again and the body flanks grow and close dorsally (gray arrows) over the inner organs (irregular shape). The failure of katasepsis in *gbb*-RNAi embryos is proposed to be caused by a defective amnion that ruptured through the mechanical forces exerted by the contracting serosa (L-N). The embryo almost maintained its germ band orientation and the embryonic flanks grew over most limbs (gray bars in A-E, K-O) resulting in a (partially) everted embryo with exposed organ mass (white irregular shape) (N, O, T). As the embryo was slightly pulled by the contracting serosa before it lost its contact to the amnion, it became only partially everted (O). The black arrows indicate the direction in which the serosa (drawn in yellow) constricts. The embryo is drawn in gray, whereby the thickening indicates the head. The helical black line indicates stylets (O). The dashed black lines mark the posterior end of the serosa in H and I. A-E and K-O show schematic drawings; F-J display pictures of wild type embryos, P-T images of *gbb*-RNAi embryos. Abbreviation: st: stylets. The wild type katasepsis scheme was based on a drawing of Panfilio 2008.

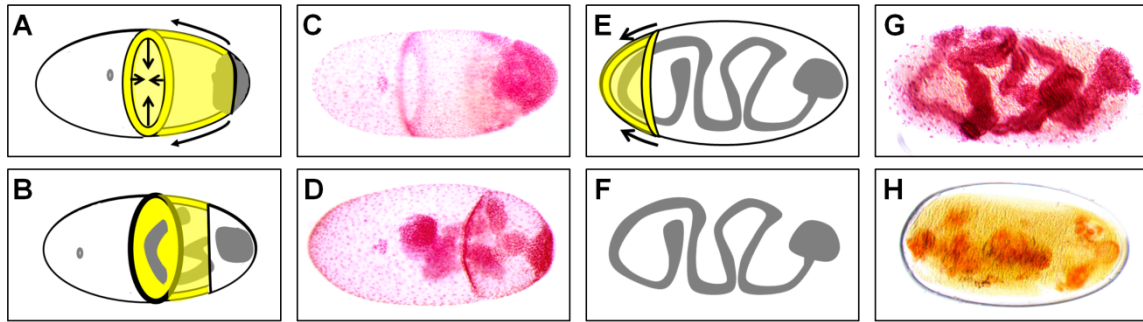


Figure 4-2: Premature serosa constriction and defective katanepsis in *BMPsc* knockdown embryos

Anterior of the egg is to the left. *BMPsc* knockdown embryos tend to form an ectopic constriction probably originating on the surface (D). This might already emerge during anatrepsis (C) and typically it was present in eggs with elongating germ bands (D). It is proposed that an "out of control" serosa (yellow) prematurely started to constrict through the yolk (A, B) instead of towards the anterior pole (Figure 4-1 A-F). *BMPsc* knockdown embryos, except *gbb*-RNAi embryos, without ectopic surface constrictions (G, H) were assumed to have had a normal functioning serosa that contracted towards the anterior pole around mid-embryogenesis (E). However, due to a (largely) absent amnion, the embryo was not pulled out of the yolk by the serosa and thus, kept its inverse orientation with respect to the egg axes (E, F, H). The arrows indicate the direction in which the serosa (drawn in yellow) constricts. The embryo is drawn in gray; the thickening indicates the head. A, B, E and F show schematic drawings; C, D display pictures of *dpp*-RNAi embryos, G, H image *tsg*-RNAi embryos.

4.2 Excursus: Crosstalk between DV and AP patterning during head specification

The establishment of the two major body axes, the AP and the DV axes, does often not occur completely independent of each other (Hashiguchi & Mullins 2013; Kotkamp et al. 2010; Schier & Talbot 2005; Tucker et al. 2008). Indeed, knockdown of Toll signaling components impaired not only DV axis formation, but also certain AP patterning aspects in *O. fasciatus* (unpublished data of Yen-Ta Chen). The influence of Toll signaling on AP patterning was most pronounced in the anterior 25% of the blastoderm. It seemed that the expansion of *twi*, *sog* and *sim* into the anterior region in *Toll-dpp* knockdown embryos was dependent on the disruption of Toll signaling (3.3.5.1; Figure 3-28; Table 3-11; unpublished data of Yen-Ta Chen). Hence, the anterior AP patterning system, referred to as the anterior terminal system, which is required to pattern the pregnathal head, might receive direct or indirect inputs from the DV patterning system. Intriguingly, differences in AP patterning between the pregnathal head region and the gnathal head plus trunk region are suggested to be ancestral for arthropods (Chipman 2010). Such differences could also account for a crosstalk of only this part of the AP patterning system with the DV patterning system.

In agreement with this assumption, *BMPsc* knockdown embryos appeared to establish all En-expressing segments¹⁰, but exhibited severe head defects (3.2). However, the head is a very complex structure, which might be therefore sensitive to a variety of developmental perturbations. In fact the head was also described to be defective in many naturally occurring mutants in *O. fasciatus* (Panfilio et al. 2006). Therefore, head patterning of the knockdown phenotypes was analyzed with the help of blastoderm marker gene expression. Intriguingly, *msh* expression is reduced or even lost in *dpp*-RNAi embryos during late blastoderm stages (3.3.2.1; Figure 3-10 O, P; Table 3-3). One would expect that the ventral expression domain, present in late blastoderm stages, would expand around the whole circumference in completely ventralized embryos. Likewise, *msh* appeared to be down regulated in *sog*-RNAi embryos, although an expansion of the dorsal-lateral domain of strong *msh* expression was expected (3.3.4.1; Figure 3-21 H, H'). The unexpected behavior of *msh* expression in these knockdown embryos might reflect a special interaction between the terminal patterning system and BMP signaling. Alternatively, the regulation of *msh* expression might be peculiar. Interestingly, *msh* is directly regulated by BMP signaling in many bilaterians (Oh et al. 2002; Alvarez Martinez et al. 2002; Tribulo et al. 2003; Suzuki et al. 1997). It is conceivable that high BMP signaling levels are required to initiate *msh* expression on the dorsal side and that more ventral *msh* expression depends on the prior establishment of the dorsal *msh* domain¹¹. However, the anterior *sog* expression domain, which is presumably located within the pregnathal head anlage, was not simply dorsally expanded upon a *gbb* knockdown but in addition it was thinner and abnormally shaped (Figure 3-13 K). Furthermore, preliminary expression analysis of *crocodile* (*croc*), which is expressed in the ventral labrum anlage, indicated *croc* expression to be expanded in ventralized as well as in dorsalized/lateralized *BMPsc* knockdown embryos at the blastoderm stage (Birkan et al. 2011; data not shown). These results suggest that expression patterns in the pregnathal head region of the blastoderm deviate from their expected behavior in *BMPsc* knockdown embryos. However, expression patterns in the pregnathal head region need to be analyzed in more detail in *BMPsc* knockdown and wild type embryos to explore if and why they might be influenced by BMP signaling in a different manner than the ones expressed in the posterior 75% of the blastoderm.

In conclusion, the DV and the anterior terminal patterning system appear to interact via Toll signaling to restrict the expression of several genes to the posterior 75% of the

¹⁰ pregnathal head segments do not express En (Liu & Kaufman 2004).

¹¹ In uniform blastoderm stages *msh* is only dorsally expressed (3.3.1.3; Figure 3-7 D).

blastoderm. However, the role of BMP signaling in the crosstalk between the terminal and DV patterning system still remains elusive.

4.3 BMP gradient formation requires Tsg and Sog

The severe morphological defects probably resulting in part from misspecification of extraembryonic tissue impressively demonstrate that the proper formation of a BMP signaling activity gradient is indispensable for normal development. But how is this gradient established?

The BMP antagonist Sog is famous for its involvement in BMP localization and gradient formation throughout the animal kingdom (Dorfman & Shilo 2001; Mizutani et al. 2005; van der Zee et al. 2006; Lapraz et al. 2009; Akiyama-Oda & Oda 2006; Wagner & Mullins 2002; De Robertis & Kuroda 2004). Indeed, the pMad gradient (the readout of the BMP gradient) was strongly impaired upon depletion of *sog* in *O. fasciatus* (3.3.4.1; Figure 3-19). This suggests that Sog is required for BMP activity gradient formation, presumably via binding and transporting BMP ligands. The similarity of the *tsg* knockdown phenotype to the one caused by *sog* depletion further confirmed this assumption (3.3.4.1; compare Figure 3-21, 3-23 with Figure 3-22, 3-24). Tsg is important for the efficient action of Sog, as complexes of Tsg and Sog have a much higher affinity to BMP ligands than either of these proteins alone in vertebrates and invertebrates (Shimmi & O'Connor 2003; Ross et al. 2001; Shimmi et al. 2005). Thus, Tsg assists Sog in binding and shuttling BMP ligands. The knockdown of *tsg* affects pMad distribution even more severely than that of *sog* in *O. fasciatus* (3.3.4.1; Table 3-10). The absence of a detectable pMad asymmetry in many of these knockdown embryos indicated that a strong depletion of *tsg* is accompanied by an entirely symmetric pMad distribution (3.3.4.1; Figure 3-20; Table 3-10). However, while *sog* is expressed at very high levels in wild type and could still be weakly detected by *in situ* hybridization in *sog*-RNAi embryos, *tsg* expression was not even detectable in wild type embryos (3.3.1.2; 3.3.4.1; Figure 3-6 D, 3-7 B, F, J, 3-21 F). This implies that *tsg* is either expressed at very low levels or maternally provided. The failure to detect it in pre-blastoderm embryos as well as in ovaries points to the first possibility (data not shown). In addition, it was possible to amplify *tsg* transcripts from cDNA of blastoderm embryos (7.2). Hence, the higher frequency of *sog* knockdown embryos with a DV asymmetric pMad distribution compared to *tsg* knockdown embryos is probably simply due to a different knockdown efficiency based on distinct

expression levels (3.3.4.1). In conclusion, the complete depletion of *sog* or *tsg* would probably result in equal levels of BMP signaling activity along the egg circumference. Furthermore, the symmetric expression of dorsal and ventral ectoderm markers along the DV axis of *sog* and *tsg* knockdown germ band embryos indicates a loss of DV polarity in the absence of *tsg* or *sog* (3.3.4.1; Figure 3-23, 3-24). The consequences for the early embryonic fate map in embryos depleted for *sog* or *tsg* are also very similar in *D. melanogaster* (Mason et al. 1994; Ross et al. 2001; Decotto & Ferguson 2001). However, the complete loss of function (lof) of *sog* causes a dramatic impairment of pMad distribution in *D. melanogaster*, but pMad is still localized to the dorsal side of the blastoderm (Dorfman & Shilo 2001; Sutherland et al. 2003). The residual DV polarity of the pMad distribution in *sog*-depleted *D. melanogaster* embryos might rely on the local restriction of several BMP components to the dorsal side as well as on a feedback mechanism that helps to establish the later, step-like pMad gradient (Shimell et al. 1991; Mason et al. 1994; Jackson & Hoffmann 1994; Wang & Ferguson 2005). The local restriction of BMP signaling components in *D. melanogaster* depends on their transcriptional control by Toll signaling, which restricts *dpp* expression to the dorsal 40% of the egg circumference and activates the BMP repressor *brinker* (*brk*) (Jaźwińska et al. 1999).

In summary, Sog and Tsg are required to establish embryonic DV polarity in *O. fasciatus*. This indicates a high impact of BMP signaling on the DV patterning system of *O. fasciatus*.

4.4 The main DV patterning function of Tsg is dependent on Sog

In various species Tsg/Cv-1 is known to modulate BMP signaling also independently of Sog (Wang & Ferguson 2005; Nunes da Fonseca et al. 2010; Oelgeschlager et al. 2003; Xie & Fisher 2005; Little & Mullins 2004). It was proposed to either help to present BMP ligands to their receptors, to antagonize another extracellular inhibitor of BMP, or even to be required for Dpp intracellular processing or secretion (Wang & Ferguson 2005; Nunes da Fonseca et al. 2010; Little & Mullins 2004). The evidence for such a Sog-independent BMP-promoting function of Tsg greatly differs in distinct species. In *D. melanogaster* and *Xenopus* such a role of Tsg is largely masked by its Sog-dependent functions (Blitz et al. 2003; Harland 2001; Ross et al. 2001; Shimmi et al. 2005; Wills et al. 2006). In contrast, the knockdown of *tsg* in the zebrafish *Danio rerio* revealed its pro BMP function, as markers expressed on the neural

side (dorsal in vertebrates) were expanded in these embryos (Xie & Fisher 2005). Most obvious is its Sog-independent, BMP-promoting function in *T. castaneum* and *N. vitripennis* where its depletion mimics that of *dpp* (Nunes da Fonseca et al. 2010; Özüak 2014). Intriguingly, BMP-promoting or BMP-antagonizing functions of *tsg* may vary in a tissue-dependent manner. For example, the lof of *tsg* causes an atrophic thymus in mice with elevated pSmad1 levels in thymocytes, which is indicative of enhanced BMP signaling activity in this tissue, whereas skeletogenesis is also impaired, a phenotype associated with diminished BMP signaling activity (Nosaka et al. 2003). Furthermore, BMP signaling is known to be required for the self-renewal of germline stem cells in *D. melanogaster* (Xie & Spradling 1998). A BMP-promoting role of Tsg during this process in *O. fasciatus* could account for the cumulative sterility effect upon a synchronous knockdown of *dpp* and *tsg* (3.3.4.4). Hence, the different weight of Tsg's Sog-dependent and -independent functions in distinct species during DV patterning are likely due to different molecular environments. Thus, whether Tsg mainly exerts a positive (Sog-independent) or negative (Sog-dependent) influence on BMP signaling activity likely depends on the presence or absence of other molecules. Among such molecules could be components of the extracellular matrix (ECM), which are shown to be involved in BMP signaling (Bornemann et al. 2008; Jiao et al. 2007; Lapraz et al. 2009; Wang et al. 2008; Yanagita 2009). For instance, heparan sulfate proteoglycans (HSPGs) and Collagen IV can bind to BMP ligands in insects, sea urchins¹², worms¹³ and vertebrates (Bornemann et al. 2008; Jiao et al. 2007; Lapraz et al. 2009; Wang et al. 2008; Yanagita 2009). In *D. melanogaster* Tsg was reported to facilitate the release of BMP from Collagen IV (Wang et al. 2008). Unfortunately, it was not possible to amplify *collagen IV* transcripts from embryonic cDNA of *O. fasciatus*. Furthermore, the knockdown of several genes encoding ECMs (*pcan*: 3.3.1.3, *syndecan*: encodes core protein of HSPGs, *dally*: encodes a glypican and *slalom*: involved in HSPG synthesis) caused either no phenotype at all (*slalom* and *dally*), or no DV defects (*pcan* and *syndecan*) (Spring et al. 1994; Nosaka et al. 2003; Lüders et al. 2003; Friedrich et al. 2000; data not shown). These negative results might be due to a failure of pRNAi, or to pleiotropy and redundancy of ECM components (Weisbrod et al. 2013).

Nevertheless, the main DV patterning function of Tsg appears to be to establish DV polarity most likely in concert with Sog by protecting the ventral side from BMP signaling activity in the *O. fasciatus* embryo.

¹² only evidence for a physical interaction of HSPG and BMP.

¹³ only evidence for a physical interaction of Collagen IV and BMP.

4.5 Growth zone patterning might dependent on posterior signaling centers established at the onset of gastrulation

In many species posterior segments are sequentially formed from a posteriorly located region of undifferentiated cells (Peel & Akam 2003). For example, somites (mesoderm units) are progressively established from a posterior region of the vertebrate embryo (Hester et al. 2011). The short germ mode of embryogenesis, which is considered as ancestral mode of development in insect, also involves successive formation of posterior segments (Roth 2004; Davis & Patel 2002). Since the best understood and analyzed insect model organism, *D. melanogaster*, is a long germ insect, patterning of the growth zone is not well understood, yet. However, knockdown of *gbb* or *sax* mainly impairs DV patterning of the growth zone in *T. castaneum*, indicating that DV fates of growth zone-derived segments are established by a mechanism partially distinct from that setting up the DV pattern of more anterior segments (Weber 2006; unpublished data of Rodrigo Nunes da Fonseca and Siegfried Roth).

The knockdown of *gbb* in *O. fasciatus* also revealed differences in DV patterning of blastoderm- and growth zone-derived segments. Thus, while the head and thorax appear to be lateralized, the abdomen of *gbb*-RNAi embryos is ventralized (3.3.2.4; Figure 3-14; Table 3-9). *gbb* appears to be required for the establishment of a dorsal, posterior domain of high BMP signaling activity at the onset of gastrulation (3.3.2.3; Figure 3-12; Table 3-6). The absence of this domain might be responsible for the posteriorly restricted ventralization in late blastoderm stages of *gbb* knockdown embryos (3.3.2.3; Figure 3-13 I, I', K').

But what is the reason for the strong dependency of this posterior peak of pMad concentration on *gbb*? It is unlikely that Gbb homodimers are responsible for this observed high posterior BMP signaling activity. Homodimeric BMP ligands, especially of the BMP5/6/7/8/Gbb/Scw group, are reported to have a lower signaling activity than BMP heterodimers (Valera et al. 2010; Shimmi et al. 2005; Zhu et al. 2006; Israel et al. 1996; Hazama et al. 1995). For instance, Scw homodimers produce only 10% to 20% of the BMP signal that Dpp homodimers generate when expressed in S2 cells, and Dpp-Scw heterodimers could be demonstrated to activate BMP signaling ten times more efficiently than Dpp homodimers in *D. melanogaster* (Shimmi et al. 2005). Consequently, the high posterior pMad levels in late blastoderm stages of *O. fasciatus* embryos are probably dependent on Dpp-Gbb heterodimers. The different signaling potential of Gbb-Gbb, Dpp-Dpp and Dpp-Gbb BMP dimers is presumably dependent on their distinct preference for BMP type I receptors

(Nguyen et al. 1998; Neul & Ferguson 1998; Haerry et al. 1998).¹⁴ High signaling activity of BMP (Dpp-Gbb) heterodimers is believed to be based on the efficient formation of BMP receptor complexes containing Sax (homolog to vertebrate Alk2/8) and Tkv (homolog to vertebrate Alk3/6) (Little & Mullins 2009; Shimmi et al. 2005).

Therefore, it was quite puzzling that *sax*-RNAi embryos neither exhibited a stronger ventralization of the posterior pole region compared to the remaining germ rudiment in late blastoderm stages, nor of abdominal segments (3.3.3.3; Figure 3-17; 3.3.3.4; Figure 3-18). In addition, the presence of a second *sax* gene in *O. fasciatus* is unlikely, as no second *sax* homolog could be identified in closely related species.¹⁵ It is conceivable that an increased amount of Tkv, in addition with an enlarged quantity of BMP ligands, might compensate for a *sax* depletion. This would require a feedback mechanism, which ensures that enough BMP signaling activity is produced above the posterior indentation at the onset of gastrulation.¹⁶ Interestingly, Sax can also antagonize BMP signaling by trapping of Gbb ligands in an inert receptor complex (containing Sax-Sax), *i.e.* *sax* depletion itself could increase the amount of BMP ligands that are available for signaling (Bangi & Wharton 2006b). This might also ameliorate the *sax*-RNAi phenotype.

Interestingly, the region of high BMP signaling activity close to the posterior pole in late blastoderm stages matches a domain of strong *dpp* expression (3.3.1.1; 3.3.1.2; compare Figure 3-5 B with Figure 3-6 B). The action of Dpp homodimers is often quite locally restricted as they are trapped by receptors and other ECM components (Bangi & Wharton 2006a; Eldar et al. 2002; Ohkawara et al. 2002). For instance, during wing disc patterning Gbb homodimers and Dpp-Gbb heterodimers can act in a much longer distance from the site of their secretion than Dpp homodimers (Bangi & Wharton 2006a). Hence, this local source of high Dpp levels might help to concentrate BMP signaling activity in this area. Intriguingly, in contrast to other *BMPsc*-RNAi embryos, the posterior pole and the abdominal segments were more resistant to ventralization than the anterior segments in weak *dpp*-RNAi phenotypes (3.3.2.2; compare Figure 3-11 with Figure 3-14, 3-23). BMP monomers were

¹⁴ Sax preferentially binds Gbb, while Tkv preferentially binds Dpp (Neul & Ferguson 1998; Nguyen et al. 1998; Haerry et al. 1998).

¹⁵ No second *sax* homolog could be identified by BLAST searches in the closely related species, *Acyrtosiphon pisum* (an aphid), *Pediculus humanus* (a louse) or *Rhodnius prolixus* (a blood-sucking bug). Yet the genome sequence of the latter is incomplete so that it was not possible to retrieve the sequence of any BMP type I receptor encoding gene (data not shown).

¹⁶ This in turn would be responsible for an upregulation of the expression of BMP type I receptors and maybe also of BMP ligands in *sax*-RNAi embryos. This could (partially) restore wild type-like BMP signaling activity in this region through lowering the knockdown efficiency and/or through increasing the concentration of Tkv and/ or BMP ligands. Monitoring *dpp* and *tkv* expression in *gbb* and *sax* knockdown embryos could reveal if this feedback mechanism is impaired or alleviates the knockdown effect, respectively.

reported to form rather hetero- than homodimers (Hazama et al. 1995). On this assumption the residual, posteriorly localized, Dpp monomers of weak *dpp*-RNAi embryos could have efficiently formed heterodimers with Gbb, which was newly synthesized and possibly also re-up taken.¹⁷ A higher Tsg-Sog to BMP ligand ratio could have facilitated the shuttling of BMP ligands (including Dpp-Gbb in weak *dpp* knockdown embryos) to the dorsal side of the posterior pole in *dpp*-RNAi embryos.¹⁸ Hence, the stronger resistance of the posterior pole region to ventralization in weak *dpp* knockdown compared to other *BMPsc* knockdown embryos would require Sog, Tsg and Gbb. Indeed, *dpp-sog* double knockdown embryos with an incomplete ventralization exhibited a stronger ventralization around the posterior pole in late blastoderm stages compared to the remaining germ rudiment (3.3.4.3; Figure 3-25 E).

The findings described above suggest that the establishment of the posterior peak BMP signaling activity requires Dpp-Gbb heterodimers from different sources: directly locally secreted as well as shuttled towards this site by Tsg-Sog complexes.¹⁹

But what is the purpose of such a locally restricted high BMP signaling activity? There was a clear connection between ventralization around the posterior pole and of the abdominal segments. The strength of posterior ventralization, or rather restoration of ventral fates, relative to the remaining germ rudiment during late blastoderm stages correlated to that of the abdomen during germ band stages in *BMPsc*-RNAi embryos (e.g. both were most pronounced in *gbb* knockdown embryos) (3.3.2.4; Figure 3-13, 3-14). Differences of DV pattern along the AP axis were presumably too subtle to detect it by *in situ* hybridization already during blastoderm stages in those *BMPsc* knockdowns where these became only apparent during germ band stages (3.3.4.2; Figure 3-21, 3-23).

To account for growth zone specific phenotypes, it is assumed that DV patterning of the growth zone requires the establishment of two "signaling centers" at the onset of

¹⁷ Internalized ligands are reported to recycle, probably dependent on their ability to bind their receptors at an acidic pH (Fazio et al. 2000). However, while BMP receptors were demonstrated to be either degraded or to recycle through the Golgi apparatus, little is known about the fate of the simultaneously internalized BMP ligands (Jortikka et al. 1997; Kim et al. 2012; Gleason et al. 2014). In rat myoblasts internalized BMP ligands become mainly degraded (Jortikka et al. 1997). Interestingly, BMP receptor recycling is dependent on auxiliary proteins, which can be tissue and receptor specific (Kim et al. 2012; Gleason et al. 2014). It is conceivable that BMP ligands can recycle as well depending on other factors, e.g. co-receptors which tighten the binding of BMPs to their receptors at an acidic pH.

¹⁸ The localization of Dpp would not be affected by this ratio because of a high concentration of "Dpp-trapping" molecules, *i.e.* receptors and other Dpp-binding ECM components, around the posterior pole. The different susceptibility to posterior ventralization upon a *gbb* and a *dpp* knockdown could be explained by assuming that many of these "Dpp-trapping" molecules are not BMP receptors and bind Dpp but not Gbb with high affinity.

¹⁹ Locally secreted Dpp-Dpp ligands might be mainly trapped by ECM components without subsequent signal transduction. Gbb-Gbb dimers might mainly contribute to the signaling by being taken up by cells in the posterior region in which they dissociate from each other, become bound to Dpp instead and re-secreted as Dpp-Gbb dimers.

gastrulation: firstly, a ventral signaling center, which is marked by a high *twi* expression level and auto-enhancement (maybe even via self-enhancement of *twi*). Prevention of a ventralization through this self-enhancing mechanism of the ventral signaling center is achieved by a second, dorsal signaling center with very high BMP signaling activity, which requires BMP heterodimers. These signaling centers retain their embryonic-posterior position during anatrepsis and are consequently located in the growth zone in germ band stages. Presumably, their signals not only assure proper DV patterning of growth zone-derived segments, but also influence the DV pattern of segments established during the blastoderm stage (Figure 4-3). This might, for example, occur via diffusion of secreted ventralizing and dorsalizing molecules, which influence the DV pattern of adjacent cells and also activate secretion of such signaling molecules in these cells. This could explain the graded weakening of ventral marker expression towards the anterior of the germ rudiment in some *BMP_{sc}*-RNAi embryos, especially *gbb*-RNAi embryos (3.3.2.4; Figure 3-14; 3.3.4.2; Figure 3-23). In addition, it could account for the alteration of blastoderm-derived DV pattern during the germ band stage, which was observed in several *BMP_{sc}* knockdown embryos (3.3.2.4-3.3.3.4; compare Figure 3-13 and 3-17 with Figure 3-14 and 3-18).

Intriguingly, BMP signaling activity becomes also enhanced dorsal to the posteriorly localized, primitive pit at the onset of gastrulation in *T. castaneum* (van der Zee et al. 2006). Further investigation of growth zone DV patterning in *O. fasciatus* and *T. castaneum* could elucidate more common and potentially ancestral features of this patterning system.

In summary, DV fates that are established prior to gastrulation, still exhibit some plasticity, and proper DV patterning of growth zone-derived segments requires a locally restricted source of high BMP signaling activity in *O. fasciatus*.

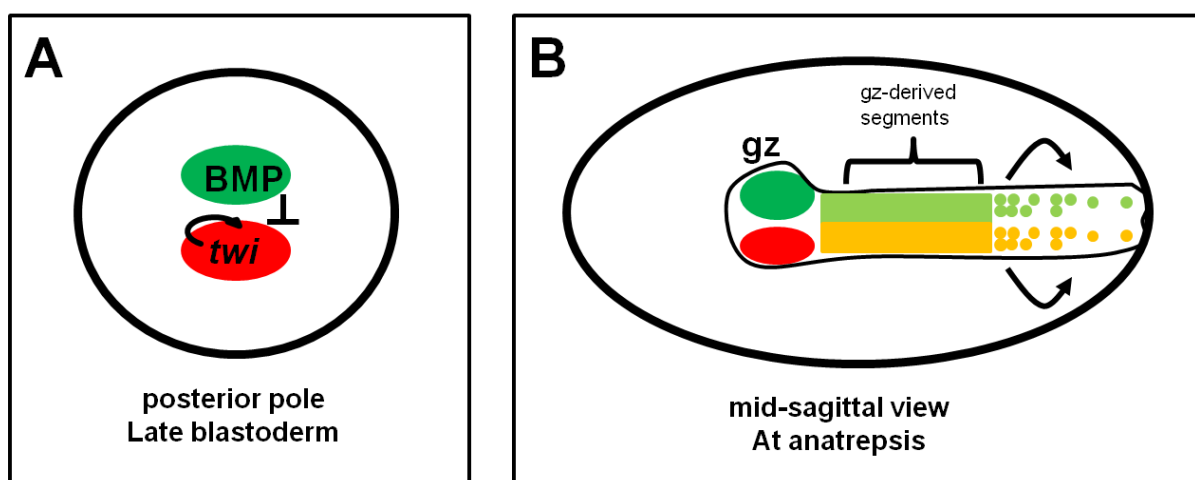


Figure 4-3: Model of DV patterning in the growth zone of *O. fasciatus* and its influence on anterior segments

It is proposed that at the onset of gastrulation a "dorsal signaling center" (green oval) and a "ventral signaling center" (red oval) are established above or below the posterior indentation, respectively (A). The dorsal signaling center is marked by high BMP signaling activity, which is required to prevent expansion of the self-enhancing "ventralizing, *twi*-expressing center" (A). These signaling centers retain their embryonic-posterior position as tissue invaginates, hence they are localized in the growth zone in germ band stages. They establish ventral and ventral-lateral (orange bar: ventral and ventral-lateral fates specified by the ventral gz signaling center) as well as dorsal and dorsal-lateral (light green bar: dorsal and dorsal-lateral fates specified by the dorsal gz signaling center) fates in the segments arising from the growth zone (B). In addition, the DV pattern of blastoderm-derived segments becomes influenced by the growth zone DV patterning system: the stronger the closer the respective segments are to the growth zone-originated segments (B). Colored dots in blastoderm-derived segments indicate this influence. The arrows indicate local signaling activity influence. Abbreviation: DV: dorsal-ventral, gz: growth zone.

4.6 BMP heterodimers might be required for shaping of the BMP signaling activity gradient

BMP heterodimers also play a role in DV patterning prior to gastrulation in *O. fasciatus*. The use of two BMP ligands to pattern the DV axis, one from the BMP2/4 group and one of the BMP5/6/7/8 group, seems to be very widespread within the animal kingdom (Schmid et al. 2000; Saina et al. 2009; Shimmi et al. 2005; Nishimatsu & Thomsen 1998; Özüak 2014). However, while the depletion of one of both BMP ligands leads in many species to the almost complete prevention of BMP signaling during early DV patterning, this does not apply to *O. fasciatus* (Schmid et al. 2000; Saina et al. 2009; Dorfman & Shilo 2001; Raftery & Sutherland 2003; Özüak 2014). Only the loss of *dpp*, but not of *gbb*, appeared to entirely inhibit BMP signaling activity in the *O. fasciatus* blastoderm (3.3.2.1; Figure 3-9; 3.3.2.3; Figure 3-12; Table 3-6). Interestingly, Tsg-Sog complexes preferentially bind to BMP heterodimers in *D. melanogaster* (Shimmi et al. 2005). A higher affinity of Tsg-Sog complexes to BMP heterodimers (Dpp-Gbb) than homodimers (Dpp-Dpp) could explain the early *gbb*-RNAi phenotype of *O. fasciatus*. The depletion of *gbb* would lead to the formation of more Dpp homodimers, which are less mobile than Dpp-Gbb (in part) because of their lower affinity to Tsg-Sog complexes (and because of the aforementioned immobilization of Dpp via trapping by ECM components) (Bangli & Wharton 2006a; Eldar et al. 2002; Ohkawara et al. 2002; Shimmi et al. 2005). This would result in the observed higher BMP signaling activity on the ventral side accompanied by less BMP signaling activity on the dorsal side, *i.e.* a flatter pMad gradient after *gbb*-RNAi (3.3.2.3; Figure 3-12; Table 3-6; Figure 4-4). The negative influence

of BMP signaling on ventral fates most likely caused the lateralization of *gbb*-RNAi uniform blastoderm embryos (3.3.2.3; Figure 3-13; Figure 4-4).

In summary, Dpp-Dpp homodimers and Dpp-Gbb heterodimers both seem able to fully activate BMP signaling, but Dpp-Gbb dimers are probably required to sharpen the BMP signaling activity gradient.

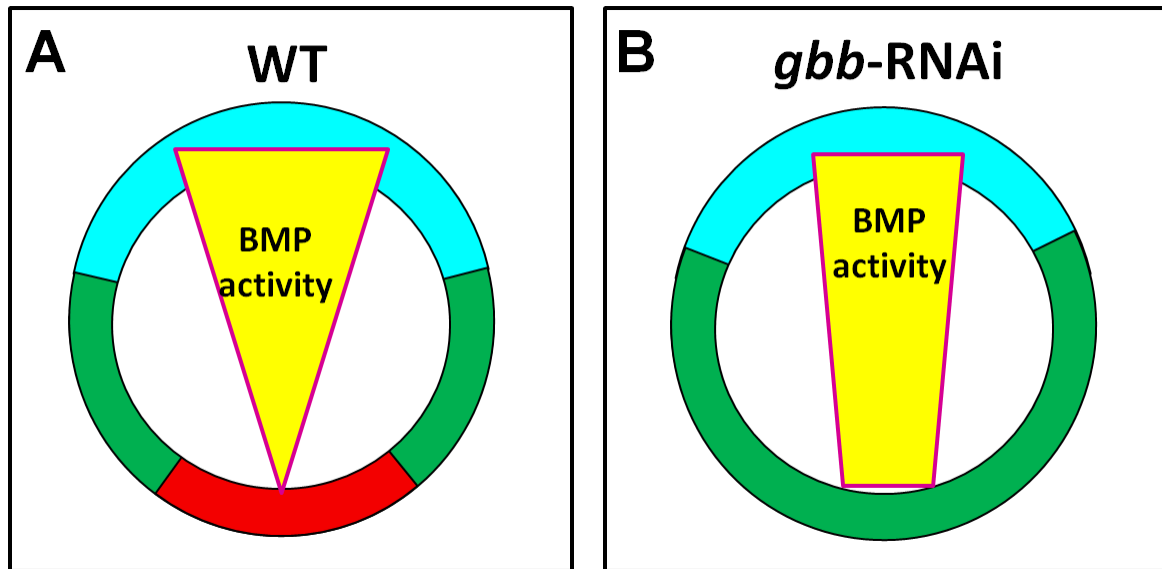


Figure 4-4: *gbb*-RNAi embryos exhibited a flattened pMad gradient

The observed lateralization (elucidated in this section), *i.e.* the expansion of the prospective neuroectoderm (green) at the expense of the future dorsal ectoderm (blue) and mesoderm (red) of *gbb*-RNAi embryos might be caused by a flattened BMP activity gradient (yellow triangle or trapezoid with pink outline). A schematic transection of a WT (A) and a *gbb*-RNAi (B) blastoderm embryo at 26 hpf is shown. Abbreviation: hpf: hours post fertilization, WT: wild type.

4.7 BMP heterodimers might contribute to robust patterning

The use of BMP heterodimers during DV patterning might also have a further reason. It could be demonstrated by computational modeling that the DV patterning system of *D. melanogaster* is more robust if BMP heterodimers are available. Thus, the formation of Dpp-Scw heterodimers strongly increased the ability to compensate for fluctuations in gene dosage in the model (Shimmi et al. 2005). Indeed, there is also evidence for such a role of Dpp-Gbb heterodimers in *O. fasciatus*. The knockdown of *gbb* caused a very broad range of different DV phenotypes, from embryos without DV polarity (3.3.2.3; Table 3-6; Figure 3-12 C, F) to those with a very clear, or even wild type-like DV asymmetry (3.3.2.3; Table 3-6; Figure 3-12 B, E). This is consistent with the similarly variable DV phenotypes of *sax*-RNAi embryos, as

gbb and *sax* are both involved in BMP signaling via heterodimers (3.3.3.3; Figure 3-17; Shimmi et al. 2005; Little & Mullins 2009). The observed phenotypic diversity upon knockdown of *gbb* or *sax* might reflect decreased buffering of random gene dosage fluctuations in those embryos.

Hence, Dpp-Gbb BMP heterodimers might contribute to robustness of the *O. fasciatus* DV patterning system.

4.8 BMP signaling restricts mesoderm formation

The different power of Toll and BMP signaling in DV patterning systems of distinct insects becomes most obvious in comparing the influence of both pathways on mesoderm specification. Toll signaling is most active on the ventral side in insects (Roth et al. 1989; Chen et al. 2000; Cande et al. 2009; Buchta 2014; unpublished data of Yen-Ta Chen). Therefore, it is not surprising that the formation of the ventral-most fate is entirely, or almost entirely, dependent on Toll signaling in the fly *D. melanogaster* and the beetle *T. castaneum*. Thus, the mesoderm is not or only slightly affected by lof or gain of function (gof) (e.g. via depletion of *sog*) of *dpp* in *D. melanogaster* and *T. castaneum*, respectively (Nunes da Fonseca et al. 2008; Jaźwińska et al. 1999; Markstein et al. 2002; van der Zee et al. 2006). In contrast, BMP signaling was demonstrated to be required to restrict the mesodermal fate in *O. fasciatus*, as the germ rudiment consists only of mesoderm in strong *dpp*-RNAi embryos (3.3.2.1; Figure 3-10, 3-11). Furthermore, the correlation of elevated ventral pMad levels, which were observed upon knockdown of *gbb*, *sog* and *tsg*, with depletion of the mesoderm, indicated that BMP signaling can even completely repress mesodermal fate (3.3.4.1; 3.3.2.3; Figure 3-12, 3-13, 3-19, 3-20, 3-21, 3-22). A restriction of mesodermal fate by BMP signaling could also be revealed by the expansion of *twi* upon *dpp* knockdown in the wasp *Nasonia vitripennis* (Özüak 2014). Toll signaling directly activates *twi* and *sog* in *D. melanogaster* and in *T. castaneum* (Stappert 2014; Markstein et al. 2002). Furthermore, Toll signaling was also shown to be indispensable for *twi* activation in *N. vitripennis* (Buchta 2014). In contrast, this cannot apply to *O. fasciatus*, as both *twi* and *sog* were expanded upon the synchronous knockdown of *Toll* and *dpp* (3.3.5.1; Figure 3-28). In addition, the initial ubiquitous expression of *sog* was not affected in *Toll*-RNAi embryos (3.3.5.2; Figure 3-30). We found that uniform *sog* expression is gradually transformed into ventral *sog* expression, which is present in blastoderm embryos from 25 hpf onwards (Figure 3-30 A-C, 3-7 B). Thus, *sog*

becomes ventrally enhanced and dorsally repressed. Hence, the ventral side, or rather the side where *sog* expression becomes enhanced, has to be determined. Determining the ventral side is probably achieved by asymmetric Toll signaling, as ventral *sog* enhancement is lost in *Toll* knockdown embryos (unpublished data of Yen-Ta Chen).

In summary, BMP signaling is required to restrict the mesodermal fate and can also entirely repress it, whereas Toll signaling appears to be required for the maintenance of this fate but not for its induction in *O. fasciatus*.

4.9 BMP signaling represses *sog*

Compared to holometabolous insects, Toll signaling has less influence not only on the activation of *sog* in *O. fasciatus* but also on its restriction during DV patterning. *O. fasciatus* embryos with a knockdown of *dpp*, *gbb* or *sax* exhibited an expanded *sog* domain (3.3.2.1; Figure 3-10 K, L; 3.3.2.3; Figure 3-13 J, P, K; 3.3.3; Figure 3-17 F-G'). This strongly indicated that BMP signaling negatively regulates *sog* expression in *O. fasciatus*. In contrast, the loss of *dpp* does not influence the expression of *sog* in *D. melanogaster*, although it causes an expansion of the neuroectoderm, which harbors the expression domain of *Dm-sog* (Ferguson & Anderson 1992b; Irish & Gelbart 1987; Wharton et al. 1993; Srinivasan et al. 2002).

The opposite also holds true: if *dpp* expression is expanded and overlaps the *sog* expression domain, the latter is not reduced in *D. melanogaster* (Ferguson & Anderson 1992b; Jaźwińska et al. 1999). This has been shown through the analysis of the *brinker* (*brk*) mutant. The lof of *brk* leads to a strong impairment of the negative regulation of *dpp* by Toll signaling, while the remaining regulatory capacity of Toll signaling is not affected (Jaźwińska et al. 1999). This demonstrated that the localization of *sog* expression is entirely dependent on Toll signaling in *D. melanogaster*. The same seems to be true for *T. castaneum*, as *sog* expression is not altered in *dpp*-depleted embryos (unpublished data of Rodrigo Nunes da Fonseca and Siegfried Roth).

Interestingly, negative regulation of *sog/chd* by BMP signaling was found in vertebrates and spiders (Akiyama-Oda & Oda 2006; De Robertis & Kuroda 2004; Reversade & De Robertis 2005). This suggests that negative feedback regulation of *chd/sog* by BMP is ancestral. However, the nature of this regulation is still unexplored in these animals. Thus, it remains unclear if BMP signaling leads directly to the repression of *sog*, or indirectly, for

example, via activation of a repressor. The frequent presence of a negative influence of BMP signaling on *sog* expression across the phylogeny could also be a product of analogous evolution. It is conceivable that a feedback mechanism where BMP signaling negatively regulates its own inhibitor *sog* contributed to the self-regulatory capacity of DV patterning systems and was therefore invented several times in evolution. Further investigation of this regulation in different lineages, e.g. searching for conserved pMad-Medea binding sites in *sog* promoters, could clarify the situation.

4.10 The evolution of Toll signaling in DV patterning: From a trigger to a ruler

In this section I will integrate results of this study with those of my colleague Yen-Ta Chen in a model of the DV patterning system of *O. fasciatus*.

We have seen that BMP signaling is required for the restriction of the ventral-most fate, the mesoderm, and of its own inhibitor *sog*, and that it is even able to completely repress both (4.8; 4.9). Furthermore, BMP signaling activity needs to be inhibited on the ventral side by Tsg and Sog to break DV symmetry (4.3). Toll signaling is also necessary to break DV symmetry (3.3.5.2; Figure 3-29; Table 3-12). Therefore, it is tempting to speculate that Toll signaling does this by influencing the activity of *sog* or *tsg*. However, as elucidated in 4.8 it is not required for the initial activation of *sog*, and by semi-quantitative PCR (semi-qPCR) it was indicated that *tsg* expression levels are not significantly changed upon the knockdown of *Toll* (7.2).

DV polarity in *O. fasciatus* embryos might be established as shown in Figure 4-5. We assume that, not only *sog* but also *tsg* and *dpp*, are initially ubiquitously expressed, although we were not able to monitor the early *tsg* and *dpp* expression, probably because of their low levels (it is, however, possible to amplify *tsg* and *dpp* transcripts from cDNA of blastoderm embryos) (3.3.1.2; Figure 3-6 A, D). This would be consistent with the finding of initially approximately ubiquitous expression of *dpp* in several animals (e.g. *T. castaneum*, *N. vitripennis*, the Leech *Helobdella austinensis*, *D. rerio*) (Kuo & Weisblat 2011; Hammerschmidt et al. 1996; Sharma et al. 2013; Özüak 2014). Sog inhibits BMP signaling, while BMP signaling represses *sog* expression, *i.e.* *sog* and *dpp* are in an equilibrium of mutual inhibition. This symmetric state is perturbed through Toll signaling that enhances *sog* on one side of the embryo. This side is now determined as ventral. The higher ventral levels of Sog lead to a decrease of BMP signaling in this region as more BMP ligands are

sequestered there. Simultaneously, Sog and Sog-Tsg-BMP complexes diffuse away from the source of Sog towards the dorsal side, where free Sog and complex-bound Sog is cleaved by Tld²⁰ (this happens presumably also on the ventral side but there BMP is rapidly re-bound by excess Sog). Consequently, BMP ligands are released from Sog-Tsg complexes and BMP signaling is enhanced in the dorsal region of the embryo, leading there to a more efficient repression of *sog* expression. In this manner a BMP morphogen gradient is established, which could then be used for early fate specification along the DV axis of *O. fasciatus*.

According to this model the loss of *sog* upon knockdown of *Toll* could be explained by a different stability of BMP ligands and Sog-Tsg complexes. If BMP ligands would be more stable than Sog and/or Tsg, the BMP/Sog-Tsg ratio would increase over time. This would result in a complete repression of *sog* expression in later blastoderm stages. Indeed, Sog might be rapidly degraded by Tld, which is indicated by the complete ventralization of *tld*-RNAi embryos (3.3.4.5; Figure 3-27). This probably depends on a massively enhanced Sog concentration, which is responsible for sequestering all or almost all BMP ligands in *tld*-depleted embryos. Hence, Sog (in the presence of Tld) likely exhibits a high degradation rate and, correlating with its high expression levels, also a high production rate.

Interestingly, a computational model based on the DV patterning mechanism proposed above, required a high production as well as a high degradation rate of Sog to explain the rapid diffusion of Sog and Sog-BMP complexes. This model was computationally analyzed by a cooperating group (AG Lässig) in order to test for robust pattern formation, which is considered to be a general principle of biochemical networks (von Dassow et al. 2000; Barkai & Shilo 2007). The system of model equations was minimalistic, as only Dpp, Sog and Dpp-Sog complexes were included. In addition, Dpp was assumed to have a very low diffusion rate if not bound by Sog. Concentrations and biochemical properties were assumed to be roughly similar as suggested for *D. melanogaster* by Peluso et al. 2011. In the model Sog concentration needs to locally exceed a certain threshold (which would be dependent on Toll) to initiate pattern formation. Most parameters (production, decay, complex formation and diffusion constants) lead to robust *sog* stripe formation over a range of at least an order of magnitude (unpublished data of Michael Lässig and Johannes Berg). Although this model is strongly simplified it could account for the experimental observation of my colleague Yen-Ta Chen and me. Furthermore, the model allowed twin formation, *i.e.* the emergence of two complete embryos out of a single initial primordium. This phenomenon was observed in

²⁰ The conserved metalloprotease Tld is responsible for the cleavage of Sog (or Chordin) in invertebrates as well as vertebrates (Ben-zvi et al. 2008; Connors et al. 1999; Little & Mullins 2006; Marqués et al. 1997; Shimmi & O'Connor 2003).

several basally branching insects, e.g. the leaf hopper *Euschelis*, as well as in vertebrates and sea urchins and is believed to be a hallmark of high self-regulatory capacity (De Robertis 2009; Lee et al. 2006; Lynch & Roth 2011).

In summary, DV patterning of *O. fasciatus* appears to be mediated by a BMP signaling-based self-regulatory system, which is only polarized by Toll signaling. Hence, Toll signaling has probably only the role to trigger an otherwise BMP-dependent DV patterning system in *O. fasciatus*, while it serves as master regulator in the DV patterning system of *D. melanogaster* (Moussian & Roth 2005; Reeves & Stathopoulos 2009).

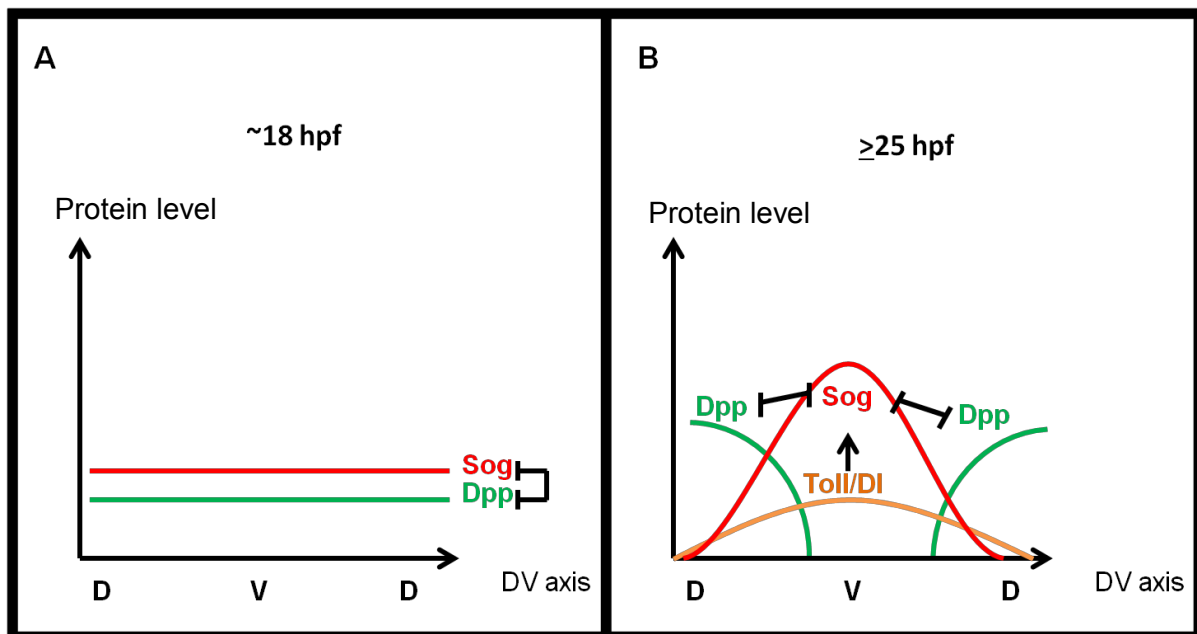


Figure 4.5: Toll signaling might act as trigger for a self-regulating BMP system during DV patterning of *O. fasciatus*

The model assumes that *dpp* (green) and *sog* (red) are initially both expressed at low levels (A). In this early phase (~18 hpf) they are in an equilibrium due to mutual negative regulation, as Sog sequesters Dpp and BMP signaling represses *sog* (A). Toll/DI signaling (orange) polarizes the embryo by enhancing *sog* expression on the ventral side (B). An elevated Sog concentration on the ventral side leads to an efficient sequestering of BMP ligands and consequently to a loss of BMP signaling-mediated *sog* repression in this region (B). Simultaneously, BMP ligands are transported by Sog to the dorsal side, where in turn the BMP signaling activity becomes enhanced, causing a complete repression of *sog* expression on this side (B). Abbreviations: D: dorsal, DI: Dorsal, DV: dorsal-ventral, hpf: hours post fertilization, V: ventral.

4.11 Evolution of DV patterning

This is one of plenty studies that demonstrate that BMP signaling has a large impact on DV patterning in almost all bilaterians, indicating that this is the ancestral state for bilaterians (Akiyama-Oda & Oda 2006; Ben-zvi et al. 2008; De Robertis & Kuroda 2004; Kishimoto et al. 1997; Lapraz et al. 2009; Lowe et al. 2006; van der Zee et al. 2006; Kuo et al. 2012; Raftery & Sutherland 2003). Intriguingly, cnidarians, which are considered to be a sister group of bilaterians, use BMP signaling to pattern their directive axis. The directive axis is comparable to the DV axis of bilaterians, although these diploblastic animals are considered to be radially symmetric (Saina et al. 2009). Hence, it might be that BMP signaling was already involved in DV axis formation prior to the emergence of triploblastic animals.

Despite the common deployment of the BMP pathway for patterning the DV axis, many aspects of this process differ in distinct lineages. Wnt signaling is required for DV axis formation in vertebrates, Nodal/Activin signaling in echinoderms, Hedgehog signaling in spiders and Toll signaling in insects. One typical function of these pathways is to regulate BMP signaling (De Robertis & Kuroda 2004; Lapraz et al. 2009; Moussian & Roth 2005; Nunes da Fonseca et al. 2009). So they can be considered as a kind of frame of the BMP-Chd system. For instance, Wnt signaling is required to activate *chd* expression in the organizer of *Xenopus* embryos and exerts negative transcriptional regulation on *bmp2b* in zebrafish embryos (De Robertis & Kuroda 2004). It appears that the "frames" of the BMP-Chd system exhibit much more differences than the system itself, comparing DV axis formation of bilaterally symmetric animals. As the signal transduction pathways, which trigger or regulate the BMP-Chd DV patterning systems, are distinct in different taxa, it is not possible to propose any of them to be ancestrally involved in DV axis formation (Akiyama-Oda & Oda 2010; De Robertis & Kuroda 2004; Lapraz et al. 2009; Moussian & Roth 2005; Nunes da Fonseca et al. 2009). It is conceivable that only the initial activation of the BMP/Chd system was ancestrally independent of the system itself. Different strategies of oogenesis might have facilitated a change of the pathway applied for the regulation or activation of the BMP/Chd system in distinct bilaterian lineages (Gilbert 2000). Subsequently, the respective signaling pathway could have invaded the BMP-Chd system thereby expanding its power.

Our group was able to trace back such an invasion by analyzing the role of Toll signaling in insect DV patterning (Figure 4-6). The first role of Toll signaling in DV patterning might have been to trigger a self-regulating BMP signaling-dependent DV patterning system, similar to its, in this study, indicated role in DV patterning of *O. fasciatus*

(4.8; 4.9; 4.10; Figure 4-6 A, A'). Then Toll might have become an inducer of mesoderm, like it is today the case in the wasp *N. vitripennis* (Özüak 2014; Buchta 2014; Figure 4-6 B, B'). This might have been facilitated by the presence of a conserved *NF-κB-twi-snail* module (Huber et al. 2005; Šošić et al. 2003; Zhang & Klymkowsky 2009). This module is known to be required for early mesoderm formation in both, vertebrates and insects (Zhang & Klymkowsky 2009). Thus, this conserved module was probably required for mesoderm formation already early in evolution. Finally, Toll signaling might have started to establish a nuclear Dorsal (Dl) morphogen gradient, initially with a low number of threshold levels and extensive feedback regulation as observed for *T. castaneum* (Nunes da Fonseca et al. 2008; Figure 4-6 C, C'). This morphogen gradient presumably became more decisive in the lineage leading to *Drosophila* until it activated and repressed target genes by establishing at least three different concentration thresholds (Moussian & Roth 2005; Reeves & Stathopoulos 2009; Figure 4-6 D, D').

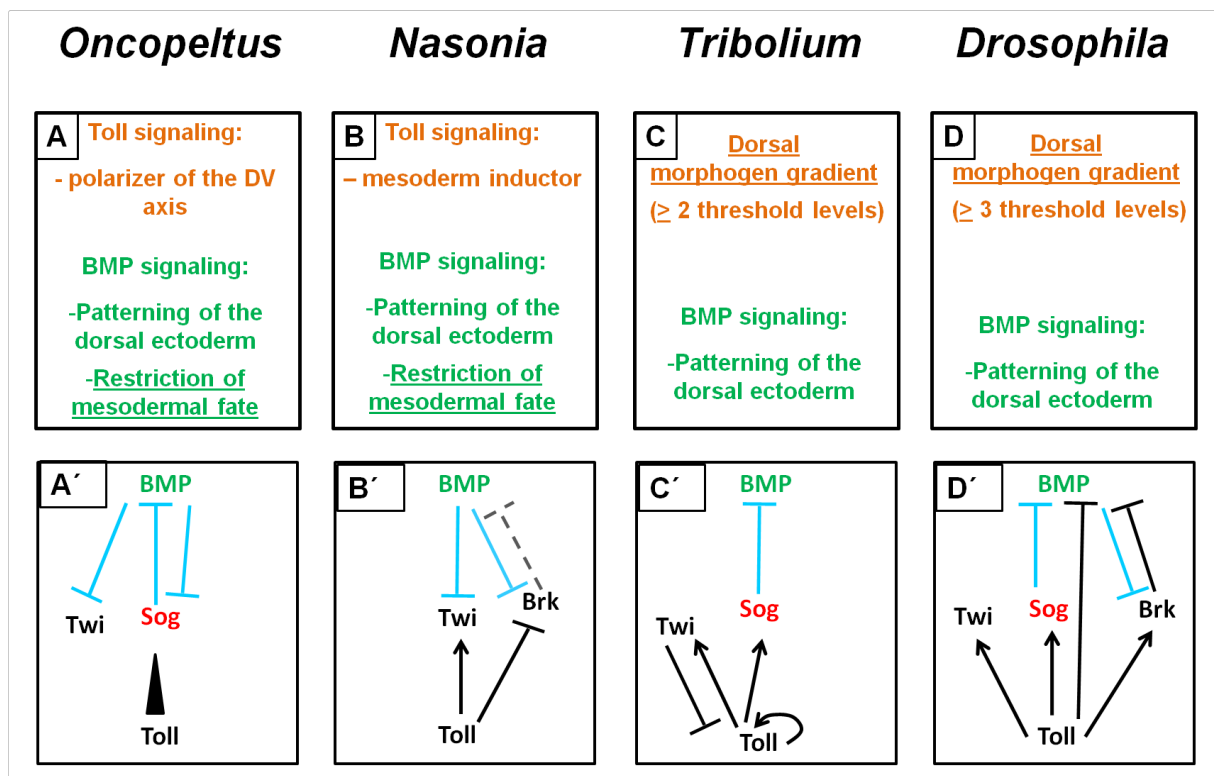


Figure 4-6: The relevance of Toll signaling in DV patterning decreases towards basally branching insects
Toll signaling appears only to polarize the DV axis of *O. fasciatus* by ventrally enhancing *sog* expression, while BMP signaling restricts the expression of *twi* and its inhibitor *sog* (A, A'). In the DV patterning system of the wasp *N. vitripennis* Toll signaling activates *twi* and induces the mesoderm, which is restricted by BMP signaling (B, B'). The fly *D. melanogaster* and the beetle *T. castaneum* form a Dorsal morphogen gradient, which regulates gene expression via at least three or two different threshold levels, respectively (D, D', C, C'). However, in *T. castaneum* the gradient formation is under extensive feedback regulation, as Toll signaling

positively (via activation of *Toll*) and negatively (via direct and indirect activation of the Dorsal inhibitor *cactus*) regulates its activity (C'). In *D. melanogaster* Toll signaling rather acts in a hierarchical fashion and also restricts BMP signaling activity by direct repression of *dpp* transcription as well as by activation of the transcriptional repressor *brk* (D'). Additionally to its aforementioned roles, BMP signaling is probably required for patterning of the dorsal ectoderm in the DV patterning system of all these species (A-D). Arrows represent activation, blunt-end lines inhibition and dashed lines uncertain regulatory interactions. Regulatory interactions can be direct or indirect. The arrowhead indicates an enhancement of expression that was initially independent of this activator. Abbreviations: DV: dorsal-ventral.

But the reason for the involvement of Toll signaling in the DV patterning system remains obscure. It is widely believed that the ancestral function of Toll signaling is defense against pathogens as Toll and Toll like receptors (TLRs) are involved in immunity throughout the whole animal kingdom (Hughes & Piontkivska 2008; Satake & Sasaki 2010; Zhong et al. 2012; Zheng et al. 2012; Pradeep et al. 2013; Yeh et al. 2013; Han-Ching Wang et al. 2010; Satake & Sekiguchi 2012). However, most of the nine *Toll* genes of *D. melanogaster* are involved in developmental processes, whereas only *Toll1*, *Toll7*, *Toll9* and eventually *Toll5* are also required for pathogen response (Bilak et al. 2003; Eldon et al. 1994; Moussian & Roth 2005; Valanne et al. 2011; Nakamoto et al. 2012). Furthermore, several studies suggested a role for Toll receptors in immunity and development in arthropods (Han-Ching Wang et al. 2010; Zheng et al. 2012; Pradeep et al. 2013; Chen et al. 2000; Tauszig et al. 2000; Nunes da Fonseca et al. 2008; Lemaitre et al. 2014; unpublished data of Matthias Pechmann). Expression analysis of an amphioxus *TLR* also suggested a developmental role (Yuan et al. 2009). Thus, it cannot be excluded that the ancestral function of Toll receptors was not, or not exclusively pathogen recognition. Alternatively, different kinds of Toll receptors could have emerged very early in evolution and the ones with developmental functions were lost in mammals. Interestingly, the functional deviation of arthropod Toll receptors is accompanied by a structural difference from other investigated TLRs. All deuterostome TLRs, analyzed so far, are activated by direct or co-receptor-mediated binding of pathogen associated molecular patterns (PAMPs) or damage associated molecular patterns (DAMPs), whereas *Toll1* and perhaps also *Toll2*, 5, 6 and 7 are activated by the binding of endogenous²¹ ligands, referred to as Spätzle (Spz) 1-6 (Valanne et al. 2011; Gangloff et al. 2013; Satake & Sekiguchi 2012). A Toll signal transduction pathway applying an endogenous ligand is a prerequisite for its recruitment for DV patterning. Therefore, the presence of Spz ligands is in line with the suggestions of a developmental role of *Toll* genes in addition to

²¹ Endogenous ligand is here used as expression for a genome encoded ligand, which does not include DAMPs, e.g. fragments of gene products which are only formed upon an injury.

their immune function in crustaceans (Zheng et al. 2012). Unraveling the evolutionary origin of *spz* and Spz-binding Toll receptors might help to infer the ancestral mode and function of Toll signaling.

Independent of the ancestral function of Toll, there is a link between Toll signaling in immunity and DV patterning in *D. melanogaster*, as both are partially dependent on *Toll1* (Tauszig et al. 2000; Lemaitre et al. 2014). Furthermore, Toll/Dl signaling is suggested to be involved in host defense during early embryogenesis of insects. The serosa is indicated to protect the egg against pathogens, e.g. via expression of antimicrobial peptides in *T. castaneum* (Chen et al. 2000; Jacobs & van der Zee 2013). The uptake of nuclear Dl from ventral serosa cells during early embryogenesis in *T. castaneum* suggested Toll signaling to be involved in the immune function of the serosa (Chen et al. 2000). The protection of the early insect embryo against pathogens might be very important as typical insect eggs are very yolk-rich and therefore a target for microorganisms (Roth 2004).

Interestingly, a hallmark of insect embryos is the very early formation of the blastoderm (Counce & Waddington 1973; Roth 2004). It is conceivable that this is also associated with creating an early line of defense against microorganisms. It might be that the blastoderm is on the one hand able to provide already some protection of the yolk and allows on the other hand a very rapid formation of the protective serosa.

A role for Toll1 in this early immune defense possibly facilitated the recruitment of Toll1 signaling for DV patterning (Moussian & Roth 2005). The cooption of a molecular network, which is already present, for a new purpose is believed to be a common evolutionary strategy and is also referred to as evolutionary tinkering (Chipman 2010). Interestingly, preliminary data suggested that *O. fasciatus* forms a very flat nuclear Dl gradient (unpublished data of Yen-Ta Chen). It could be that such a flat gradient can ventrally enhance *sog* expression, but also uniformly activate expression of anti-microbial peptides.

In summary, our group was able to draw a first draft of the evolution of DV patterning in insects, regarding Toll and BMP signaling, however, still a lot of open questions remain.

5. Outlook

5.1 The future of the system *Oncopeltus fasciatus*

Future research regarding the DV patterning system of *O. fasciatus* requires a better understanding of the animal system itself. One current drawback of this system is its partially unresolved fate map. Especially the location of the serosa and also the time point of its differentiation are still obscure. A classical way to trace back the origin of this tissue would be to perform dye injections. For example, the local injection of vital, lipophilic, fluorescent dyes (e.g., DiI²², DiO²³, Di Asp²⁴) into certain blastoderm cells would enable to trap these labeled cells (for example via time-laps imaging) (Clarke & Tickle 1999). Unraveling the blastoderm fate map of *O. fasciatus* could help to understand the morphological perturbations of *BMPsc* knockdown embryos, as the location and the shape of the border of the serosa anlage would be a first hint if its formation is (partially or completely) independent of DV patterning. In the case of *gbb*-RNAi embryos, nuclear staining of embryos around mid-embryogenesis, maybe in combination with monitoring the late serosa marker *zen*, could provide further insights into the extraembryonic membrane defects of these embryos (Panfilio et al. 2006). However, most convenient would be the availability of early, dorsal and extraembryonic marker genes. As more than 20 candidate marker genes from holometabolous insects were not appropriate as dorsal or extraembryonic markers in *O. fasciatus* the candidate gene approach appears not to be reasonable in this regard (data not shown). One unbiased approach to identify genes that can be used as fate markers and are involved in DV patterning would be a comparison of transcriptomes from knockdown embryos with an altered DV fate map and wild type embryos. This experiment is already planned and probably the transcriptomes of *sog*-RNAi, *gbb*-RNAi, *dpp*-RNAi and *Toll*-RNAi will be investigated for differentially expressed genes. For the bioinformatic analysis of these transcriptomes a reference genome is of advantage (Garber et al. 2011).

Within the scope of the ik5 project (PMID: 23940263) the *O. fasciatus* genome was recently sequenced and our group will participate in its annotation. Beside its supporting role in the transcriptome project the genome will help to obtain more sequence information for

²² DiI: Dioctadecyl-indocarbocyanine

²³ DiO: Dioctadecyl-oxycarbocyanine (DiO)

²⁴ Di Asp: N-4(4-dilinoyleylaminostyryl)-N-methylpyridinium iodide and related molecules

genes of already identified transcripts and will help to identify new potential DV patterning genes or lineage-specific duplications. This could, for instance, clarify if vertebrate-typical BMP signaling components, like the BMP ligand encoding gene *anti dorsalizing morphogenic protein (admp)* or the BMP inhibitor *bambi* are present in the *O. fasciatus* genome. *bambi* was identified in the beetle *T. castaneum* and, like *admp*, is generally associated with autoregulatory feedback loops (Van der Zee et al. 2008; Ben-zvi et al. 2008; Reversade & De Robertis 2005; Nunes da Fonseca et al. 2008). More sequence information will also facilitate the analysis of promoters and identification of putative transcription factor binding sites. The latter could be validated by several experimental approaches, e.g., electrophoretic mobility shift assay (EMSA) or Chromatin immunoprecipitation (ChIP) (Buck & Lieb 2004; Park 2009; Hellman & Fried 2007). In this manner direct target genes of the BMP and Toll signaling pathways could be identified.

Furthermore, a second *sax* homolog could be searched. This together with repeating the *sax* knockdown but injecting a higher concentration of dsRNA to overcome a possible reduction of the knockdown efficiency during development due to a feedback loop might help to understand the recovery of *sax* knockdown embryos. In addition, complete sequences of coding regions are a prerequisite to analyze gene functions by overexpression via injection of capped sense mRNA (Krieg & Melton 1984). For example, one could test if injection of *sog* mRNA can induce a second DV axis similar to the effect seen by *chd* injections in *Xenopus* (Sasai et al. 1994). Furthermore, the injection of GFP encoding transcripts could supplement dye injections.

However, although embryonic injections were already performed in *O. fasciatus* this technique seems to be difficult and needs to be re-established. This will be indispensable not only to perform sense RNA injections, or embryonic RNAi for genes which are resistant for pRNAi knockdown (e.g. possibly *dally*), but most important to establish transgenesis. The establishment of transgenesis will enable a variety of experimental possibilities. One could do different screens, e.g. for enhancer trap lines or for DV mutants, by random mutation, for example via random insertions of transposons. Targeted mutagenesis could be established with the help of site specific DNases and homologous recombination (Hartenstein & Jan 1992; St Johnston 2002; Gaj et al. 2013; Rajewsky et al. 1996; Mortensen 2006).

5.2 Towards a broader perspective

Apart from new techniques and deeper analysis of the embryonic DV patterning system, unraveling the maternal contribution to this process, *i.e.* the DV axis pre-forming in the ovary, is also crucial to complete the picture. It will be interesting to investigate the role of EGF signaling since the activity of this pathway during oogenesis appears to be required for proper establishment of the blastoderm Dorsal gradient in *T. castaneum* and *D. melanogaster* (Lynch et al. 2010; Roth & Schüpbach 1994).

Furthermore, as we want to understand evolution of DV patterning, we aim to create more sampling points, *i.e.* to investigate DV patterning in more organisms. This comprises an expansion of our focus towards more basally branching insects as well as to non-insect arthropods. To that end, our group started to culture and investigate the beetles *Atrachya menetriesi* and *Callosobruchus sp.* as well as *Orchesella cincta* a collembolan, *i.e.* a non-insect hexapod and several spider species .

Analyses of the DV patterning systems of these species might enable us to further narrow down the time point in evolution when Toll was recruited for DV patterning. In addition we could unravel if its participation in AP patterning, which was observed in *O. fasciatus*, is the result of lineage-specific evolution or represents an ancestral role of Toll in arthropods, which was lost during insect evolution (4.10). Furthermore these studies could help to identify ancestral regulatory interactions and feedback loops with regard to DV patterning and might also give insights into the evolution of growth zone DV patterning.

6. References

- Ahn, K. et al., 2001. BMPR-IA signaling is required for the formation of the apical ectodermal ridge and dorsal-ventral patterning of the limb. *Development (Cambridge, England)*, 128(22), pp.4449–61.
- Akiyama-Oda, Y. & Oda, H., 2006. Axis specification in the spider embryo: dpp is required for radial-to-axial symmetry transformation and sog for ventral patterning. *Development (Cambridge, England)*, 133(12), pp.2347–57.
- Akiyama-Oda, Y. & Oda, H., 2010. Cell migration that orients the dorsoventral axis is coordinated with anteroposterior patterning mediated by Hedgehog signaling in the early spider embryo. *Development (Cambridge, England)*, 137(8), pp.1263–73.
- Alvarez Martinez, C.E. et al., 2002. Characterization of a Smad motif similar to Drosophila mad in the mouse Msx 1 promoter. *Biochemical and biophysical research communications*, 291(3), pp.655–62.
- Anderson, K. V, Bokla, L. & Nüsslein-Volhard, C., 1985. Establishment of dorsal-ventral polarity in the Drosophila embryo: the induction of polarity by the Toll gene product. *Cell*, 42(3), pp.791–8.
- Angelini, D.R. & Kaufman, T.C., 2005. Functional analyses in the milkweed bug *Oncopeltus fasciatus* (Hemiptera) support a role for Wnt signaling in body segmentation but not appendage development. *Developmental biology*, 283(2), pp.409–23.
- Armstrong, N.J. et al., 1998. Conserved Spätzle/Toll signaling in dorsoventral patterning of Xenopus embryos. *Mechanisms of development*, 71(1-2), pp.99–105.
- Armstrong, N.J. et al., 2012. Maternal Wnt/ β -catenin signaling coactivates transcription through NF- κ B binding sites during Xenopus axis formation. *PLoS one*, 7(5), p.e36136.
- Arora, K., Levine, M.S. & O'Connor, M.B., 1994. The screw gene encodes a ubiquitously expressed member of the TGF-beta family required for specification of dorsal cell fates in the Drosophila embryo. *Genes & development*, 8(21), pp.2588–601.
- Arora, K. & Nüsslein-Volhard, C., 1992. Altered mitotic domains reveal fate map changes in Drosophila embryos mutant for zygotic dorsoventral patterning genes. *Development (Cambridge, England)*, 114(4), pp.1003–24.
- Bangi, E. & Wharton, K., 2006a. Dpp and Gbb exhibit different effective ranges in the establishment of the BMP activity gradient critical for Drosophila wing patterning. *Developmental biology*, 295(1), pp.178–93.
- Bangi, E. & Wharton, K., 2006b. Dual function of the Drosophila Alk1/Alk2 ortholog Saxophone shapes the Bmp activity gradient in the wing imaginal disc. *Development (Cambridge, England)*, 133(17), pp.3295–303.
- Barkai, N. & Shilo, B.-Z., 2007. Variability and robustness in biomolecular systems. *Molecular cell*, 28(5), pp.755–60.
- Belvin, M.P. & Anderson, K. V, 1996. A conserved signaling pathway: the Drosophila toll-dorsal pathway. *Annual review of cell and developmental biology*, 12, pp.393–416.

- Ben-David, J. & Chipman, A.D., 2010. Mutual regulatory interactions of the trunk gap genes during blastoderm patterning in the hemipteran *Oncopeltus fasciatus*. *Developmental biology*, 346(1), pp.140–9.
- Ben-zvi, D. et al., 2008. Scaling of the BMP activation gradient in *Xenopus* embryos. *Nature*, 453(June), pp.1205–1211.
- Biehs, B. et al., 1996. The *Drosophila* short gastrulation gene prevents Dpp from autoactivating and suppressing neurogenesis in the neuroectoderm. *Genes & development*, 10(22), pp.2922–2934.
- Bilak, H., Tauszig-Delamasure, S. & Imler, J.-L., 2003. Toll and Toll-like receptors in *Drosophila*. *Biochemical Society transactions*, 31(Pt 3), pp.648–51.
- Birkan, M., Schaeper, N.D. & Chipman, A.D., 2011. Early patterning and blastodermal fate map of the head in the milkweed bug *Oncopeltus fasciatus*. *Evolution & Development*, 13(5), pp.436–447.
- Blank, U. et al., 2008. An in vivo reporter of BMP signaling in organogenesis reveals targets in the developing kidney. *BMC developmental biology*, 8, p.86.
- Blitz, I.L., Cho, K.W.Y. & Chang, C., 2003. Twisted gastrulation loss-of-function analyses support its role as a BMP inhibitor during early *Xenopus* embryogenesis. *Development (Cambridge, England)*, 130(20), pp.4975–88.
- Bornemann, D.J. et al., 2008. A translational block to HSPG synthesis permits BMP signaling in the early *Drosophila* embryo. *Development (Cambridge, England)*, 135(6), pp.1039–47.
- Bowles, J., Schepers, G. & Koopman, P., 2000. Phylogeny of the SOX family of developmental transcription factors based on sequence and structural indicators. *Developmental biology*, 227(2), pp.239–55.
- Buchta, T., 2014. *Analysis of the dorsal-ventral gene regulatory network of Nasonia vitripennis*. Universität zu Köln.
- Buchta, T. et al., 2013. Patterning the dorsal-ventral axis of the wasp *Nasonia vitripennis*. *Developmental biology*, 381(1), pp.189–202.
- Buck, M.J. & Lieb, J.D., 2004. ChIP-chip: considerations for the design, analysis, and application of genome-wide chromatin immunoprecipitation experiments. *Genomics*, 83(3), pp.349–360.
- Buescher, M., Hing, F.S. & Chia, W., 2002. Formation of neuroblasts in the embryonic central nervous system of *Drosophila melanogaster* is controlled by SoxNeuro. *Development (Cambridge, England)*, 129(18), pp.4193–203.
- Butt, F.H., 1949. Embryology of the Milkweed Bug *Oncopeltus fasciatus* (Hemiptera). *Memoir Cornell University Agricultural Experiment Station*, 283, pp.1–43.
- Cande, J., Goltsev, Y. & Levine, M.S., 2009. Conservation of enhancer location in divergent insects. *Proceedings of the National Academy of Sciences of the United States of America*, 106(34), pp.14414–9.
- Chen, G., Handel, K. & Roth, S., 2000. The maternal NF-kappaB/dorsal gradient of *Tribolium castaneum*: dynamics of early dorsoventral patterning in a short-germ beetle. *Development (Cambridge, England)*, 127(23), pp.5145–56.

- Chipman, A.D., 2010. Parallel evolution of segmentation by co-option of ancestral gene regulatory networks. *BioEssays : news and reviews in molecular, cellular and developmental biology*, 32(1), pp.60–70.
- Clarke, J.D. & Tickle, C., 1999. Fate maps old and new. *Nature cell biology*, 1(4), pp.E103–9.
- Connors, S. a et al., 1999. The role of tolloid/mini fin in dorsoventral pattern formation of the zebrafish embryo. *Development (Cambridge, England)*, 126(14), pp.3119–30.
- Constam, D.B. & Robertson, E.J., 1999. Regulation of bone morphogenetic protein activity by pro domains and proprotein convertases. *The Journal of cell biology*, 144(1), pp.139–49.
- Counce, S.J. & Waddington, C.H., 1973. *Developmental systems: insects* 2nd ed. S. J. Counce & C. H. Waddington, eds., Academic Press London and New York.
- Cui, Y. et al., 1998. BMP-4 is proteolytically activated by furin and/or PC6 during vertebrate embryonic development. *The EMBO journal*, 17(16), pp.4735–43.
- Dale, L. et al., 1992. Bone morphogenetic protein 4: a ventralizing factor in early *Xenopus* development. *Development (Cambridge, England)*, 115(2), pp.573–85. Available at: <http://www.ncbi.nlm.nih.gov/pubmed/1425340>.
- Von Dassow, G. et al., 2000. The segment polarity network is a robust developmental module. *Nature*, 406(6792), pp.188–92.
- Davis, G.K. & Patel, N.H., 2002. SHORT, LONG, AND BEYOND: Molecular and Embryological Approaches to Insect Segmentation. *Annual review of Entomology*, 47, pp.669–699.
- Decotto, E. & Ferguson, E.L., 2001. A positive role for Short gastrulation in modulating BMP signaling during dorsoventral patterning in the *Drosophila* embryo. *Development (Cambridge, England)*, 128(19), pp.3831–41.
- Dereeper, a et al., 2008. Phylogeny.fr: robust phylogenetic analysis for the non-specialist. *Nucleic acids research*, 36(Web Server issue), pp.W465–9.
- Ten Dijke, P. et al., 1994. Identification of Type I Receptors for Osteogenic Protein-1 and Bone Morphogenetic Protein 4. *The Journal of biological chemistry*, 269, pp.16985–16988.
- Dorfman, R. & Shilo, B.Z., 2001. Biphasic activation of the BMP pathway patterns the *Drosophila* embryonic dorsal region. *Development (Cambridge, England)*, 128(6), pp.965–72.
- Drechsler, A., 2007. Studien zur dorsoventralen Musterbildung und Gastrulation in *Oncopeltus fasciatus* und *Gryllus bimaculatus*. *Diploma thesis, University of cologne*.
- Dutko, J. a & Mullins, M.C., 2011. SnapShot: BMP signaling in development. *Cell*, 145(4), pp.636, 636.e1–2.
- Eldar, A. et al., 2002. Robustness of the BMP morphogen gradient in *Drosophila* embryonic patterning. *Nature*, 419(September).
- Eldon, E. et al., 1994. The *Drosophila* 18 wheeler is required for morphogenesis and has striking similarities to Toll. *Development (Cambridge, England)*, 120(4), pp.885–99.

- Ewen-Campen, B. et al., 2011. The maternal and early embryonic transcriptome of the milkweed bug *Oncopeltus fasciatus*. *BMC genomics*, 12(1), p.61.
- Ewen-Campen, B., Jones, T.E.M. & Extavour, C.G., 2013. Evidence against a germ plasm in the milkweed bug *Oncopeltus fasciatus*, a hemimetabolous insect. *Biology open*, 2(6), pp.556–68.
- Fazio, S., Linton, M.F. & Swift, L.L., 2000. The cell biology and physiologic relevance of ApoE recycling. *Trends in cardiovascular medicine*, 10(1), pp.23–30.
- Feng, X.H. & Derynck, R., 1997. A kinase subdomain of transforming growth factor-beta (TGF-beta) type I receptor determines the TGF-beta intracellular signaling specificity. *The EMBO journal*, 16(13), pp.3912–23.
- Ferguson, E.L. & Anderson, K. V, 1992a. Decapentaplegic acts as a morphogen to organize dorsal-ventral pattern in the *Drosophila* embryo. *Cell*, 71(3), pp.451–61.
- Ferguson, E.L. & Anderson, K. V, 1992b. Localized enhancement and repression of the activity of the TGF-beta family member, decapentaplegic, is necessary for dorsal-ventral pattern formation in the *Drosophila* embryo. *Development (Cambridge, England)*, 114(3), pp.583–97.
- Fossett, N. et al., 2000. The multitype zinc-finger protein U-shaped functions in heart cell specification in the *Drosophila* embryo. *Proceedings of the National Academy of Sciences of the United States of America*, 97(13), pp.7348–53.
- Francois, V. et al., 1994. Dorsal-ventral patterning of the *Drosophila* embryo depends on a putative negative growth factor encoded by the short gastrulation gene. *Genes & Development*, 8(21), pp.2602–2616.
- Friedrich, M. V et al., 2000. Perlecan domain V of *Drosophila melanogaster*. Sequence, recombinant analysis and tissue expression. *European journal of biochemistry / FEBS*, 267(11), pp.3149–59.
- Gaj, T., Gersbach, C. a & Barbas, C.F., 2013. ZFN, TALEN, and CRISPR/Cas-based methods for genome engineering. *Trends in biotechnology*, 31(7), pp.397–405.
- Gangloff, M. et al., 2013. Functional insights from the crystal structure of the N-terminal domain of the prototypical toll receptor. *Structure (London, England : 1993)*, 21(1), pp.143–53.
- Garber, M. et al., 2011. Computational methods for transcriptome annotation and quantification using RNA-seq. *Nature methods*, 8(6), pp.469–77.
- Gilbert, F., 2000. *Developmental Biology* 6th ed., Sunderland (MA).
- Gleason, R.J. et al., 2014. BMP signaling requires retromer-dependent recycling of the type I receptor. *Proceedings of the National Academy of Sciences of the United States of America*, 111(7), pp.2578–83.
- Goltsev, Y. et al., 2007. Evolution of the dorsal-ventral patterning network in the mosquito, *Anopheles gambiae*. *Development (Cambridge, England)*, 134(13), pp.2415–24.
- Guo, J. & Wu, G., 2012. The signaling and functions of heterodimeric bone morphogenetic proteins. *Cytokine & growth factor reviews*, 23(1-2), pp.61–7.
- Guo, X. & Wang, X.-F., 2009. Signaling cross-talk between TGF-beta/BMP and other pathways. *Cell research*, 19(1), pp.71–88.

- Haerry, T.E. et al., 1998. Synergistic signaling by two BMP ligands through the SAX and TKV receptors controls wing growth and patterning in *Drosophila*. *Development (Cambridge, England)*, 125(20), pp.3977–87.
- Hammerschmidt, M., Serbedzija, G.N. & McMahon, a P., 1996. Genetic analysis of dorsoventral pattern formation in the zebrafish: requirement of a BMP-like ventralizing activity and its dorsal repressor. *Genes & Development*, 10(19), pp.2452–2461.
- Han-Ching Wang, K. et al., 2010. RNAi knock-down of the *Litopenaeus vannamei* Toll gene (LvToll) significantly increases mortality and reduces bacterial clearance after challenge with *Vibrio harveyi*. *Developmental and comparative immunology*, 34(1), pp.49–58.
- Handel, K. et al., 2005. *Tribolium castaneum* twist: gastrulation and mesoderm formation in a short-germ beetle. *Development genes and evolution*, 215(1), pp.13–31.
- Harland, R.M., 2001. A twist on embryonic signalling. *Nature*, 410(March), pp.423–424.
- Hartenstein, V. & Jan, Y.N., 1992. Studying *Drosophila* embryogenesis with P-lacZ enhancer trap lines. *Roux's Archives of Developmental Biology*, 201, pp.194–220.
- Hashiguchi, M. & Mullins, M.C., 2013. Anteroposterior and dorsoventral patterning are coordinated by an identical patterning clock. *Development (Cambridge, England)*, 140(9), pp.1970–80.
- Hazama, M. et al., 1995. Efficient expression of a heterodimer of bone morphogenetic protein using a baculovirus expression system. *Biochemical and biophysical research communications*, 209(3), pp.859–866.
- Hellman, L.M. & Fried, M.G., 2007. Electrophoretic mobility shift assay (EMSA) for detecting protein-nucleic acid interactions. *Nature protocols*, 2(8), pp.1849–61.
- Hester, S.D. et al., 2011. A multi-cell, multi-scale model of vertebrate segmentation and somite formation. *PLoS computational biology*, 7(10), p.e1002155.
- Hibino, T. et al., 2006. The immune gene repertoire encoded in the purple sea urchin genome. *Developmental biology*, 300(1), pp.349–65.
- Hogan, B.L., 1996. Bone morphogenetic proteins: multifunctional regulators of vertebrate development. *Genes & Development*, 10(13), pp.1580–1594.
- Huber, M. a, Kraut, N. & Beug, H., 2005. Molecular requirements for epithelial-mesenchymal transition during tumor progression. *Current opinion in cell biology*, 17(5), pp.548–58.
- Hughes, A.L. & Piontkivska, H., 2008. Functional diversification of the toll-like receptor gene family. *Immunogenetics*, 60(5), pp.249–56.
- Irish, V.F. & Gelbart, W.M., 1987. The decapentaplegic gene is required for dorsal-ventral patterning of the *Drosophila* embryo. *Genes & Development*, 1(8), pp.868–879.
- Israel, D. et al., 1996. Heterodimeric bone morphogenetic proteins show enhanced activity in vitro and in vivo. *Growth Factors*, 13(3-4), pp.291–300.

- Jackson, P.D. & Hoffmann, F.M., 1994. Embryonic expression patterns of the *Drosophila* decapentaplegic gene: separate regulatory elements control blastoderm expression and lateral ectodermal expression. *Developmental dynamics : an official publication of the American Association of Anatomists*, 199(1), pp.28–44.
- Jacobs, C.G.C. & van der Zee, M., 2013. Immune competence in insect eggs depends on the extraembryonic serosa. *Developmental and comparative immunology*, 41(2), pp.263–9.
- Jagla, T. et al., 1999. Plasticity within the lateral somatic mesoderm of *Drosophila* embryos. *The International journal of developmental biology*, 43(6), pp.571–3.
- Jażwińska, a, Rushlow, C. & Roth, S., 1999. The role of brinker in mediating the graded response to Dpp in early *Drosophila* embryos. *Development (Cambridge, England)*, 126(15), pp.3323–34.
- Jiao, X. et al., 2007. Heparan sulfate proteoglycans (HSPGs) modulate BMP2 osteogenic bioactivity in C2C12 cells. *The Journal of biological chemistry*, 282(2), pp.1080–6.
- Jiménez, F. et al., 1995. vnd, a gene required for early neurogenesis of *Drosophila*, encodes a homeodomain protein. *The EMBO journal*, 14(14), pp.3487–95.
- Jinek, M. & Doudna, J. a, 2009. A three-dimensional view of the molecular machinery of RNA interference. *Nature*, 457(7228), pp.405–12.
- Jockusch, E.L. et al., 2000. Leg development in flies versus grasshoppers: differences in dpp expression do not lead to differences in the expression of downstream components of the leg patterning pathway. *Development (Cambridge, England)*, 127(8), pp.1617–26.
- Johnston, R.D.S. & Gelbart, W.M., 1987. Decapentaplegic transcripts are localized along the dorsal-ventral axis of the *Drosophila* embryo. *EMBO Journal*, 6(9), pp.2785–2791.
- Jortikka, L. et al., 1997. Internalization and intracellular processing of bone morphogenetic protein (BMP) in rat skeletal muscle myoblasts (L6). *Cellular signalling*, 9(1), pp.47–51.
- Kasai, Y. et al., 1992. Dorsal-ventral patterning in *Drosophila*: DNA binding of snail protein to the single-minded gene. *Proceedings of the National Academy of Sciences of the United States of America*, 89(8), pp.3414–8.
- Kim, J.-D. et al., 2012. Context-dependent proangiogenic function of bone morphogenetic protein signaling is mediated by disabled homolog 2. *Developmental cell*, 23(2), pp.441–8.
- Kishimoto, Y. et al., 1997. The molecular nature of zebrafish swirl: BMP2 function is essential during early dorsoventral patterning. *Development (Cambridge, England)*, 124(22), pp.4457–66.
- Kotkamp, K., Klingler, M. & Schoppmeier, M., 2010. Apparent role of *Tribolium* orthodenticle in anteroposterior blastoderm patterning largely reflects novel functions in dorsoventral axis formation and cell survival. *Development (Cambridge, England)*, 186(2), pp.1853–1862.
- Krieg, P.A. & Melton, D.A., 1984. Functional messenger RNAs are produced by SP6 in vitro transcription of cloned cDNAs. *Nucleic Acids Research*, 12(18), pp.7057–7070.
- Kuo, D.-H., Shankland, M. & Weisblat, D. a, 2012. Regional differences in BMP-dependence of dorsoventral patterning in the leech *Helobdella*. *Developmental biology*, 368(1), pp.86–94.

- Kuo, D.-H. & Weisblat, D. a, 2011. A new molecular logic for BMP-mediated dorsoventral patterning in the leech *Helobdella*. *Current biology : CB*, 21(15), pp.1282–8.
- Lall, S. & Patel, N.H., 2001. Conservation and divergence in molecular mechanisms of axis formation. *Annual review of genetics*, 35, pp.407–437.
- Lapraz, F., Besnardeau, L. & Lepage, T., 2009. Patterning of the dorsal-ventral axis in echinoderms: insights into the evolution of the BMP-chordin signaling network. *PLoS biology*, 7(11), p.e1000248.
- Lee, H.X. et al., 2006. Embryonic dorsal-ventral signaling: secreted frizzled-related proteins as inhibitors of tolloid proteinases. *Cell*, 124(1), pp.147–59.
- Lemaitre, B. et al., 2014. Pillars Article : The Dorsoventral Regulatory Gene Cassette *spätzle* / Toll / *cactus* Controls the Potent Antifungal Response in.
- Leptin, M., 2004. Gastrulation in *Drosophila*. In *Gastrulation - From Cells to Embryo*. Cold Spring Harbor Laboratory Press, pp. 91–104.
- Leptin, M., 1991. *twist* and *snail* as positive and negative regulators during *Drosophila* mesoderm development. *Genes & Development*, 5(9), pp.1568–1576.
- Letsou, a et al., 1995. *Drosophila* Dpp signaling is mediated by the *punt* gene product: a dual ligand-binding type II receptor of the TGF beta receptor family. *Cell*, 80(6), pp.899–908.
- Little, S.C. & Mullins, M.C., 2009. Bone morphogenetic protein heterodimers assemble heteromeric type I receptor complexes to pattern the dorsoventral axis. *Nature cell biology*, 11(5), pp.637–43.
- Little, S.C. & Mullins, M.C., 2006. Extracellular modulation of BMP activity in patterning the dorsoventral axis. *Birth defects research. Part C, Embryo today : reviews*, 78(3), pp.224–42.
- Little, S.C. & Mullins, M.C., 2004. Twisted gastrulation promotes BMP signaling in zebrafish dorsal-ventral axial patterning. *Development (Cambridge, England)*, 131(23), pp.5825–35.
- Liu, P.Z. & Kaufman, T.C., 2005. *even-skipped* is not a pair-rule gene but has segmental and gap-like functions in *Oncopeltus fasciatus*, an intermediate germband insect. *Development (Cambridge, England)*, 132(9), pp.2081–92.
- Liu, P.Z. & Kaufman, T.C., 2004. *hunchback* is required for suppression of abdominal identity, and for proper germband growth and segmentation in the intermediate germband insect *Oncopeltus fasciatus*. *Development (Cambridge, England)*, 131(7), pp.1515–27.
- Lowe, C.J. et al., 2006. Dorsoventral patterning in hemichordates: insights into early chordate evolution. *PLoS biology*, 4(9), p.e291.
- Lüders, F. et al., 2003. *Slalom* encodes an adenosine 3'-phosphate 5'-phosphosulfate transporter essential for development in *Drosophila*. *The EMBO journal*, 22(14), pp.3635–44.
- Lynch, J. a et al., 2010. EGF Signaling and the Origin of Axial Polarity among the Insects. *Current biology : CB*, 20(11), pp.1042–1047.
- Lynch, J. a et al., 2006. Localized maternal orthodenticle patterns anterior and posterior in the long germ wasp *Nasonia*. *Nature*, 439(7077), pp.728–32.

- Lynch, J. a & Roth, S., 2011. The evolution of dorsal-ventral patterning mechanisms in insects. *Genes & development*, 25(2), pp.107–18.
- Markstein, M. et al., 2002. Genome-wide analysis of clustered Dorsal binding sites identifies putative target genes in the Drosophila embryo. *Proceedings of the National Academy of Sciences of the United States of America*, 99(2), pp.763–8.
- Marqués, G. et al., 1997. Production of a DPP activity gradient in the early Drosophila embryo through the opposing actions of the SOG and TLD proteins. *Cell*, 91(3), pp.417–26.
- Mason, E.D. et al., 1994. Dorsal midline fate in Drosophila embryos requires twisted gastrulation, a gene encoding a secreted protein related to human connective tissue growth factor. *Genes & Development*, 8(13), pp.1489–1501.
- Miller-Bertoglio, V.E. et al., 1997. Differential regulation of chordin expression domains in mutant zebrafish. *Developmental biology*, 192(2), pp.537–50.
- Miyazono, K., Maeda, S. & Imamura, T., 2005. BMP receptor signaling: transcriptional targets, regulation of signals, and signaling cross-talk. *Cytokine & growth factor reviews*, 16(3), pp.251–63.
- Mizutani, C.M. et al., 2005. Formation of the BMP activity gradient in the Drosophila embryo. *Developmental cell*, 8(6), pp.915–24.
- Mortensen, R., 2006. Overview of gene targeting by homologous recombination. *Current protocols in molecular biology*, p.Supplement 76.
- Moussian, B. & Roth, S., 2005. Dorsoventral axis formation in the Drosophila embryo--shaping and transducing a morphogen gradient. *Current biology : CB*, 15(21), pp.R887–99.
- Nakamoto, M. et al., 2012. Virus recognition by Toll-7 activates antiviral autophagy in Drosophila. *Immunity*, 36(4), pp.658–67.
- Nambu, J.F. et al., 1990. The single-minded Gene of Drosophila for the Expression of Genes Important Development of CNS Midline Cells Is Required for the . , 63, pp.63–75.
- Nambu, J.R. et al., 1991. The Drosophila single-minded Gene Encodes a Helix-Loop-Helix Protein That Acts as a Master Regulator of CNS Midline Development. *Cell*, 67, pp.1157–1167.
- Nellen, D., Affolter, M. & Basler, K., 1994. Receptor serine/threonine kinases implicated in the control of Drosophila body pattern by decapentaplegic. *Cell*, 78(2), pp.225–37.
- Nentwig, W., Bacher, S. & Brandl, R., 2007. *Ökologie kompakt* first edit., Spektrum.
- Neul, J.L. & Ferguson, E.L., 1998. Spatially restricted activation of the SAX receptor by SCW modulates DPP/TKV signaling in Drosophila dorsal-ventral patterning. *Cell*, 95(4), pp.483–94.
- Newfeld, S.J., Wisotzkey, R.G. & Kumar, S., 1999. Molecular Evolution of a Developmental Pathway : Phylogenetic Analyses of Transforming Growth Factor- β Family Ligands, Receptors and Smad Signal Transducers. *Genetics*, 152, pp.183–95.
- Nguyen, M. et al., 1998. Interpretation of a BMP activity gradient in Drosophila embryos depends on synergistic signaling by two type I receptors, SAX and TKV. *Cell*, 95(4), pp.495–506.

- Nishimatsu, S. & Thomsen, G.H., 1998. Ventral mesoderm induction and patterning by bone morphogenetic protein heterodimers in *Xenopus* embryos. *Mechanisms of development*, 74(1-2), pp.75–88.
- Nosaka, T. et al., 2003. Mammalian Twisted Gastrulation Is Essential for Skeleto-Lymphogenesis. *Society*, 23(8), pp.2969–2980.
- Nose, a, Isshiki, T. & Takeichi, M., 1998. Regional specification of muscle progenitors in *Drosophila*: the role of the *msh* homeobox gene. *Development (Cambridge, England)*, 125(2), pp.215–23.
- Nunes da Fonseca, R. et al., 2008. Self-regulatory circuits in dorsoventral axis formation of the short-germ beetle *Tribolium castaneum*. *Developmental cell*, 14(4), pp.605–15.
- Nunes da Fonseca, R., Lynch, J.A. & Roth, S., 2009. Evolution of axis formation: mRNA localization, regulatory circuits and posterior specification in non-model arthropods. *Current opinion in genetics & development*, 19(4), pp.404–11.
- Nunes da Fonseca, R., van der Zee, M. & Roth, S., 2010. Evolution of extracellular Dpp modulators in insects: The roles of *tolloid* and *twisted-gastrulation* in dorsoventral patterning of the *Tribolium* embryo. *Developmental biology*, 345(1), pp.80–93.
- Oelgeschlager, M. et al., 2003. The pro-BMP activity of Twisted gastrulation is independent of BMP binding. *Development*, 130(17), pp.4047–4056.
- Oh, C.T. et al., 2002. Local inhibition of *Drosophila* homeobox-containing neural dorsoventral patterning genes by Dpp. *FEBS letters*, 531(3), pp.427–31.
- Ohkawara, B. et al., 2002. Action range of BMP is defined by its N-terminal basic amino acid core. *Current biology : CB*, 12(3), pp.205–9.
- Özüak, O., 2014. *The role of the BMP and Toll pathways in patterning the dorsal-ventral axis in Nasonia virtipennis*. Universität zu Köln.
- Panfilio, K. a, 2008. Extraembryonic development in insects and the acrobatics of blastokinesis. *Developmental biology*, 313(2), pp.471–91.
- Panfilio, K. a, 2009. Late extraembryonic morphogenesis and its *zen*(RNAi)-induced failure in the milkweed bug *Oncopeltus fasciatus*. *Developmental biology*, 333(2), pp.297–311.
- Panfilio, K. a et al., 2006. *Oncopeltus fasciatus zen* is essential for serosal tissue function in *katatrepsis*. *Developmental biology*, 292(1), pp.226–43.
- Panfilio, K.A., 2006. Extraembryonic development in the milkweed bug *Oncopeltus fasciatus* and the role of insect *zen* genes. *Ph.D Dissertation, University of Cambridge*.
- Park, P.J., 2009. ChIP-seq: advantages and challenges of a maturing technology. *Nature reviews. Genetics*, 10(10), pp.669–80.
- Patel, N.H. et al., 1989. Expression of engrailed proteins in arthropods, annelids, and chordates. *Cell*, 58(5), pp.955–68.
- Peel, A. & Akam, M., 2003. Evolution of Segmentation: Rolling Back the Clock. , 13(03), pp.708 – 710.

- Peluso, C.E. et al., 2011. Shaping BMP morphogen gradients through enzyme-substrate interactions. *Developmental cell*, 21(2), pp.375–83.
- Petersen, C.P. & Reddien, P.W., 2009. Wnt signaling and the polarity of the primary body axis. *Cell*, 139(6), pp.1056–68.
- Piccolo, S. et al., 1996. Dorsoventral patterning in *Xenopus*: inhibition of ventral signals by direct binding of chordin to BMP-4. *Cell*, 86(4), pp.589–98.
- Pradeep, A.N.R. et al., 2013. Activation of autophagic programmed cell death and innate immune gene expression reveals immuno-competence of integumental epithelium in *Bombyx mori* infected by a dipteran parasitoid. *Cell and tissue research*, 352(2), pp.371–85.
- Prothmann, C., Armstrong, N.J. & Rupp, R. a, 2000. The Toll/IL-1 receptor binding protein MyD88 is required for *Xenopus* axis formation. *Mechanisms of development*, 97(1-2), pp.85–92.
- Rafiqi, A.M. et al., 2012. BMP-dependent serosa and amnion specification in the scuttle fly *Megaselia abdita*. *Development (Cambridge, England)*, 139(18), pp.3373–82.
- Rafiqi, A.M. et al., 2008. Evolutionary origin of the amnioserosa in cyclorrhaphan flies correlates with spatial and temporal expression changes of zen. *Proceedings of the National Academy of Sciences of the United States of America*, 105(1), pp.234–9.
- Rafiqi, A.M., Lemke, S. & Schmidt-Ott, U., 2010. Postgastrular zen expression is required to develop distinct amniotic and serosal epithelia in the scuttle fly *Megaselia*. *Developmental biology*, 341(1), pp.282–90.
- Raftery, L. a. & Sutherland, D.J., 2003. Gradients and thresholds: BMP response gradients unveiled in *Drosophila* embryos. *Trends in Genetics*, 19(12), pp.701–708.
- Rajewsky, K. et al., 1996. Conditional Gene Targeting. *The American Society for Clinical Investigation*, 98(3), pp.600–603.
- Reeves, G.T. & Stathopoulos, A., 2009. Graded dorsal and differential gene regulation in the *Drosophila* embryo. *Cold Spring Harbor perspectives in biology*, 1(4), p.a000836.
- Reversade, B. & De Robertis, E.M., 2005. Regulation of ADMP and BMP2/4/7 at opposite embryonic poles generates a self-regulating morphogenetic field. *Cell*, 123(6), pp.1147–60.
- De Robertis, E.M., 2009. Spemann's organizer and the self-regulation of embryonic fields. *Mechanisms of development*, 126(11-12), pp.925–41.
- De Robertis, E.M. & Kuroda, H., 2004. Dorsal-ventral patterning and neural induction in *Xenopus* embryos. *Annual review of cell and developmental biology*, 20, pp.285–308.
- Ross, J.J. et al., 2001. Twisted gastrulation is a conserved extracellular BMP antagonist. *Nature*, 410(6827), pp.479–83.
- Roth, S., 2004. Gastrulation in other insects. In *Gastrulation - From Cells to Embryo*. Cold Spring Harbor Laboratory Press, pp. 105–121.
- Roth, S. & Schüpbach, T., 1994. The relationship between ovarian and embryonic dorsoventral patterning in *Drosophila*. *Development (Cambridge, England)*, 120(8), pp.2245–57.

- Roth, S., Stein, D. & Nüsslein-Volhard, C., 1989. A gradient of nuclear localization of the dorsal protein determines dorsoventral pattern in the *Drosophila* embryo. *Cell*, 59(6), pp.1189–202.
- Rusch, J. & Levine, M., 1996. Threshold responses to the dorsal regulatory gradient and the subdivision of primary tissue territories in the *Drosophila* embryo. *Current opinion in genetics & development*, 6(4), pp.416–23.
- Rushlow, C. et al., 1987. Molecular characterization of the *zerknüllt* region of the Antennapedia gene complex in *Drosophila*. *Genes & Development*, 1(10), pp.1268–1279.
- Sachs, L., 2011. *The role of BMP signaling in Dorsoventral patterning in the milkweed bug *Oncopeltus fasciatus**. University of Cologne.
- Sachs, L.M., 2009. *Dorsoventral patterning in the milkweed bug *Oncopeltus fasciatus**. Universität zu Köln.
- Saina, M. et al., 2009. BMPs and chordin regulate patterning of the directive axis in a sea anemone. *Proceedings of the National Academy of Sciences of the United States of America*, 106(44), pp.18592–7.
- Santegoets, K.C.M. et al., 2011. Toll-like receptors in rheumatic diseases: Are we paying a high price for our defense against bugs? *FEBS letters*.
- Sasai, Y. et al., 1994. Xenopus chordin: a novel dorsalizing factor activated by organizer-specific homeobox genes. *Cell*, 79(5), pp.779–90.
- Satake, H. & Sasaki, N., 2010. Comparative overview of toll-like receptors in lower animals. *Zoological science*, 27(2), pp.154–61.
- Satake, H. & Sekiguchi, T., 2012. Toll-like receptors of deuterostome invertebrates. *Frontiers in immunology*, 3(February), p.34.
- Schier, A.F. & Talbot, W.S., 2005. Molecular genetics of axis formation in zebrafish. *Annual review of genetics*, 39, pp.561–613.
- Schmid, B. et al., 2000. Equivalent genetic roles for *bmp7/snailhouse* and *bmp2b/swirl* in dorsoventral pattern formation. *Development (Cambridge, England)*, 127(5), pp.957–67.
- Schmidt, J. et al., 1995. *Drosophila* short gastrulation induces an ectopic axis in *Xenopus*: evidence for conserved mechanisms of dorsal-ventral patterning. *Development (Cambridge, England)*, 121(12), pp.4319–28.
- Schmidt-Ott, U., 2000. The amnioserosa is an apomorphic character of cyclorrhaphan flies. *Development genes and evolution*, 210(7), pp.373–6.
- Sharma, R., Beermann, A. & Schröder, R., 2013. The dynamic expression of extraembryonic marker genes in the beetle *Tribolium castaneum* reveals the complexity of serosa and amnion formation in a short germ insect. *Gene expression patterns : GEP*, 13(8), pp.362–71.
- Shimell, M.J. et al., 1991. The *Drosophila* dorsal-ventral patterning gene *tollid* is related to human bone morphogenetic protein 1. *Cell*, 67(3), pp.469–81.
- Shimmi, O. et al., 2005. Facilitated transport of a Dpp/Scw heterodimer by Sog/Tsg leads to robust patterning of the *Drosophila* blastoderm embryo. *Cell*, 120(6), pp.873–86.

- Shimmi, O. & O'Connor, M.B., 2003. Physical properties of Tld, Sog, Tsg and Dpp protein interactions are predicted to help create a sharp boundary in Bmp signals during dorsoventral patterning of the Drosophila embryo. *Development (Cambridge, England)*, 130(19), pp.4673–82.
- Solnica-Krezel, L. & Sepich, D.S., 2012. Gastrulation: making and shaping germ layers. *Annual review of cell and developmental biology*, 28, pp.687–717.
- Sommer, R. & Tautz, D., 1994. Expression patterns of twist and snail in Tribolium (Coleoptera) suggest a homologous formation of mesoderm in long and short germ band insects. *developmental genetics*, 15(1), pp.32–7.
- Sonnenfeld, M. et al., 1997. The Drosophila tango gene encodes a bHLH-PAS protein that is orthologous to mammalian Arnt and controls CNS midline and tracheal development. *Development (Cambridge, England)*, 124(22), pp.4571–82.
- Šošić, D. et al., 2003. Twist regulates cytokine gene expression through a negative feedback loop that represses NF-kappaB activity. *Cell*, 112(2), pp.169–80.
- Spring, J. et al., 1994. Drosophila syndecan: conservation of a cell-surface heparan sulfate proteoglycan. *Proceedings of the National Academy of Sciences of the United States of America*, 91(8), pp.3334–8.
- Srinivasan, S., Rashka, K.E. & Bier, E., 2002. Creation of a Sog morphogen gradient in the Drosophila embryo. *Developmental cell*, 2(1), pp.91–101.
- St Johnston, D., 2002. The art and design of genetic screens: Drosophila melanogaster. *Nature reviews. Genetics*, 3(3), pp.176–88.
- Stappert, D., 2014. *Two novel , complementary next generation sequencing approaches to reveal the dorso-ventral gene regulatory network of Tribolium castaneum*. Universität zu Köln.
- Sun, P.D. & Davies, D.R., 1995. The cysteine-knot growth-factor superfamily. *annual review of biophysics and biomolecular structure*, 24, pp.269–91.
- Sutherland, D.J. et al., 2003. Stepwise formation of a SMAD activity gradient during dorsal-ventral patterning of the Drosophila embryo. *Development (Cambridge, England)*, 130(23), pp.5705–16.
- Suzuki, a, Ueno, N. & Hemmati-Brivanlou, a, 1997. Xenopus msx1 mediates epidermal induction and neural inhibition by BMP4. *Development (Cambridge, England)*, 124(16), pp.3037–44.
- Tauszig, S. et al., 2000. Toll-related receptors and the control of antimicrobial peptide expression in Drosophila. *Proceedings of the National Academy of Sciences of the United States of America*, 97(19), pp.10520–5.
- Thisse, B., Messal, M. El & Perrin-Schmitt, F., 1987. The twist gene: isolation of a Drosophila zygotic gene necessary for the establishment of dorso-ventral pattern. *Nucleic Acids Research*, 15(8), pp.3439–3453.
- Towb, P., Sun, H. & Wasserman, S. a, 2009. Tube Is an IRAK-4 homolog in a Toll pathway adapted for development and immunity. *Journal of innate immunity*, 1(4), pp.309–21.
- Tribulo, C. et al., 2003. Regulation of Msx genes by a Bmp gradient is essential for neural crest specification. *Development (Cambridge, England)*, 130(26), pp.6441–52.

- Tucker, J. a, Mintzer, K. a & Mullins, M.C., 2008. The BMP signaling gradient patterns dorsoventral tissues in a temporally progressive manner along the anteroposterior axis. *Developmental cell*, 14(1), pp.108–19.
- Valanne, S., Wang, J.-H. & Rämetsä, M., 2011. The Drosophila toll signaling pathway. *Journal of immunology (Baltimore, Md. : 1950)*, 186(2), pp.649–56.
- Valera, E. et al., 2010. BMP-2/6 heterodimer is more effective than BMP-2 or BMP-6 homodimers as inductor of differentiation of human embryonic stem cells. *PloS one*, 5(6), p.e11167.
- Vuilleumier, R. et al., 2010. Control of Dpp morphogen signalling by a secreted feedback regulator. *Nature cell biology*, 12(6), pp.611–7.
- Wagner, D.S. & Mullins, M.C., 2002. Modulation of BMP activity in dorsal-ventral pattern formation by the chordin and noggin antagonists. *Developmental biology*, 245(1), pp.109–23.
- Wan, M. & Cao, X., 2005. BMP signaling in skeletal development. *Biochemical and biophysical research communications*, 328(3), pp.651–7.
- Wang, X. et al., 2008. Type IV collagens regulate BMP signalling in Drosophila. *Nature*, 455(7209), pp.72–7.
- Wang, Y. & Ferguson, E.L., 2005. Spatial bistability of Dpp – receptor interactions during Drosophila dorsal – ventral patterning. *Nature*, 702(December 2004), pp.601–604.
- Weber, M., 2006. *Bone Morphogenetic Proteins (BMP) in der Embryonalentwicklung von Tribolium castaneum*. Ludwig-Maximilians-Universität München.
- Weisbrod, A., Cohen, M. & Chipman, A.D., 2013. Evolution of the insect terminal patterning system--insights from the milkweed bug, *Oncopeltus fasciatus*. *Developmental biology*, 380(1), pp.125–31.
- Wharton, K. a, Ray, R.P. & Gelbart, W.M., 1993. An activity gradient of decapentaplegic is necessary for the specification of dorsal pattern elements in the Drosophila embryo. *Development (Cambridge, England)*, 117(2), pp.807–22.
- Wills, A., Harland, R.M. & Khokha, M.K., 2006. Twisted gastrulation is required for forebrain specification and cooperates with Chordin to inhibit BMP signaling during *X. tropicalis* gastrulation. *Developmental biology*, 289(1), pp.166–78.
- Xie, J. & Fisher, S., 2005. Twisted gastrulation enhances BMP signaling through chordin dependent and independent mechanisms. *Development (Cambridge, England)*, 132(2), pp.383–91.
- Xie, T. & Spradling, a C., 1998. decapentaplegic is essential for the maintenance and division of germline stem cells in the Drosophila ovary. *Cell*, 94(2), pp.251–60.
- Yanagita, M., 2009. BMP modulators regulate the function of BMP during body patterning and disease progression. *BioFactors (Oxford, England)*, 35(2), pp.113–9.
- Yeh, D.-W. et al., 2013. Toll-like receptor 9 and 21 have different ligand recognition profiles and cooperatively mediate activity of CpG-oligodeoxynucleotides in zebrafish. *Proceedings of the National Academy of Sciences of the United States of America*, 110(51), pp.20711–6.

- Yuan, S. et al., 2009. An amphioxus TLR with dynamic embryonic expression pattern responses to pathogens and activates NF-kappaB pathway via MyD88. *Molecular immunology*, 46(11-12), pp.2348–56.
- Van der Zee, M. et al., 2006. Sog/Chordin is required for ventral-to-dorsal Dpp/BMP transport and head formation in a short germ insect. *Proceedings of the National Academy of Sciences of the United States of America*, 103(44), pp.16307–12.
- Van der Zee, M., da Fonseca, R.N. & Roth, S., 2008. TGFbeta signaling in Tribolium: vertebrate-like components in a beetle. *Development genes and evolution*, 218(3-4), pp.203–13.
- Zelzer, E., Wappner, P. & Shilo, B.-Z., 1997. The PAS domain confers target gene specificity of Drosophila bHLH/PAS proteins. *Genes & Development*, 11(16), pp.2079–2089.
- Zhang, C. & Klymkowsky, M.W., 2009. Unexpected functional redundancy between Twist and Slug (Snail2) and their feedback regulation of NF-kappaB via Nodal and Cerberus. *Developmental biology*, 331(2), pp.340–9.
- Zheng, L.-P. et al., 2012. Cloning and the expression pattern of Spätzle gene during embryonic development and bacterial challenge in Artemia sinica. *Molecular biology reports*, 39(5), pp.6035–42.
- Zhong, X. et al., 2012. A Toll-Spätzle pathway in the tobacco hornworm, Manduca sexta. *Insect biochemistry and molecular biology*, 42(7), pp.514–24.
- Zhu, W. et al., 2006. Noggin regulation of bone morphogenetic protein (BMP) 2/7 heterodimer activity in vitro. *Bone*, 39(1), pp.61–71.

7. Supplementary Information

7.1 Cell distributions differ between *dpp*-RNAi and *Toll-dpp*-RNAi embryos at the onset of gastrulation

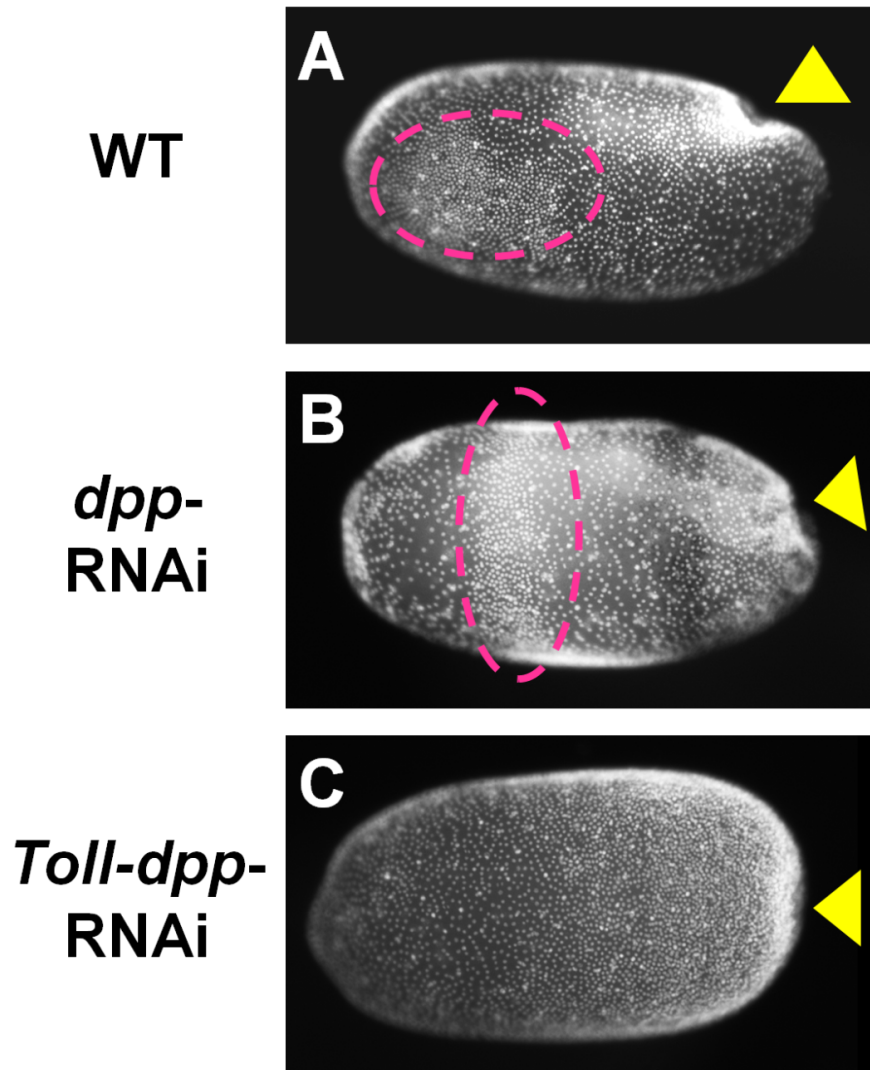


Figure 7-1: Nuclei distribution differs between *dpp*-RNAi and *Toll-dpp*-RNAi embryos at the onset of gastrulation

Anterior of the egg is to the left. The view is lateral with ventral down in A and not determinable in B and C. At the onset of gastrulation lateral patches of high nuclear density are observed in WT (A). *dpp* knockdown embryos exhibited instead an anterior transversal stripe of closely packed cells (B). *Toll-dpp*-RNAi embryos rather seemed to form a gradual nuclear distribution with highest density at the posterior pole at the onset of gastrulation (C). Pink dashed-line ovals highlight regions of high nuclear density and yellow arrowheads point towards invagination sites or the posterior indentation. Embryos shown in A and B are already at the anatrepsis stage, while the embryo pictured in C is slightly younger. The pictured *dpp*-RNAi embryo exhibited not the strongest phenotype, *i.e.* it mainly consist of mesoderm but it also contains some mesectodermal tissue (this is known as *sim* expression was monitored in this embryo). Abbreviation: WT: wild type.

7.2 *tsg* expression is not lost in *Toll*-RNAi embryos

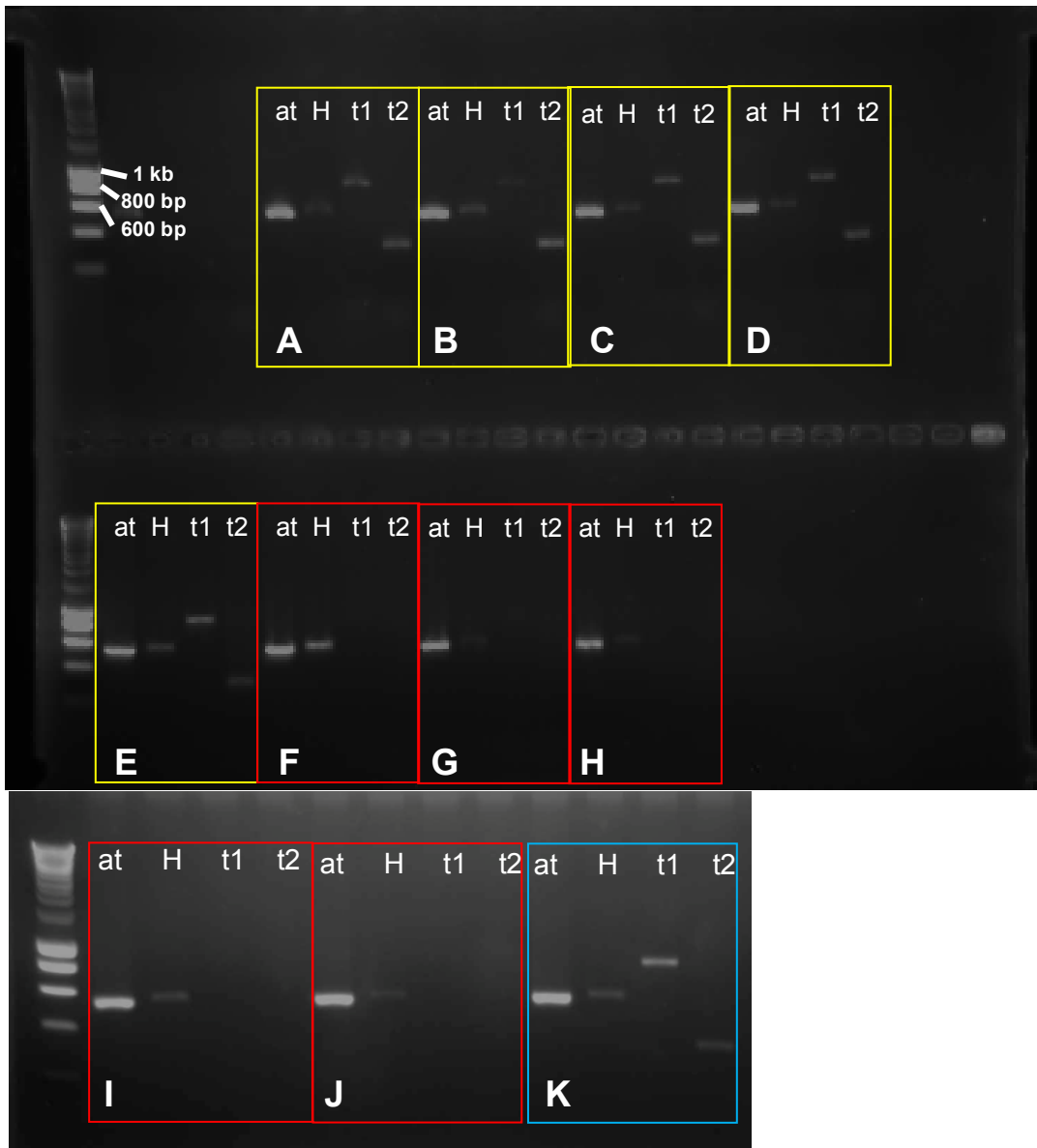


Figure 7-2: *tsg* transcript levels of *Toll*-RNAi and wild type embryos are similar

alpha-tubulin (at), *HMBS* (H) and two different *tsg* (t1, t2) amplicons were amplified by PCR and loaded on an agarose gel. The origin of the cDNA is indicated by colors of the squares that separate amplicons derived from different cDNAs (yellow: cDNA of *Toll*-RNAi embryos, red: cDNA of *tsg*-RNAi embryos, blue: cDNA from wild type embryos). Applied primers (Table 2-3): LS_Of_qPCR_HMBS Fwd 1 & Rev 2 (HMBS), LS_Of_qPCR_atubulin Fwd 3 & Rev 2 (at), Of-*tsg* marginal forward & reverse (t1), LS_Of *tsg* intern FWD & Of-*tsg* marginal reverse (t2). The annealing temperature was 58°C (more detailed PCR conditions are provided in 2.1.5). The SMART ladder (Fermentas) was used as size indicator.

Semi-quantitative PCR was performed to reveal if *Toll* regulates *tsg* transcription. Therefore, embryos from single egg batches were staged to 26 hpf to 32 hpf and used for RNA isolation

and subsequent cDNA synthesis (2.2.7). Each 1 µl of cDNA (each the same amount of RNA was used as cDNA template) was used as template for the PCR. *HMBS* and *alpha-tubulin* transcripts were amplified as control. *tsg* transcript levels appeared not to be significantly altered upon *Toll* knockdown (Figure 7-2 compare K with A-E). Subtle differences are assumed to be due to technical issues (e.g. pipetting). In cDNA of *tsg* knockdown embryos no *tsg* transcripts were detected (Figure 7-2 compare K with F-J). Although it cannot be excluded that *tsg* transcript levels are slightly altered in *Toll*-RNAi embryos they are clearly more similar to wild type *tsg* levels (Figure 7-2 compare K with A-E) than to that of *tsg*-RNAi embryos (Figure 7-2 F-J). Hence, the loss of DV polarity upon a *Toll* knockdown is not caused by a loss of *tsg* expression (3.3.5.2).

7.3 Transcript sequences

Table 7-1: Identifiers of transcript sequences

Orthologous genes were identified as described in 2.2.8. Sequences which were obtained by other approaches are either shown below or it is referred to the person who obtained the respective sequence information. Abbreviation: ID: identifier.

gene	ID
<i>twisted gastrulation/ crossveinless 1</i>	isotig 19489
<i>decapentaplegic</i>	AY899334.1 (Gene bank), cap3_Contig13540, unpublished data of Jeremy Lynch
<i>glass bottom boat</i>	isotig19379, isotig15491, Figure 7-3
<i>short gastrulation</i>	cap3_Contig14795, cap3_Contig18465, unpublished data of Yen-Ta Chen
<i>single minded</i>	unpublished data of Yen-Ta Chen
<i>Toll</i>	isotig03359 (Yen-Ta Chen)
<i>perlecan</i>	isotig17083
<i>pentagone</i>	cap3_Contig7096
<i>sox21b</i>	isotig05762
<i>punt</i>	isotig05130
<i>saxophone</i>	cap3_Contig17917
<i>thickveins</i>	cap3_Contig15135
<i>muscle specific homeobox</i>	unpublished data of Yen-Ta Chen
<i>tolloid / tolkin</i>	isotig14297
<i>twist</i>	unpublished data of Yen-Ta Chen
<i>dally</i>	cap3_singlet_GEQE5QV01DEFOF
<i>slalom</i>	isotig06519
<i>syndecan</i>	cap3_singlet_GEQE5QV01DZ2LX
<i>SoxNeuro</i>	unpublished data of Yen-Ta Chen

GGCCGCGGTTGAAGTCCGTAACAATGAAGTTCATTGTTCTAGTATTTTTTCGAGCGTTCATGAATCTGCTTTTGTGCACTGTCTGGTCTGTACATAGATAACGGA
ATTGATCAAACGGTTattCAAAGAGTCATgactTTGCGTGAAAAGCAGGAAGTTCAACATgaAATTTaAatTACTTGGtctACCTGACAgGCcCCACCCGAAAAA
AATTGTTACAAGGAGAGCAGTTAGAAGTtCtgctCCgAAATTTCTCCTTAATGTTTATAAGTCTCTtcTTGATTACCCCTCTCcAAGAAGTGCAGGAGTGAATTTA
ATCTTAGCGACAAAGATCTTCAGTCTATTGATGAAAGTGATATGATTATCAGCTTTTCTGGACATCGTCAACCTCCGGCTCTGAGAAAAGgGAATGTGATATGGTTT
GATGTCTCAGAAGTTTCTGTCAAGTAACTATGTTGGAGCAGAACTAAGACTGTATCACAACCTAACTATAATATTAGTCTTCAGCAATACACTTAAAGAGTTTA
TCTTTTAACTGAAGGAGTACATGGGGGAAAAATTTGGAGCTCATTGATACTTCTAACTTACTTCAGACTATGAAGGATGGCTAATATGTAATGTGACACATGTAT
TGACTTCCTGGGTTGTTTTCTCATTC TAATAAGGGATTATATGTTTCACTTACCTCTCTGCCTGGTACAGAGATATCTCTTGAAGATGGTGGCATAACACTTGAT
GAAGATGATGAAAAGCAGCCATTTATGGTAGCATTCTACAGGGCAGTGTACAAAACCAACGAACCTCATCTCGTGTTCGAAGGCAACAAGACTAAGAAAAAGAA
GGCTGATCATCAGAGTAAAAGCCACGAAATCCATTCCAAGATACAAGTGGATCCTGGACTCATTCAAAAAAGCTGTCAAATCCAAACTTTATATGTGAGTTTC
GAGACTTAAAGTGGCAGGATTGGATTATTGCTCCTGACGGTTATGGTGCTTTCTATGTCAGTGGTGAATGCAATTTCCCTTAAATGCACATATGAATGCAACAAC
CATGCAATTGTTCAAACCTCTGTTCATCTCATGAATCCTCTGCAGGTGCCTAAGCCTTGTGTGCTCCAAGCCCCGGG

Figure 7-3: incomplete *gbb* transcript sequence

The sequence was obtained by PCR with primers located in two non-overlapping *gbb* transcript sequence fragments present in the transcriptome (Table 7-1).

Acknowledgments/Danksagungen

Lieber Siegfried, vielen Dank, dass Du es mir ermöglichst hast an diesem spannenden Projekt mitzuarbeiten und mich während dieser Zeit so toll unterstützt hast! Außerdem möchte ich mich dafür bedanken, dass Du immer ein offenes Ohr für Fragen und Probleme hast. Ich schätze die wissenschaftlichen Diskussionen mit Dir sehr. Ich habe Dank Dir sehr viel Wissen und Erfahrung während meiner Zeit als Student mitnehmen können. Außerdem bin ich sehr froh einen Gruppenleiter zu haben der gleichzeitig so viel Kompetenz und so viele gute menschliche Qualitäten in sich vereinbart wie Du. Vielen Dank!!

Ich möchte mich bei meinem Zweitgutachter und Mitglied meines Thesis-Komitees Herr Prof. Dr. Plickert bedanken. Sie sind ein enthusiastischer und intelligenter Wissenschaftler und zudem immer hilfsbereit und freundlich. Ich freue mich sehr, dass Sie sich bereit erklärt haben meine Arbeit zu begutachten. Dafür und für ihren wissenschaftlichen Rat möchte ich mich herzlich bedanken! Außerdem möchte ich mich auch für den spannenden und interessanten Einblick in die Arbeit ihrer Forschungsgruppe während meines Rotations-Praktikums bedanken!

Vielen Dank Frau Prof. Dr. Ute Höcker dass Sie den Vorsitz bei meiner Prüfung übernehmen!

Vielen Dank Herr Dr. Hans-Martin Pogoda dass Sie sich bereit erklärt haben als Beisitzer in meinem Prüfungskomitee teilzuhaben!

Ich möchte Frau Prof. Dr. Korsching danken. Vielen Dank für Ihre wissenschaftlichen Ratschläge als Mitglied meines Thesis-Komitees und für das spannende Rotations-Projekt!

I would like to thank Dr. Kristen Panfilio. You supervized me in the beginning of my studies and inspired me for Evo-Devo science! Also after this time and even when you already started your own research group you still scientifically supported me a lot. Thank you very much for all your help!

I would also like to thank Dr. Jeremy Lynch. You did not only supervize me in the beginning of my scientific career but afterwards you also gave good advises and helped me in terms of technical issues. In addition, all the BBQs and sport events you planned for the lab community were always great and I enjoyed them a lot! You are a great person! Thank you very much!

I would also like to thank all my colleagues. It is very nice to work and drink Mauer-beer together with you! I enjoyed the atmosphere in the lab a lot! In addition, you all gave me good scientific advises, helped and supported me a lot! However, most important was for me that you all are very nice people and that it was always fun to celebrate and have BBQ with you! Thank you all very much!! Special thanks to you Yen-Ta for the nice and fruitful collaboration!!

Im Speziellen möchte ich mich bei meinen Büro Kollegen sowie Walde, Meike und Thorsten bedanken. Lieber Dominik, liebe Nadine, lieber Thomas, lieber Thorsten ihr alle habt mich beim Schreiben dieser Arbeit super unterstützt! Außerdem habt ihr mir alle (inkl. Orhan, Walde und Meike) immer mit Rat und Tat bei Seite gestanden, das gilt natürlich besonders für die "älteren Hasen". Dafür bist Du mir, liebe Nadine, umso schneller ans Herz gewachsen! Ich schätze euch alle sehr und könnte mir keine besseren Kollegen (in der Arbeit, beim Feiern und natürlich beim Mauer-Bier) als euch vorstellen! Vielen lieben Dank!!!!

Ich möchte Dir, liebe Isabell, für dein unendliches Engagement, deine Hilfsbereitschaft und Unterstützung danken! Auch vielen Dank an Dein tolles Mitarbeiter-Team!

Ich möchte mich für die Finanzierung meiner Arbeit beim SFB 680 und der International Graduate School in Development Health and Disease von Köln bedanken.

Liebe Mama, lieber Papa, liebe Familie und Freunde ich möchte euch allen für eure Liebe, euren Rückhalt und Unterstützung danken. Und für die vielen super Oster-, Nikolaus- und Geburtstagspäckle! Ich liebe euch alle!

Lieber Hubert, vielen Dank für deine Liebe und deinen Rückhalt! Du warst immer für mich da und hast es mir niemals übel genommen oder mich unter Druck gesetzt wenn ich Dich wegen des Studiums vernachlässigt habe. Vielen Dank! Ich liebe Dich und werde Dich immer lieben!

Erklärung

Ich versichere, dass ich die von mir vorgelegte Dissertation selbständig angefertigt, die benutzten Quellen und Hilfsmittel vollständig angegeben und die Stellen der Arbeit - einschließlich Tabellen, Karten und Abbildungen -, die anderen Werken im Wortlaut oder dem Sinn nach entnommen sind, in jedem Einzelfall als Entlehnung kenntlich gemacht habe; dass diese Dissertation noch keiner anderen Fakultät oder Universität zur Prüfung vorgelegen hat; dass sie - abgesehen von unten angegebenen Teilpublikationen - noch nicht veröffentlicht worden ist sowie, dass ich eine solche Veröffentlichung vor Abschluss des Promotionsverfahrens nicht vornehmen werde. Die Bestimmungen der Promotionsordnung sind mir bekannt. Die von mir vorgelegte Dissertation ist von Herrn Prof. Dr. Siegfried Roth betreut worden.

Köln, den 05.05.2014

Lena Sachs

Teilpublikationen

Sachs, L. M., 2009. Dorsoventral patterning in the milkweed bug *Oncopeltus fasciatus*. Bachelor thesis, University of Cologne

Sachs, L. M., 2011. The role of BMP signaling in Dorsoventral patterning in the milkweed bug *Oncopeltus fasciatus*. Master thesis, University of Cologne

Lebenslauf

Name: Lena Mareike Sachs

Geburtstag und -ort: 19.11.1985, Dachau

Staatsangehörigkeit: deutsch

Schulbildung: 1992-1996: Grundschule in Eching
1996- 2005: Camerloher-Gymnasium in Freising
Juli 2005: Allgemeine Hochschulreife

Studienverlauf: 2006 - 2009: Bachelor of Science in Biologie
an der Universität zu Köln
Bachelor Arbeit:
Dorsoventrale Musterbildung in der Wanze
Oncopeltus fasciatus betreut durch Prof. Dr. S. Roth

2009 - 2011: Master of Science in Biologie an der Universität zu Köln
Teilnahme am Fast Track Programm der International
Graduate School in Development Health and Disease
(IGSDHD), Köln

Promotion: Seit 2010: Promotion und Master Arbeit im Rahmen des Fast Track
Programms am Institut für Entwicklungsbiologie der
Universität zu Köln, betreut durch Prof. Dr. S. Roth

2010-2011: Master Arbeit: The role of BMP signaling during
Dorsoventral patterning of the milkweed bug
Oncopeltus fasciatus

2010-2013: Finanzierung durch den SFB 680

2013-2014: Forschungstipendium der IGSDHD, Köln

